Westinghouse

EC 232

ATTENUATION OF BEARING TRANSMITTED NOISE

Volume 2

August 1964

performed in conjunction with

subcontractor

Mechanical Technology Incorporated

in fulfillment of

Contract NO. NOBS-86914

Bureau of Ships

Department of Navy

U. S. of America

Westinghouse Electric Corporation
Lester, Pennsylvania

EC 232

ATTENUATION OF BEARING TRANSMITTED NOISE

Volume 2

August 1964

performed in conjunction with

subcontractor

Mechanical Technology Incorporated

in fulfillment of

Contract NO. NOBS-86914

Bureau of Ships

Department of Navy

U. S. of America

Westinghouse Electric Corp.

Lester, Pennsylvania

Volume 2

Part I

Attenuation of Rotor Unbalance Forces by Flexible Bearing Supports

by

Jorgen Lund
Mechanical Technology Incorporated

Preface

This volume, the second of three volumes which examine the noise attenuation value of a flexibly-supported bearing, is divided into two parts:

Part I - Attenutation of Rotor Unbalance Forces By Flexible Bearing Supports

Part II - Unbalance Response Of A Uniform Elastic Rotor, Supported In Damped Flexible Bearings

The other two volumes complete a study aimed specifically at an investigation into the effect of a hydraulically supported, tilting-pad, journal bearing on the attenuation of noise originating from rotor unbalance. Volume 1, Spring and Damping Coefficients For The Tilting-Pad Journal Bearing, provides an analytical method for determining the spring and damping properties of the bearing oil-film with the results presented in curves for typical tilting-pad bearing geometries. The third volume includes (1) a generalized-rotor analysis and (2) experimental results.

Mechanical Technology Incorporated was primarily responsible for the analytical portion of this study - while Westinghouse Electric Corporation designed and conducted the experimental test.

TABLE OF CONTENTS

	Pg.
ABSTRACT	1
INTRODUCTION	2
DISCUSSION	3
RESULTS:	5
Description of the Charts	5
Interpretation of the Charts	7
Numerical Example	10
ANALYSIS	14
CONCLUSIONS	25
RECOMMENDATIONS	26
REFERENCES	27
APPENDIX:	28
Computer Program PN0125: Transmitted Force and Response of a Two-Mass Rotor in Rigid Pedestals -	28
Computer Program PN0132: Transmitted Force and Response of a Two-Mass Rotor in Flexible Pedestals-	32
FIGURES 1 to 25	35
NOMENCLATURE	60

ABSTRACT

This report is concerned with the attenuation of the force transmitted by an unbalanced rotor. The attenuation is achieved by a flexible bearing support. The report presents an analysis of the unbalance vibrations of a flexible, symmetrical, two-mass rotor supported in fluid film bearings which in turn are mounted in flexible supports. The fluid film in the bearings possesses both flexibility and damping. The analysis takes into account both static and dynamic rotor unbalance and gives results for the rotor amplitudes and the transmitted force as functions of the system parameters. The analysis has been programmed for a digital computer and a description of the two computer programs is included. Numerical results have been obtained and are summarized in 24 design charts.

INTRODUCTION

Among the principal noise sources on board a ship are the vibrations transmitted from the various pieces of rotating machinery such as the main propulsion unit, the auxiliary machinery, etc. In attempting to reduce the transmitted vibrations two general approaches are available:

a) eliminate the causes responsible for the generated noise by better rotor balancing, closer manufacturing tolerances, etc.

b) attenuate the noise by means of vibration isolation

Experience has shown that the former approach yields, at best, moderate gains due to the limitations imposed by practical considerations. Hence, increased attention is given instead to the possible methods of vibration isolation. A key consideration in the application of this approach is to attenuate the noise as close to its source as feasible and prevent the vibrations from setting too heavy masses in motion. This may be accomplished by mounting the bearing housings on flexible supports.

It is the purpose of this report to present an analysis of the noise attenuating characteristic of a flexible bearing support. Specifically the analysis establishes the equations for determining the support stiffness which will achieve a desired noise attenuation. The analysis takes into account the flexibility of the rotor, the damping and stiffness characteristics of the bearing film, the mass of the bearing housing and the stiffness and damping of the support. Both static and dynamic rotor unbalance is considered.

Numerical results have been computed for a wide range of support and rotor parameters. The results are presented in 24 graphs giving the transmitted force and the rotor amplitude as functions of the rotor speed. The graphs are intended to be used for selecting the support parameters (e.g. stiffness) to achieve a desired noise attenuation over a given speed range.

DISCUSSION

The unbalance which is always present in a rotor gives rise to a dynamical force at the bearings with the same frequency as the speed of the rotor. Some attenuation of the force takes place in the bearings since the fluid film possesses both flexibility and damping (see Refs 1,2,3, 4 and 5). However, to obtain an appreciable force attenuation it becomes necessary to vibration isolate the bearings by means of a flexible support (e.g. a hydraulic support). The magnitude of the resulting attenuation depends on the stiffness of the support and the dynamical characteristics of the rotor-bearing system. It is the purpose of the present report to study this attenuation and to determine the effect of the parameters of the system

The system is represented by the model in Fig. 1. It consists of a flexible, symmetrical, two-mass rotor supported in two journal bearings. Having two rotor masses makes it possible to consider both static and dynamic rotor unbalance. Each bearing is mounted on a flexible support with a specified stiffness and a specified damping. The journal bearing is characterized by 4 spring coefficients and 4 damping coefficients derived from lubrication theory (Refs.1,2,3,4,5). The mass of the bearing housing is also included since it affects the force transmission.

On the basis of the selected model the equations of motion are set up for the rotor and the support. Because of the large number of parameters it is of limited value to derive a closed form solution. Instead, the equations are reduced to a form convenient for numerical evaluation and programmed for a digital computer. Two computer programs, both for the IBM 1620 computer, have been written. They are described in detail in the Appendix including instructions for using the programs. The results from the programs include the force transmitted to the foundation, the rotor amplitudes and the amplitude of the bearing housing. Extensive calculations have been performed and the data have been plotted in Figs.2 to 25. The employed values of rotor stiffness and weight and of support stiffness are selected to cover the range normally encountered in Navy applications. The use of the graphs is explained in the following section.

A study of the graphs reveals that a very significant attenuation of the transmitted force can be obtained, at least in theory. Note that the "unattenuated" force is not shown in the graphs but would appear as a series of straight lines. They are determined by a simple relationship given in the following section. However, even small amounts of damping in the support diminish the attenuation and in practice this is unavoidable. Furthermore, system resonances tend to become accentuated in a way not found in the conventional construction, e g. the resonance of the bearing housing becomes important. Therefore, the graphs should serve as a guide line only, they are not intended to be final design charts.

Since it is known that a flexible support may adversely affect the stability of the bearing, i.e. the speed at onset of oil whip may be lowered, a study of the stability is also undertaken. It is concluded that even if a flexible support does lower the oil whip speed when there is no damping in the support it takes only a rather small amount of damping to restore, and even increase the stability limit.

RESULTS

The main purpose of the numerical results (Fig.2 to 25) is to illustrate the attenuation of the transmitted force due to a flexible support. To obtain a high attenuation as required in Naval applications the support is very soft in comparison with the bearing stiffness.

The rotor configuration is shown in Fig. 1. The rotor is symmetric and consists of two masses M on a flexible shaft. There are two bearings which are flexibly supported with the support stiffness, K_p. In addition, the mass m of the bearing housing is included because the support resonance may become important when the stiffness is small. The support damping has been neglected since it is in general kept small in order to achieve the force attenuation.

The results are given in form of dimensionless parameters:

dimensionless transmitted force: $\frac{\xi C F}{W \delta}$

dimensionless journal amplitude: $\frac{\xi X_2}{\delta}$

dimensionless rotor mass amplitude: $\frac{X_1}{\delta}$

speed ratio: $\frac{\omega}{\omega_n}$

The rotor-bearing-support parameters are:

bearing stiffness: $\frac{C K_{xx}}{W}$

bearing damping: $\frac{C \omega C_{xx}}{W}$

support stiffness: $\frac{C K_p}{W}$

support mass: $\frac{m}{\xi^2 M}$

rotor flexibility parameter: $\varrho = \frac{W \alpha}{C \xi^2}$

where:

W - bearing reaction, lbs.

M - half of the total rotor mass, lbs.sec^2/in

α - influence coefficient for rotor (inverse rotor stiffness), Equation (4), $\frac{\text{in}}{\text{lbs.}}$

ξ - distance between rotor masses divided by rotor length, Equation (5).

δ - eccentricity of rotor masses, inch

C - radial bearing clearance, inch

ω - rotor speed, rad/sec.

$\omega_n = 1/\sqrt{M\alpha}$, critical speed of rigidly supported rotor, rad/sec.

m - support mass, lbs.sec^2/in

K_p - support stiffness, lbs/in

K_{xx} - bearing stiffness, lbs/in

C_{xx} - bearing damping coefficient, lbs.sec/in

F - force transmitted to foundation, lbs.

X_1 - amplitude of rotor mass, inch

X_2 - amplitude of journal, inch.

The numerical data cover the following range of rotor-support parameters:

$$\varrho = \frac{W\alpha}{C\xi^2} = .1,\ .3,\ 1,\ 3 \text{ and } 10$$

$$\frac{CK_p}{W} = 10^{-3},\ 3\cdot10^{-3},\ 10^{-2} \text{ and } 3\cdot10^{-2}$$

$$\frac{m}{\xi^2 M} = .05 \text{ and } .15$$

Since in the present case the bearing is much stiffer than the support, it has virtually no influence on the results. For completeness the bearing is assigned the coefficients:

$$\frac{CK_{xx}}{W} = 3.75 \qquad \frac{C\omega C_{xx}}{W} = 4.70$$

which is representative of a 4-shoe tilting pad journal bearing.

Interpretation of the Charts

The data apply to both static and dynamic unbalance such that for static unbalance $\xi = 1$ and α corresponds to the first flexural rotor critical speed, whereas for dynamic unbalance ξ represents the distance between rotor masses and α corresponds to the second flexural rotor critical speed.

In Figs. 2 to 25 two resonances are evident. The first resonance is the rotor resonance which for a soft support occurs at:

$$\left(\frac{\omega}{\omega_n}\right)_{\text{system resonance}} \cong \sqrt{\rho \frac{CK_p}{W}}$$

or in dimensional form:

$$\omega_{\text{System resonance}} \cong \begin{cases} \sqrt{\frac{K_p}{M}} & \frac{\text{radians}}{\text{sec}} \quad \text{(1st mode)} \\ \sqrt{\frac{K_p}{\xi^2 M}} & \frac{\text{radians}}{\text{sec}} \quad \text{(2nd mode)} \end{cases}$$

Note that for the second mode the angular restoring stiffness is $\frac{1}{2}\ell^2 K_p$ (ℓ = span between bearings) and the transverse mass moment of inertia of the rotor is $\frac{1}{2}(\xi\ell)^2 M$ leading to the stated result for the resonant speed.

The second resonance shown by the graphs is the resonance of the support:

$$\left(\frac{\omega}{\omega_n}\right)_{\text{Support resonance}} \cong \sqrt{\frac{1+\rho\frac{CK_p}{W}}{\frac{m}{M}}} \cong \sqrt{\frac{M}{m}}$$

or in dimensional form:

$$\omega_{\text{Support resonance}} \cong \sqrt{\frac{\frac{1}{\alpha}+K_p}{m}} \cong \sqrt{\frac{1}{\alpha m}} \quad \frac{\text{radians}}{\text{sec}}$$

where $1/\alpha$ represents the rotor stiffness. Hence, in schematic form Figs. 2 to 25 become:

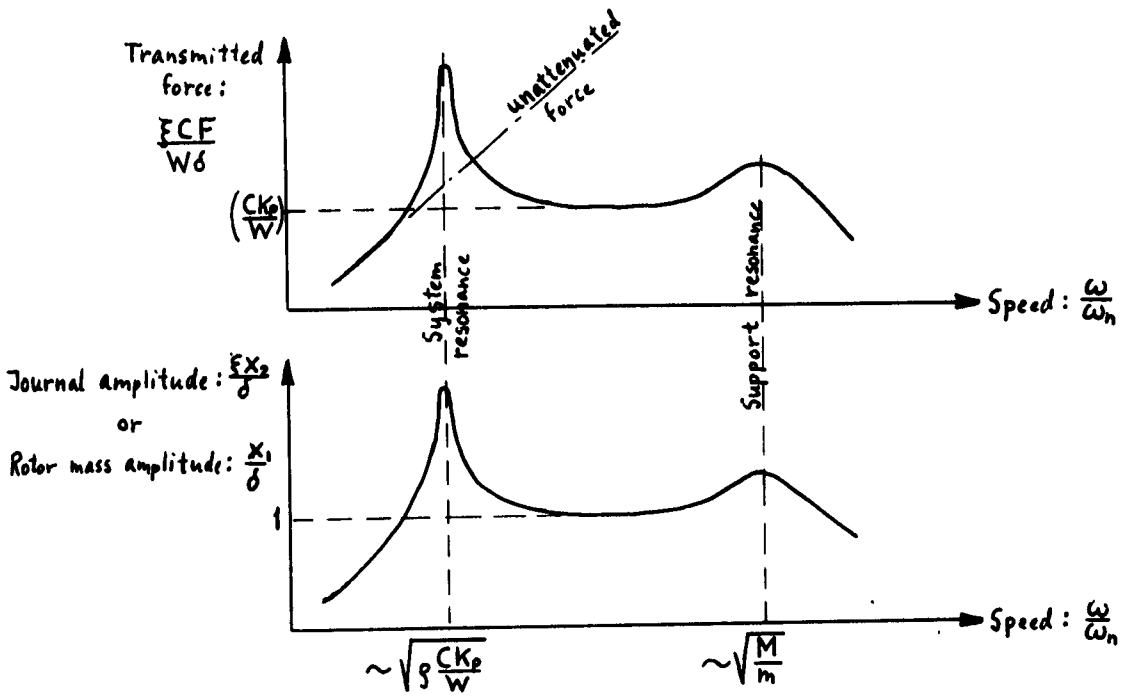

Since the support damping has been neglected the resonance values are very large in the graphs. However, some damping is always present in the support and an estimate of the peak amplitude and transmitted force at the rotor resonance can be obtained from:

peak journal amplitude: $$\left(\frac{\xi X_2}{\delta}\right)_{peak} \cong \frac{\sqrt{\frac{1}{\rho}\frac{CK_p}{W}}}{\left(1-\rho\frac{CK_p}{W}\right)\omega_n\frac{Cd}{W}} \cong \frac{\sqrt{\frac{1}{\rho}\frac{CK_p}{W}}}{\frac{C\omega_n d}{W}}$$

peak transmitted force: $$\left(\frac{\xi CF}{W\delta}\right)_{peak} \cong \frac{CK_p}{W}\left(\frac{\xi X_2}{\delta}\right)_{peak}$$

In dimensional form:

journal amplitude: $$(X_2)_{peak} \cong \frac{\delta\sqrt{K_p M}}{d} \quad \text{inch}$$

transmitted force: $$F_{peak} \cong K_p (X_2)_{peak} \quad \text{lbs}$$

where:

d - support damping, lbs.sec/in

When the rotor is considered rigid and the bearings are also taken to be rigid the transmitted force becomes:

$$F = \xi M \delta \omega^2 \quad \text{lbs.} \quad \text{(rigid rotor)}$$

or in dimensionless form:

$$\frac{\xi CF}{W\delta} = \frac{1}{\rho}\left(\frac{\omega}{\omega_n}\right)^2 \qquad \text{(unattenuated force)}$$

Comparing this value with the values of the transmitted force for a flexible support the magnitude of the force attenuation can be estimated. The above "unattenuated" force would appear as straight lines with a slope of 2 in Figs. 2 to 9. There would be a line for each rotor flexibility parameter.

Numerical Example

Let it be desired to vibration isolate a steam turbine rotor with the following data:

Total weight: 4,400 lbs.
Transverse mass moment of inertia around CG: $I = 1.35 \cdot 10^6$ lbs.in^2
Span between bearings: = 74 inch.
First flexural critical speed: = 25,200 RPM
Second flexural critical speed: = 73,000 RPM

The rotor is approximately symmetrical around the CG so that:

Bearing reaction: W = 2,200 lbs
Rotor mass per bearing: M = 2,200 lbs = 5.7 lbs.sec^2/in.

From the formula:

$$\omega_n = \sqrt{\frac{1}{M\alpha}}$$

the influence coefficient α is calculated as:

$$\alpha = \begin{cases} 2.5 \cdot 10^{-8} \ \frac{in}{lb} & \text{(1st mode)} \\ 3 \cdot 10^{-9} \ \frac{in}{lb} & \text{(2nd mode)} \end{cases}$$

For the second mode the two rotor masses M are separated by the distance (ξl) where l is the rotor span. Thus:

$$\tfrac{1}{2}(\xi l)^2 M = I$$

from which:

$$\xi = \frac{1}{74}\sqrt{\frac{2 \cdot 1.35 \cdot 10^6}{2200}} = .475$$

For the first mode $\xi = 1$ by definition.

Setting the radial bearing clearance:

$C = 4.10^{-3}$ inch

the rotor flexibility parameter ϱ becomes:

$$\varrho = \frac{W\alpha}{C\xi^2} = \begin{cases} 1.37 \cdot 10^{-2} & \text{(1st mode)} \\ 7.3 \cdot 10^{-3} & \text{(2nd mode)} \end{cases}$$

These values are outside the range used in the graphs making it necessary to employ a scale factor on the influence coefficient. This can be done because the rotor is very stiff. Hence, if α is multiplied by 7.3 and 13.7 respectively the new values becomes $\varrho = .1$ for both the first and second mode. The corresponding flexural critical speeds become:

$$\omega_1 = \frac{25,200}{\sqrt{7.3}} = 9,300 \text{ RPM} \quad \text{(by scaling)}$$

$$\omega_2 = \frac{73,000}{\sqrt{13.7}} = 19,700 \text{ RPM} \quad \text{(by scaling)}$$

In order to select the support stiffness K_p it is seen from Figs. 2 to 9 that it is necessary to specify the lowest speed at which attenuation is required. Then K_p must be selected such that the system resonances are well below this specified speed. In the present case it is desired to achieve a substantial attenuation at 1100 RPM or for use in the charts:

$$\frac{\omega}{\omega_1} = \frac{1,100}{9,300} = .118$$

$$\frac{\omega}{\omega_2} = \frac{1,100}{19,700} = .056$$

The "unattenuated" transmitted force becomes a straight line in Figs. 2 to 9 determined by:

$$\left(\frac{\xi CF}{W\delta}\right)_{\text{unattenuated}} = \frac{1}{\varrho}\left(\frac{\omega}{\omega_n}\right)^2 = 10\left(\frac{\omega}{\omega_n}\right)^2$$

i.e. a line passing through two points:

$$\left(\left(\frac{\omega}{\omega_n}\right), \frac{\xi CF}{W\delta}\right) = (10^{-2}, 10^{-3}) \quad \text{and} \quad (10^{-1}, 10^{-1})$$

It is found that $\frac{CK_p}{W} = 10^{-2}$ is the highest value of the support stiffness which gives attenuation for both modes at 1,100 RPM. From Fig. 6 (or 7):

	$\left(\frac{\omega}{\omega_n}\right)$ for 1,100rpm	actual force $\frac{\xi CF}{W\delta}$	"unattenuated" force $\left(\frac{\xi CF}{W\delta}\right)_{unatten.}$	Attentuation at 1,100 RPM $db = 20 \cdot \log\left(\frac{F_{unatten.}}{F}\right)$
1st mode (static unbalance)	.118	.01	.135	22.6
2nd mode (dynamic unbalance)	.056	.0135	.03	6.9

The actual value of the support stiffness K_p is calculated as:

$$K_p = \frac{W}{C} 10^{-2} = \frac{2,200}{4 \cdot 10^{-3}} 10^{-2} = 5,500 \ \frac{lbs}{in}$$

The bearing housing weighs 100 lbs. Thus:

$$\frac{m}{\xi^2 M} = \frac{100}{\xi^2 \cdot 2,200} = \begin{cases} .045 & \text{(1st mode)} \\ .20 & \text{(2nd mode)} \end{cases}$$

Hence, Fig. 6 applies for the first mode and Fig. 7 for the second mode. However, for the original calculated values of the rotor flexibility parameter the support resonance is very insignificant.

The journal and rotor amplitudes can be found from Figs. 14 and 22 (or Figs. 15 and 23 for the second mode). Since the rotor is very stiff there is no difference between the two amplitudes in the speed range of interest, say up to 10,000 RPM. Still using the scale factor on α the rotor resonances occur at:

$$\frac{\omega}{\omega_n} = .032 \sim \begin{cases} 295 \text{ RPM} & \text{(1st mode)} \\ 630 \text{ RPM} & \text{(2nd mode)} \end{cases}$$

Let the rotor unbalance be 4 oz.inch per rotor mass, i.e. the rotor eccentricity δ becomes:

$$\delta = \frac{4/16}{2,200} = .113 \cdot 10^{-3} \text{ inch}$$

At speeds above 1200 to 1300 RPM the journal amplitude is practically constant:

$$\frac{\xi X_2}{\delta} = 1 \sim X_2 = \begin{cases} .113 \cdot 10^{-3} \text{ inch} & \text{(1st mode)} \\ .24 \cdot 10^{-3} \text{ inch} & \text{(2nd mode)} \end{cases}$$

Let there by a small damping in the support, given by the damping coefficient d and assume the value:

$$d = 20 \ \frac{lbs \cdot sec}{in}$$

Hence, the peak amplitude at resonance can be calculated from the previously given formula:

$$\left(\frac{\xi x_2}{\delta}\right)_{peak} = \frac{\sqrt{\frac{1}{\zeta}\frac{CK_0}{W}}}{\frac{C\omega_n d}{W}} = \frac{\sqrt{\frac{1}{.1}\cdot 10^{-2}}}{\frac{4\cdot 10^{-3}\cdot 20}{2200}\cdot\frac{2\pi}{60}\begin{cases}9{,}300\\19{,}700\end{cases}} = \begin{cases}8.95 & \text{(1st mode)}\\ 4.2 & \text{(2nd mode)}\end{cases}$$

In actual values the peak journal amplitude becomes:

$$(x_2)_{peak} = \frac{\delta}{\xi}\cdot\begin{cases}8.95\\4.2\end{cases} = 1\cdot 10^{-3} \text{ inch}$$

ANALYSIS

In order to account for both the first and the second critical speed and also consider both static and dynamic unbalance the rotor is represented by a symmetrical two-mass rotor:

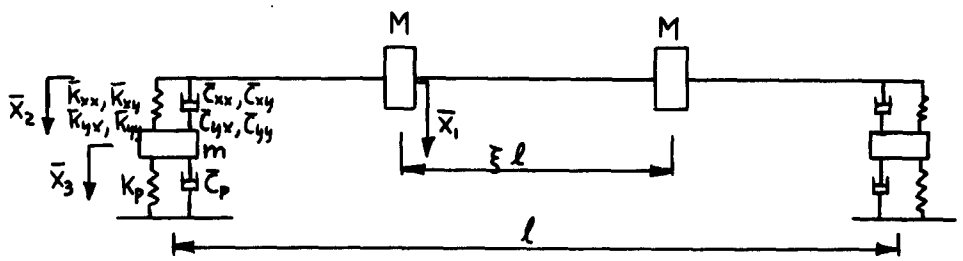

Rotor Equations

Let the rotor stiffness be described by the influence coefficients α_{aa} and α_{ab}, applying at the concentrated masses. The rotor unbalance is introduced by giving each mass an eccentricity δ. Hence, the equations of motion are

$$\bar{X}_1 = \alpha_{aa}\left(-M\ddot{\bar{X}}_1 + M\omega^2\delta\cos\omega t\right) + \alpha_{ab}\left(\mp M\ddot{\bar{X}}_1 \pm M\omega^2\delta\cos\omega t\right) + \begin{cases}\bar{X}_2\\ \xi\bar{X}_2\end{cases} \tag{1}$$

where the upper sign applies to static unbalance (first mode) and the lower sign is for the dynamic unbalance (second mode). Eq.(1) may also be written:

$$\bar{X}_1 - \xi\bar{X}_2 = -\alpha M\ddot{\bar{X}}_1 + \alpha M\omega^2\delta\cos\omega t \tag{2}$$

$$\bar{y}_1 - \xi\bar{y}_2 = -\alpha M\ddot{\bar{y}}_1 + \alpha M\omega^2\delta\sin\omega t \tag{3}$$

with the convention:

$$\alpha = \begin{cases}\alpha_{aa}+\alpha_{ab} & \text{static unbalance, first mode}\\ \alpha_{aa}-\alpha_{ab} & \text{dynamic unbalance, second mode}\end{cases} \tag{4}$$

$$\xi = \begin{cases}1 & \text{static unbalance, first mode}\\ \xi & \text{dynamic unbalance, second mode}\end{cases} \tag{5}$$

The rigid support critical speed is then given by:

(6) $$\omega_n = \sqrt{\frac{1}{M\alpha}}$$

Set:

(7) $$X_1 = Re\left\{\frac{x_1}{\delta} e^{i\omega t}\right\}$$

(8) $$X_2 = Re\left\{\frac{\xi \bar{x}_2}{\delta} e^{i\omega t}\right\}$$

(9) $$X_3 = Re\left\{\frac{\xi \bar{x}_3}{\delta} e^{i\omega t}\right\}$$

and similarly for the y-direction. Substitute into Eq.(2) and (3) to get:

(10) $$X_1 = \frac{x_2 + \left(\frac{\omega}{\omega_n}\right)^2}{1 - \left(\frac{\omega}{\omega_n}\right)^2}$$

(11) $$y_1 = \frac{y_2 - i\left(\frac{\omega}{\omega_n}\right)^2}{1 - \left(\frac{\omega}{\omega_n}\right)^2}$$

Bearing Equations

The rotor is supported in two identical bearings. Each bearing is represented by four spring coefficients: $\bar{K}_{xx}$, $\bar{K}_{xy}$, $\bar{K}_{yx}$, $\bar{K}_{yy}$ and four damping coefficients: $\bar{C}_{xx}$, $\bar{C}_{xy}$, $\bar{C}_{yx}$, $\bar{C}_{yy}$. A force balance yields:

(12) $$\xi\left[-M\ddot{\bar{x}}_1 + M\omega^2\delta\cos\omega t\right] = \frac{\xi}{\alpha}\left[\bar{x}_1 - \xi\bar{x}_2\right] = \bar{K}_{xx}(\bar{x}_2-\bar{x}_3) + \bar{C}_{xx}(\dot{\bar{x}}_2-\dot{\bar{x}}_3) + \bar{K}_{xy}(\bar{y}_2-\bar{y}_3) + \bar{C}_{xy}(\dot{\bar{y}}_2-\dot{\bar{y}}_3)$$

(13) $$\xi\left[-M\ddot{\bar{y}}_1 + M\omega^2\delta\sin\omega t\right] = \frac{\xi}{\alpha}\left[\bar{y}_1 - \xi\bar{y}_2\right] = \bar{K}_{yx}(\bar{x}_2-\bar{x}_3) + \bar{C}_{yx}(\dot{\bar{x}}_2-\dot{\bar{x}}_3) + \bar{K}_{yy}(\bar{y}_2-\bar{y}_3) + \bar{C}_{yy}(\dot{\bar{y}}_2-\dot{\bar{y}}_3)$$

Set:

(14) $$K_{xx} = \frac{C\bar{K}_{xx}}{W}$$

(15) $$\omega C_{xx} = \frac{C\omega C_{xx}}{W}.$$

and similarly for the 6 remaining coefficients. Here C is the radial bearing clearance and W is the load on the bearing. Introducing Eqs. (7) to (10), (14) and (15) into Eqs. (12) and (13) yields:

$$(16)\quad [K_{xx}-\alpha+i\omega C_{xx}]x_2+[K_{xy}+i\omega C_{xy}]y_2-[K_{xx}+i\omega C_{xx}]x_3-[K_{xy}+i\omega C_{xy}]y_3=\alpha$$

$$(17)\quad [K_{yx}+i\omega C_{yx}]x_2+[K_{yy}-\alpha+i\omega C_{yy}]y_2-[K_{yx}+i\omega C_{yx}]x_3-[K_{yy}+i\omega C_{yy}]y_3=-i\alpha$$

where:

$$(18)\qquad \alpha=\frac{\xi^2 C}{W\alpha}\;\frac{\left(\frac{\omega}{\omega_n}\right)^2}{1-\left(\frac{\omega}{\omega_n}\right)^2}$$

Support Equations

The bearing housing is supported flexibly by a spring K_p and a dashpot C_p. Denoting the mass of the bearing housing m the equations of motion are:

$$(19)\qquad m\ddot{\bar{x}}_3=-K_p\bar{x}_3-C_p\dot{\bar{x}}_3+\bar{K}_{xx}(\bar{x}_2-\bar{x}_3)+\bar{C}_{xx}(\dot{\bar{x}}_2-\dot{\bar{x}}_3)+\bar{K}_{xy}(\bar{y}_2-\bar{y}_3)+\bar{C}_{xy}(\dot{\bar{y}}_2-\dot{\bar{y}}_3)$$

and similarly for the y-direction. To make dimensionless set:

$$(20)\qquad k=\frac{CK_p}{W}$$

$$(21)\qquad \omega_n d=\frac{C\omega_n\bar{C}_p}{W}$$

$$(22)\qquad \frac{Cm\omega_n^2}{W}=\frac{C\xi^2}{W\alpha}\frac{m}{\xi^2 M}=\frac{\mu}{\rho}$$

$$(23)\qquad \rho=\frac{W\alpha}{C\xi^2}$$

$$(24)\qquad \mu=\frac{m}{\xi^2 M}$$

Solve Eq. (19) together with Eq.(16) and (17) to get:

$$(25)\qquad x_3=\frac{\alpha(x_2+1)}{k-\frac{\mu}{\rho}\left(\frac{\omega}{\omega_n}\right)^2+i\left(\frac{\omega}{\omega_n}\right)\omega_n d}$$

$$(26)\qquad y_3=\frac{\alpha(y_2-i)}{k-\frac{\mu}{\rho}\left(\frac{\omega}{\omega_n}\right)^2+i\left(\frac{\omega}{\omega_n}\right)\omega_n d}$$

System Equations

Combine Eqs. (16), (17), (25) and (26) to get the equations in their final form:

$$[K_{xx}+i\omega C_{xx}-\alpha(1+\delta_{xx})]X_2+[K_{xy}+i\omega C_{xy}-\alpha\delta_{xy}]y_2=\alpha[1+\delta_{xx}-i\delta_{xy}]$$

(27)

$$[K_{yx}+i\omega C_{yx}-\alpha\delta_{yx}]X_2+[K_{yy}+i\omega C_{yy}-\alpha(1+\delta_{yy})]y_2=-i\alpha[1+\delta_{yy}+i\delta_{yx}]$$

with the following abbreviations:

(28) $$\delta_{xx}=\frac{K_{xx}+i\omega C_{xx}}{k-\frac{M}{\rho}\left(\frac{\omega}{\omega_n}\right)^2+i\left(\frac{\omega}{\omega_n}\right)\omega_n d}$$

(29) $$\delta_{xy}=\frac{K_{xy}+i\omega C_{xy}}{k-\frac{M}{\rho}\left(\frac{\omega}{\omega_n}\right)^2+i\left(\frac{\omega}{\omega_n}\right)\omega_n d}$$

(30) $$\delta_{yx}=\frac{K_{yx}+i\omega C_{yx}}{k-\frac{M}{\rho}\left(\frac{\omega}{\omega_n}\right)^2+i\left(\frac{\omega}{\omega_n}\right)\omega_n d}$$

(31) $$\delta_{yy}=\frac{K_{yy}+i\omega C_{yy}}{k-\frac{M}{\rho}\left(\frac{\omega}{\omega_n}\right)^2+i\left(\frac{\omega}{\omega_n}\right)\omega_n d}$$

These equations may be solved for the journal amplitudes x_2 and y_2 from which the rotor amplitudes and the bearing amplitudes can be determined through Eqs. (10),(11),(25) and (26). The solution is obtained numerically by a computer.

Singularities

When the rotor speed ω is equal to one of the rigid support rotor critical speeds, i.e. $\frac{\omega}{\omega_n}=1$, α becomes infinite. If δ_{xx}, δ_{xy} etc., are finite Eq. (27) yields:

(32) $$X_2=-1$$

(33) $$y_2=i$$

$$\Big\}\ \alpha=\infty$$

The bearing housing amplitudes are found through Eq. (19):

(34) $$X_3=-1+\frac{1+\delta_{yy}+i\delta_{xy}}{(1+\delta_{xx})(1+\delta_{yy})-\delta_{xy}\delta_{yx}}$$

(35) $$y_3=i\left[1-\frac{1+\delta_{xx}-i\delta_{yx}}{(1+\delta_{xx})(1+\delta_{yy})-\delta_{xy}\delta_{yx}}\right]$$

$$\Big\}\ \frac{\alpha=\infty}{\left[k-\frac{M}{\rho}\left(\frac{\omega}{\omega_n}\right)^2\right]^2+(\omega_n d)^2\neq 0}$$

The rotor mass amplitudes are finally given through Eqs. (12) and (13):

$$\left.\begin{aligned} (36)\quad X_1 &= -1 + \varrho\left[(K_{xx}+i\omega C_{xx})(x_2-x_3)+(K_{xy}+i\omega C_{xy})(y_2-y_3)\right] \\ (37)\quad y_1 &= i + \varrho\left[(K_{yx}+i\omega C_{yx})(x_2-x_3)+(K_{yy}+i\omega C_{yy})(y_2-y_3)\right] \end{aligned}\right\} \quad \underline{\varkappa=\infty \qquad \left[k-\tfrac{\mu}{\varrho}\left(\tfrac{\omega}{\omega_n}\right)^2\right]^2+(\omega_n d)^2\neq 0}$$

If an addition to $\varkappa=\infty$, $\delta_{xx}, \delta_{xy}, \delta_{yx}$ etc are also infinite the above equations reduce to:

$$\left.\begin{aligned} (38)\quad & X_1 = X_2 = X_3 = -1 \\ (39)\quad & y_1 = y_2 = y_3 = i \end{aligned}\right\} \quad \underline{\varkappa=\infty \qquad k-\tfrac{\mu}{\varrho}\left(\tfrac{\omega}{\omega_n}\right)^2=0\ ,\ \omega_n d=0}$$

so that the amplitude is 180° out of phase with the unbalance while the center of gravity of the rotor does not move.

Eqs. (38) and (39) are actually also valid even if $\varkappa\neq\infty$ as long as $k-\tfrac{\mu}{\varrho}\left(\tfrac{\omega}{\omega_n}\right)^2=0$, $\omega_n d=0$.

Transmitted Force

The force transmitted to the bearing housing, denoted F_B, is given by:

$$F_{Bx} = \bar{K}_{xx}(\bar{x}_2-\bar{x}_3)+\bar{C}_{xx}(\dot{\bar{x}}_2-\dot{\bar{x}}_3)+\bar{K}_{xy}(\bar{y}_2-\bar{y}_3)+\bar{C}_{xy}(\dot{\bar{y}}_2-\dot{\bar{y}}_3)$$

and similarly for the y-direction. Making use of Eqs.(12), (13), (10) and (11) this equation reduces to:

$$(40)\quad \frac{C\xi}{Wd}F_{Bx} = \varkappa(1+x_2)$$

$$(41)\quad \frac{C\xi}{Wd}F_{By} = \varkappa(y_2-i)$$

The force transmitted to the foundation, denoted F, is given by:

$$F_x = K_p\,\bar{x}_3 + C_p\,\dot{\bar{x}}_3$$

$$F_y = K_p\,\bar{y}_3 + C_p\,\dot{\bar{y}}_3$$

which through Eqs. (25) and (26) becomes:

$$\frac{C\xi}{W\delta} F_x = \frac{\varkappa(x_2+1)}{1-\frac{\frac{\mu}{\rho}(\frac{\omega}{\omega_n})^2}{k+i(\frac{\omega}{\omega_n})\omega_n d}} \tag{42}$$

$$\frac{C\xi}{W\delta} F_y = \frac{\varkappa(y_2-i)}{1-\frac{\frac{\mu}{\rho}(\frac{\omega}{\omega_n})^2}{k+i(\frac{\omega}{\omega_n})\omega_n d}} \tag{43}$$

When $\varkappa = \infty$ the above equations become indeterminant. In that case use the equivalent equations.

$$\frac{C\xi}{W\delta} F_{Bx} = \frac{1}{\rho}(x_1 - x_2) \tag{44}$$

$$\frac{C\xi}{W\delta} F_{By} = \frac{1}{\rho}(y_1 - y_2) \tag{45}$$

$$\frac{C\xi}{W\delta} F_x = \left[k + i(\frac{\omega}{\omega_n})\omega_n d\right] x_3 \tag{46}$$

$$\frac{C\xi}{W\delta} F_y = \left[k + i(\frac{\omega}{\omega_n})\omega_n d\right] y_3 \tag{47}$$

Stability

Since the support flexibility and damping influences the rotor-bearing stability (oil whip) it is of interest to analyze this effect. To do this return to Eq. (27) and investigate the eigenvalues of the determinant of the homogenous equations. Introduce the symbols:

$$\gamma = \frac{\nu}{\omega} \tag{48}$$

$$s = \frac{\omega}{\omega_n} \tag{49}$$

where ν is the eigenfrequency. Hence, the determinant of Eq.(27) becomes:

$$\begin{vmatrix} [K_{xx} + i\gamma\omega C_{xx} - \varkappa(1+\delta_{xx})] & [K_{xy} + i\gamma\omega C_{xy} - \varkappa\delta_{xy}] \\ [K_{yx} + i\gamma\omega C_{yx} - \varkappa\delta_{yx}] & [K_{yy} + i\gamma\omega C_{yy} - \varkappa(1+\delta_{yy})] \end{vmatrix} = 0 \tag{50}$$

where:

$$\varkappa = \frac{1}{\rho}\,\frac{(s\gamma)^2}{1-(s\gamma)^2} \tag{51}$$

$$\sigma_{xx} = \frac{K_{xx} + i\gamma\omega C_{xx}}{k - \frac{\mu}{\rho}(s\gamma)^2 + i s\gamma\omega_n d} \tag{52}$$

$$\sigma_{xy} = \frac{K_{xy} + i\gamma\omega C_{xy}}{k - \frac{\mu}{\rho}(s\gamma)^2 + i s\gamma\omega_n d} \tag{53}$$

Look first at the case where the supports are rigid, i.e. $\sigma_{xx} = \sigma_{xy} = \cdots = 0$. Equate the real and imaginary parts of Eq. (50) to zero to get:

$$\varkappa = \frac{K_{xx}\omega C_{yy} + K_{yy}\omega C_{xx} - K_{xy}\omega C_{yx} - K_{yx}\omega C_{xy}}{\omega C_{xx} + \omega C_{yy}} \tag{54}$$

$$\gamma^2 = \frac{(K_{xx}-\varkappa)(K_{yy}-\varkappa) - K_{xy}K_{yx}}{\omega C_{xx}\omega C_{yy} - \omega C_{xy}\omega C_{yx}} \tag{55}$$

Substituting Eq. (54) into Eq.(55) allows for computing γ, i.e. the ratio between eigenfrequency and running speed. Substituting into Eq.(51) gives the value of S, i.e. the rotor speed at instability as a fraction of the natural frequency ω_n.

Next assume the supports to be flexible but without damping, i.e. $d = 0$. For abbreviation set:

$$A = k - \frac{\mu}{\rho}(s\gamma)^2 \tag{56}$$

and the solution becomes:

$$\frac{\varkappa}{1-\frac{\varkappa}{A}} = \frac{K_{xx}\omega C_{yy} + K_{yy}\omega C_{xx} - K_{xy}\omega C_{yx} - K_{yx}\omega C_{xy}}{\omega C_{xx} + \omega C_{yy}} \tag{57}$$

$$\gamma^2 = \frac{\left(K_{xx} - \frac{\varkappa}{1-\frac{\varkappa}{A}}\right)\left(K_{yy} - \frac{\varkappa}{1-\frac{\varkappa}{A}}\right) - K_{xy}K_{yx}}{\omega C_{xx}\omega C_{yy} - \omega C_{xy}\omega C_{yx}} \tag{58}$$

i.e. the eigenfrequency ratio γ is unchanged. To determine the rotor speed at instability, i.e. S, expand Eq. (57):

$$\frac{\mu}{\rho}\left[1+\rho\,\frac{\varkappa}{1-\frac{\varkappa}{A}}\right](s\gamma)^4 - \left[k\left(1+\rho\,\frac{\varkappa}{1-\frac{\varkappa}{A}}\right) + \frac{\varkappa}{1-\frac{\varkappa}{A}}\left(1+\rho\,\frac{\mu}{\rho}\right)\right](s\gamma)^2 + \rho k\,\frac{\varkappa}{1-\frac{\varkappa}{A}} = 0 \tag{59}$$

which is a quadratic equation in $(s\gamma)^2$. Hence, S can be obtained with γ known from Eq. (58).

It is seen that there are two solutions for the speed ratio S, both with the same frequency. One solution corresponds to the coincidence of the rotor critical speed (including the effect of the flexible support) with the eigenfrequency γ, the other solution stems from the instability of the pedestal mass. This was checked numerically as follows:

For rigid support $(k = \infty)$ we may use Eq. (54) and (55) to determine:

$$\gamma = \frac{\nu}{\omega_0} \qquad S = \frac{\omega_0}{\omega_n}$$

where ω_0 is the threshold speed for rigid support. Let $\omega_{c,0}$ denote the corresponding actual critical speed. Then, by hypothesis:

$$\omega_{c,0} = \nu \qquad \text{i.e} \qquad \frac{\omega_{c,0}}{\omega_n} = (S_0\gamma)$$

Introduce an equivalent bearing stiffness K_B such that:

$$\omega_{c,0}^2 = \frac{K_B}{M}$$

Hence,

$$\left(\frac{\omega_{c,0}}{\omega_n}\right)^2 = M\alpha\,\frac{K_B}{M} = \alpha K_B$$

or

$$\frac{CK_B}{W} = \frac{1}{\rho}(S_0\gamma)^2 \tag{60}$$

Now introduce the support stiffness to get an effective stiffness:

$$\frac{CK_e}{W} = \frac{\frac{CK_B}{W}\,\frac{CK_P}{W}}{\frac{CK_B}{W} + \frac{CK_P}{W}} \tag{61}$$

and the corresponding critical speed becomes:

$$\omega_c^2 = \frac{K_e}{M} = \nu^2$$

Therefore,

$$(S_1\gamma)^2 = \frac{\nu^2}{\omega_n^2} = \rho\,\frac{CK_e}{W}$$

or

$$S_1 = \frac{1}{\gamma}\sqrt{\rho\,\frac{CK_e}{W}} \tag{62}$$

which is the first solution. To evaluate the second solution, equate the support mass resonance to the eigenfrequency:

$$\frac{K_P + K_B}{m} = \nu^2$$

or:

$$\left(\frac{\nu}{\omega_n}\right)^2 = (s_2\gamma)^2 = \rho\,\frac{\frac{CK_P}{W} + \frac{CK_B}{W}}{\frac{m}{M}}$$

Thus:

$$s_2 = \frac{1}{\gamma}\sqrt{\rho\,\frac{\frac{CK_P}{W} + \frac{CK_B}{W}}{\frac{m}{M}}} \tag{63}$$

which is the second solution. It should be noted that both Eqs. (62) and (63) are approximate. Their validity has been checked numerically for selected cases and the difference was found to be less than 1 per cent. Finally when the support includes damping set:

$$A = k - \frac{M}{\rho}(s\gamma)^2 \qquad B = (s\gamma)\omega_n d \tag{64}$$

Eq. (27) becomes:

$$\begin{vmatrix} \left[K_{xx} + i\gamma\omega C_{xx} - \frac{\alpha}{1-\frac{\alpha}{A+iB}}\right] & \left[K_{xy} + i\gamma\omega C_{xy}\right] \\ \left[K_{yx} + i\gamma\omega C_{yx}\right] & \left[K_{yy} + i\omega C_{yy} - \frac{\alpha}{1-\frac{\alpha}{A+iB}}\right] \end{vmatrix} = 0 \tag{65}$$

For convenience introduce:

$$E - iF = \frac{\alpha}{1-\frac{\alpha}{A+iB}} \tag{66}$$

Expand the determinant of Eq. (65) in its real and imaginary parts:

$$(K_{xx}-E)(K_{yy}-E) - \gamma^2(\omega C_{xx}+F)(\omega C_{yy}+F) - K_{xy}K_{yx} + \gamma^2\omega C_{xy}\,\omega C_{yx} = 0 \tag{67}$$

$$(K_{xx}-E)(\omega C_{yy}+F) + (K_{yy}-E)(\omega C_{xx}+F) - K_{xy}\,\omega C_{yx} - K_{yx}\,\omega C_{xy} = 0 \tag{68}$$

Solve Eq. (68):

$$E = \frac{K_{xx}(\omega C_{yy}+F) + K_{yy}(\omega C_{xx}+F) - K_{xy}\,\omega C_{yx} - K_{yx}\,\omega C_{xy}}{(\omega C_{xx}+F) + (\omega C_{yy}+F)} \tag{69}$$

Set:

(70) $a = K_{xx} - K_{yy}$

(71) $b = \omega C_{xx} + \omega C_{yy}$

(72) $G = K_{xy}\,\omega C_{yx} + K_{yx}\,\omega C_{xy}$

(73) $X = F + \frac{1}{2}(\omega C_{xx} + \omega C_{yy})$

Substitute Eq. (69) to (73) into Eq. (67):

(74) $$\gamma^2 X^4 + \left[\frac{a^2-\gamma^2 b^2}{4} + \gamma^2(\omega C_{xx}\,\omega C_{yy} - \omega C_{xy}\,\omega C_{yx}) + K_{xy}K_{yx}\right]X^2 - \frac{1}{4}\left[G + \frac{a}{2}(\omega C_{xx} - \omega C_{yy})\right]^2 = 0$$

This equation has always two roots, a positive and a negative one. Of these only the positive one can be used as shown later in Eq. (79).

Thus Eq. (74) and, therefore, Eq. (69) can be solved for F and E as functions of the frequency ratio γ . They may be considered as frequency dependent eigenvalues such that E represents "eigen stiffness" and F "eigen damping". When F is positive the "eigen damping" becomes negative according to Eq. (66). Having determined E and F it remains to find the corresponding $\mathcal{X}$-value from Eq. (66). However, it should first be noted that the two actual unknown are γ and $s = \frac{\omega}{\omega_n}$. Since the calculation is performed for a given Sommerfeld Number S the speed ω is known and the variable is therefore ω_n, i.e. the rotor mass M . For this reason it is convenient to redefine the pedestal mass and damping as:

(75) $$\sigma = \frac{\mu}{\rho} s^2 = \frac{mC\omega^2}{W} = 2\pi^2 S^2 \left(\frac{mW}{\mu^2 L^2 D (\frac{R}{C})^5}\right)$$

(76) $$\beta = s\omega_n d = \frac{C\omega C_p}{W} = \pi S \left(\frac{C_p}{\mu L (\frac{R}{C})^3}\right)$$

Hence, Eq. (66) may be written:

(77) $$E - i\gamma F = \frac{\mathcal{X}}{1 - \frac{\mathcal{X}}{k - \sigma\gamma^2 + i\gamma\beta}}$$

Solve Eq. (77):

(78) $$E = \mathcal{X}\left[1 + \mathcal{X}\,\frac{k - \sigma\gamma^2 - \mathcal{X}}{[k - \sigma\gamma^2 - \mathcal{X}]^2 + (\gamma\beta)^2}\right]$$

$$F = \varkappa^2 \frac{\beta}{[k-\delta\gamma^2-\varkappa]^2+(\gamma\beta)^2} \tag{79}$$

Combine the two equations:

$$\varkappa = \frac{E\beta - F(k-\delta\gamma^2)}{\beta - F} \tag{80}$$

Thus, for a range of frequency ratios γ with corresponding E and F-values $\varkappa$ can be calculated from Eq.(80). Substituting into the right hand side of Eq. (79) and subtracting from F gives a difference, designated the error. Only when the error vanishes has a solution been obtained, i.e. for a correct frequency ratio.

When the denominator of Eq. (80) has a singularity a false solution occurs except in the rare case when the numerator is simultaneously zero. For this purpose it is convenient to have a check on Eq. (80) by solving Eq. (78):

$$[E+(k-\delta\gamma^2)]\varkappa^2 - [(k-\delta\gamma^2)^2+(\gamma\beta)^2+2E(k-\delta\gamma^2)]\varkappa + E[(k-\delta\gamma^2)^2+(\gamma\beta)^2] = 0 \tag{81}$$

or

$$\varkappa = \frac{1}{2[E+(k-\delta\gamma^2)]}\left[(k-\delta\gamma^2)^2+(\gamma\beta)^2+2E(k-\delta\gamma^2) \pm \sqrt{[(k-\delta\gamma^2)^2+(\gamma\beta)^2]^2-4E^2(\gamma\beta)^2}\right] \tag{82}$$

Hence, there is no root when:

$$E-\sqrt{E^2-(k-\delta\gamma^2)^2} < (\gamma\beta) < E+\sqrt{E^2-(k-\delta\gamma^2)^2} \tag{83}$$

Within the frequency ratio range from 0 to γ_{rigid} (Eq. (55)) there may be up to three roots for $(\varkappa,\gamma)$

CONCLUSIONS

1. A flexible bearing support provides an ideal method for attenuating the force transmitted by an unbalanced rotor. It introduces a minimum of extraneous resonances (namely one, the resonance of the bearing housing) and in theory the attenuation can be as high as desired by a suitable selection of the support stiffness.

2. The damping in the bearing support should be small in order not to lose the force attenuation.

3. The rotor amplitude at resonance is relatively high but since it occurs at low rotor speeds it may not be too important. Otherwise the support may be locked in passing through the resonant speeds.

4. Although the speed at onset of oil whip is lowered by the flexible support, there will always, in practice, be enough damping in the support to restore the stability.

RECOMMENDATIONS

1. The purpose of a flexible bearing support is to achieve a desired attenuation of the transmitted force. However, the use of such a support raises questions with regards to the response of the rotor during onboard-ship operation (ship motion, shock etc). An investigation should be undertaken of this problem with special emphasis on the actual design of the flexible support. Important factors in the study should be reliability, low maintenance and simplicity.

2. Although the unbalance is the principal source of noise in a piece of rotating machinery, vibrations of other frequencies are also present and may be important (subharmonic rotor vibrations, electric field forces, etc.). A study of these vibrations should be performed both analytically and experimentally.

REFERENCES

1. Lund, J.W. and Sternlicht, B., "Bearing Attenuation," Bureau of Ships Report, Contract No. Nobs 78930, April 28, 1961.

2. Lund, J.W. and Sternlicht, B., "Rotor-Bearing Dynamics with Emphasis on Attenuation," Trans. ASME, Vol. 84, series D. No.4, Journal of Basic Engineering, Dec. 1962.

3. Warner, P.C., and Thoman, R.J., "The Effect of the 150-Degree Partial Bearing on Rotor-Unbalance Vibration," ASME Paper No. 63-LubS-6, presented in Boston, June, 1963.

4. Warner, P.C., "Static and Dynamic Properties of Partial Journal Bearings," Trans. ASME, Vol: 85, series D. No. 2, Journal of Basic Engineering, June 1963.

5. Lund, J.W."Spring and Damping Coefficients for the Tilting-Pad Journal Bearing," Bureau of Ships Report, Contract No. Nobs-86914, March 1964.

APPENDIX

Computer Programs

The analysis has been programmed for the IBM 1620 digital computer. Two programs are written: PN 0125 where the bearing pedestals are assumed rigid, and PN 0132 where the pedestal flexibility is included. Separate descriptions of the programs are provided below.

PN 0125: Transmitted Force and Response of a Two-Mass Rotor in Rigid Pedestals

This program calculates the dimensionless transmitted force and the rotor amplitude for a symmetrical two mass rotor with a given unbalance. The rotor is supported in two bearings, each bearing represented by 4 spring and 4 damping coefficients. The pedestals are assumed rigid.

The transmitted force, the journal amplitude and the rotor mass amplitude are functions of the rotor speed ω expressed in dimensionless form by (ω/ω_n) where ω_n is the critical speed of the rigidly supported rotor. However, for the transmitted force and the journal amplitude a simplification is possible by use of another variable:

(a) $$\varkappa = \frac{1}{\varrho} \cdot \frac{\left(\frac{\omega}{\omega_n}\right)^2}{1-\left(\frac{\omega}{\omega_n}\right)^2}$$

where

(b) $$\varrho = \frac{W\alpha}{C\xi^2}$$ (rotor flexibility parameter)

- W - bearing reaction, lbs.
- C - radial clearance, inch
- α - influence coefficient for rotor, $\frac{in}{lbs}$ (see Eq.(4))
- ξ - distance between rotor mass, divided by rotor span (see Eq. (5))
- $\omega_n = \sqrt{1/M\alpha}$ critical speed of rotor on rigid supports, rad/sec.
- M - rotor mass per bearing, lbs-sec^2/in.

Since α is inconvenient to use directly an equivalent speed ratio may be defined by:

(c) $$\alpha = 10 \frac{\left(\frac{\omega}{\omega_n}\right)_o}{1 - \left(\frac{\omega}{\omega_n}\right)_o^2}$$

By this choice of non-dimensional parameters, a single plot of journal deflection and transmitted force against equivalent speed ratio will represent a full range of rotor flexibilities. Since the rotor deflection requires the designation of a particular flexibility, the actual speed ratio is computed in this case. However, for large values of rotor flexibility, a large range of equivalent speed ratio corresponds to only a small change in actual speed ratio. Therefore, in this case it becomes advisable to enter the actual speed ratio and so this provision is made.

The program also performs a stability analysis, providing, for a given rotor and bearing configuration, the ratio of eigenfrequency to rotor speed at the onset of instability and the corresponding rotor speed.

The output is provided in a form that makes it adaptable for automatic plotting on an X-Y plotter. Since it is anticipated that the output would be represented on logarithmic scales, the logarithm of the response values along with a code for automatic sorting is provided.

Computer Input

Card 1 - 49 columns Hollerith - descriptive text

Card 2 - (5I4, E12.4) - control parameters

Word 1 - type of computation; if this value is:

1. the input speed ratios are intended to be equivalent speed ratios
2. the input speed ratios are intended to be actual speed ratios

Word 2 - number of speed ratios, maximum 18

Word 3 - number of rotor flexibility parameters , maximum 10

Word 4 - intermediate output; if this value is 0 - no intermediate output is provided; $\neq$ 0 - intermediate output (diagnostic) is provided.

Word 5 - additional data; if this value is 0 - there is no additional data; ≠ 0 - additional input data follows the case being computed.

Word 6 - the value of eccentricity ratio corresponding to the input bearing parameters.

Card 3 - (6E12.4) - dimensionless bearing spring and damping coefficients in the order $\frac{CK_{xx}}{W}, \frac{CK_{xy}}{W}, \frac{CK_{yx}}{W}, \frac{CK_{yy}}{W}, \frac{C\omega C_{xx}}{W}, \frac{C\omega C_{xy}}{W}$

Card 4 - (6E12.4) - the remaining bearing parameters $\frac{C\omega C_{yx}}{W}$ $\frac{C\omega C_{yy}}{W}$

Card 5 - (5E6.0) - the values of the rotor flexibility parameter ϱ, Eq.(b)

Card - (6E12.) - the speed ratios

Computer output

The initial output is in the order:

- program heading
- Hollerith text provided as input
- input control parameter values
- input bearing parameters

Then for the type 1 computation the first output values with appropriate headings are, by row

- first row - the initial equivalent speed ratio
  - the maximum dimensionless journal deflection $\frac{\xi \bar{x}_2}{\delta}$
  - the value of the dimensionless parameter $\varkappa$, eq.(a)
  - a column of signs ($\pm$ 1) corresponding to the sign of the log of the speed ratio and provided for the automatic plotting facility.
  - the log of the speed ratio
  - the sign of the log of the response value
  - the log of the response value
  - a code value for automatic sorting

- second row - the same as the first row, but with the speed ratio the actual speed ratio, the deflection the maximum rotor mass deflection, and the third value the value of rotor flexibility used in the computation.
- third row - the third row is the same as the second row but for a second value of rotor flexibility, if more than one is provided. Then the additional rows correspond to any additional flexibility values.
- last row - the last row is similar to the above, with the speed ratio the equivalent speed ratio and the response value the dimensionless transmitted force $\frac{FCF}{W\delta}$ (maximum value).

From Equation (a) it can be seen that

$$\left(\frac{\omega}{\omega_n}\right)^2 = \frac{\varkappa\varrho}{1+\varkappa\varrho}$$

and so there is no real solution to $\frac{\omega}{\omega_n}$ for values of $\varkappa\varrho$ between 0 and -1. For those cases the program prints the message "no solution for kappa · rho between 0 and -1 for rho = . ." Then the program proceeds to the next value of ϱ.

The last output is the results of the stability analysis. It consists of three values:

first value - the flexibility parameter, ϱ
second value - the speed ratio of the threshold of instability, $\frac{\omega}{\omega_n}$
third value - the square of the ratio of eigenfrequency to running speed at the threshold of instability, $\frac{\chi}{\omega}$

The output for the type 2 computation is much like that of the type 1 with the exception that, since the equivalent speed ratio is a function of both the actual speed ratio and the flexibility parameter, each time a new ϱ-value is specified for a given actual speed ratio, the equivalent ratio changes and requires a new journal deflection and transmitted force computation. Therefore, the order of output is: journal deflection, rotor deflection, transmitted force, then index ϱ and again, journal deflection, rotor deflection, transmitted force, etc.

PN 0132: Transmitted Force and Response of a Two-Mass Rotor in Flexible Pedestal

This program calculates the dimensionless journal deflection and transmitted force of a symmetrical rotor supported by two similar bearings with flexible pedestals as a function of the speed ratio, $\frac{\omega}{\omega_n}$, where ω_n is the flexural critical speed of the rotor simply-supported.

The program also performs a stability analysis, providing, for a given rotor and bearing configuration, the ratio of eigenfrequency to rotor speed at the onset of instability and the corresponding rotor speed.

The output is provided in a form that makes it adaptable for automatic plotting on an X-Y plotter. Since it is anticipated that the output would be represented on logarithmic scales, the logarithm of the response along with a code for automatic sorting is provided.

Computer Input

Card 1.- 49 columns Hollerith - descriptive text

Card 2.- (6I4, E12.4) - control parameters

- Word 1 - type of computation; if this value is:
  - 2 - the program performs the rotor response computation only
  - 3 - the program performs the stability analysis only
  - 4 - the program performs both analyses
- Word 2 - the number of speed ratios, maximum 18
- Word 3 - the number of non-dimensional pedestal to rotor mass ratios, μ, where $\mu = \frac{m}{\xi^2 M}$, maximum 10.
- Word 4 - the number of rotor flexibility parameters ϱ , maximum 10
- Word 5 - intermediate output; if this value is 0 - no intermediate output is provided; $\neq 0$ - intermediate output (diagnostic) is provided.
- Word 6 - additional data, if this value is 0 - there is no additional input data; $\neq 0$ - additional input data follows the case being computed.
- Word 7 - the value of eccentricity ratio corresponding to the input bearing parameters.

Card 3. - (6E12.4) - Dimensionless bearing spring and damping coefficients in the order $\frac{CK_{xx}}{W}, \frac{CK_{xy}}{W}, \frac{CK_{yx}}{W}, \frac{CK_{yy}}{W}, \frac{C\omega C_{xx}}{W}, \frac{C\omega C_{xy}}{W}$

Card 4. - (6E12.4) - the remaining bearing coefficients, and the pedestal parameters; in the order $\frac{C\omega C_{yx}}{W}, \frac{C\omega C_{yy}}{W}, \frac{CK_e}{W}, \frac{C\omega C_e}{W}$ where the parameters are dimensionless as defined in the analysis.

Card 5. - (5E6.0) - the values of the mass ratio $\mu = \frac{m}{\rho^2 M}$

Card - (5E6.0) - the values of the rotor flexibility parameter ρ

For a type 3 computation, the above is all the necessary input; otherwise the following must be provided.

Card - (6E12.4) - the speed ratios $\left(\frac{\omega}{\omega_n}\right)$

Computer output

The initial output is in the order:

- program heading
- Hollerith text provided as input
- input control parameter values
- input bearing and pedestal parameters

Then for the type 2 computation the next output with appropriate heading is the value of mass ratio and rotor flexibility, followed by the system response, in the order

- first row - the initial speed ratio
  - the dimensionless journal deflection $\frac{\xi \bar{x}_2}{\delta}$ (max.value)
  - the value of the dimensionless parameter $\varkappa$ where

$$\varkappa = \frac{1}{\rho} \frac{\left(\frac{\omega}{\omega_n}\right)^2}{1 - \left(\frac{\omega}{\omega_n}\right)^2}$$

  - a column of signs ($\pm$ 1) corresponding to the sign of the log of the speed ratio and provided for the automatic plotting facility
  - the log of the speed ratio
  - the sign of the log of the response value
  - the log of the response value
  - a coding value for automatic sorting

- second row - the same as the first row, but with the response value now the dimensionless rotor deflection $\frac{\bar{X}_i}{\delta}$ and the third value the equivalent speed ratio.
- third row - the same as the first two rows but for the dimensionless pedestal deflection $\frac{\xi \bar{X}_3}{\delta}$ (max value).
- fourth row- the same as the above rows but for the dimensionless transmitted force $\frac{\Sigma CF}{W\delta}$ (max. values).

Then the next speed ratio is indexed and the above four values generated. When the response for all of the speed ratios are computed, a new rotor flexibility value is indexed and the above sequence repeated. When all of the flexibility values are computed a new mass ratio is indexed and the above process repeated.

For the type 3 computation a heading indicating the stability analysis follows the input. Then four columns of output as follows:

column 1 - the value of the mass ratio

column 2 - the value of rotor flexibility factor

column 3 - the ratio of running speed to rotor flexural critical speed at the threshold of instability

column 4 - the square of the ratio of eigenfrequency to running speed at the onset of instability

For the case where there are two real solutions for the running speed ratio, they are both given.

For the type 4 computation the output after the listing of the input values is the type 2 output followed by the type 3 output.

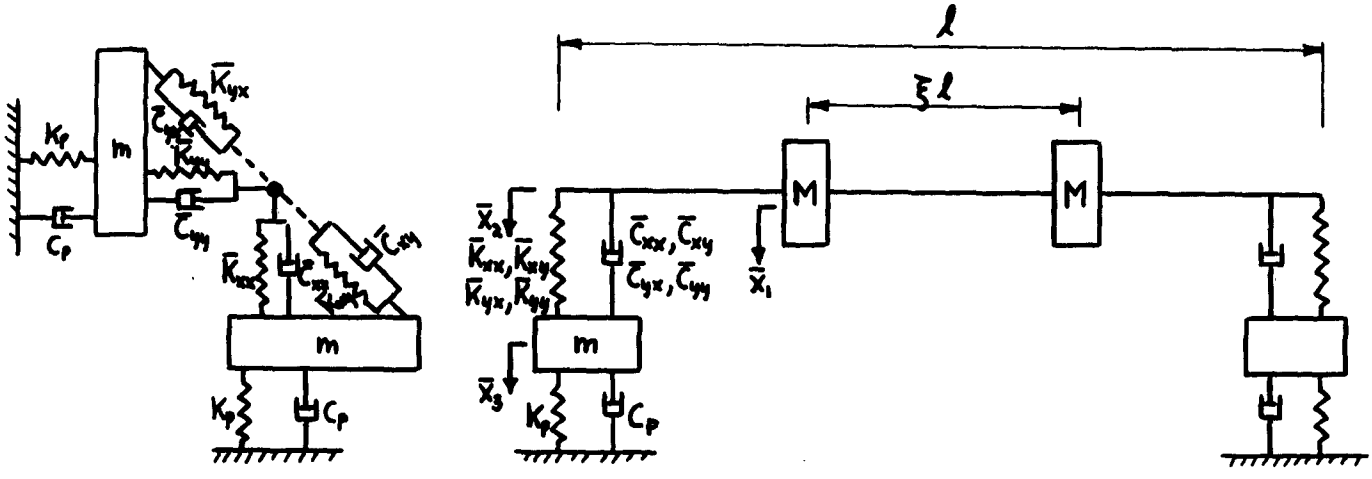

Fig. 1 Rotor-Bearing-Support System

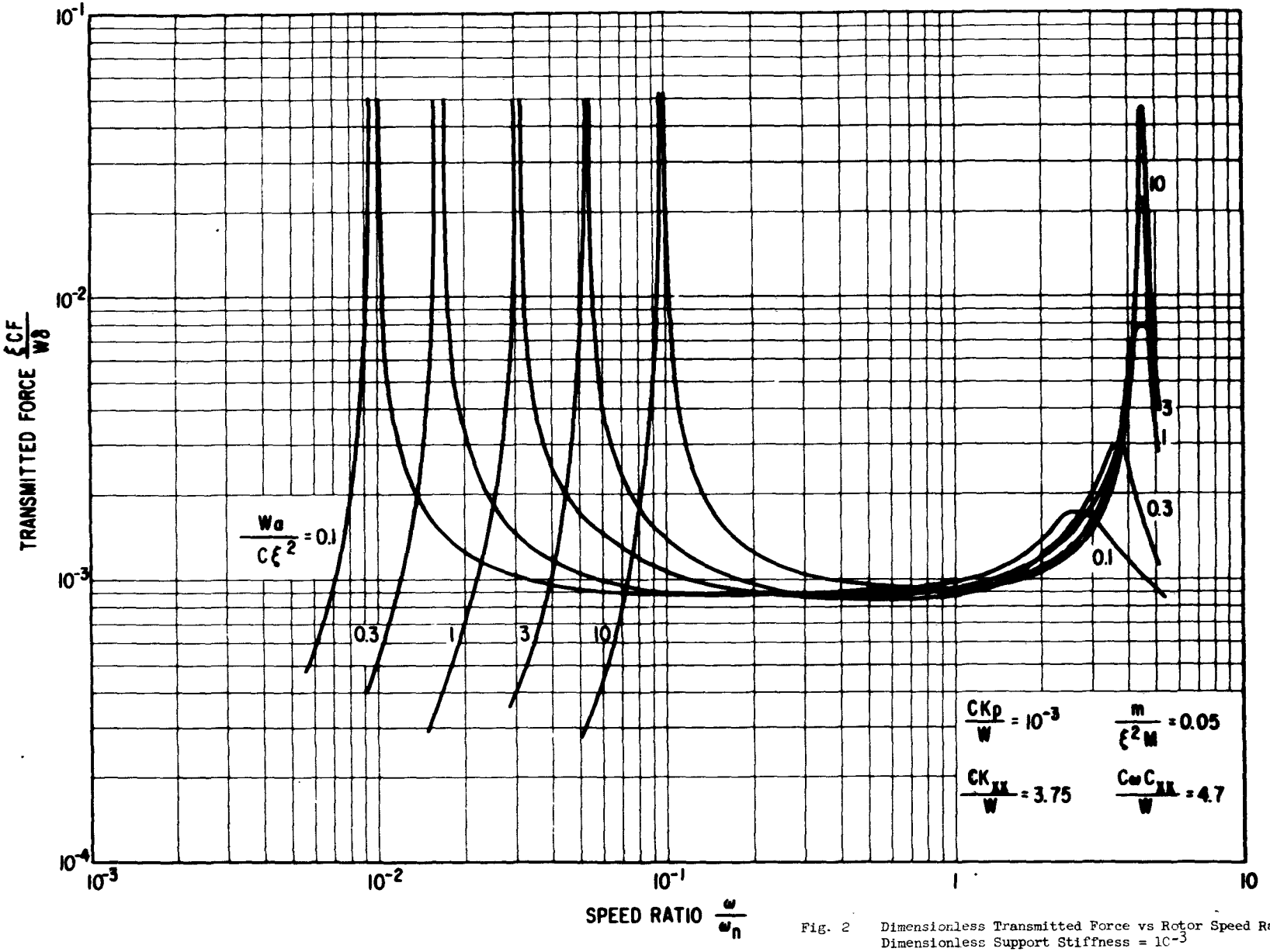

Fig. 2 Dimensionless Transmitted Force vs Rotor Speed Ratio
Dimensionless Support Stiffness = 10^{-3}
Dimensionless Bearing Mass = 0.05

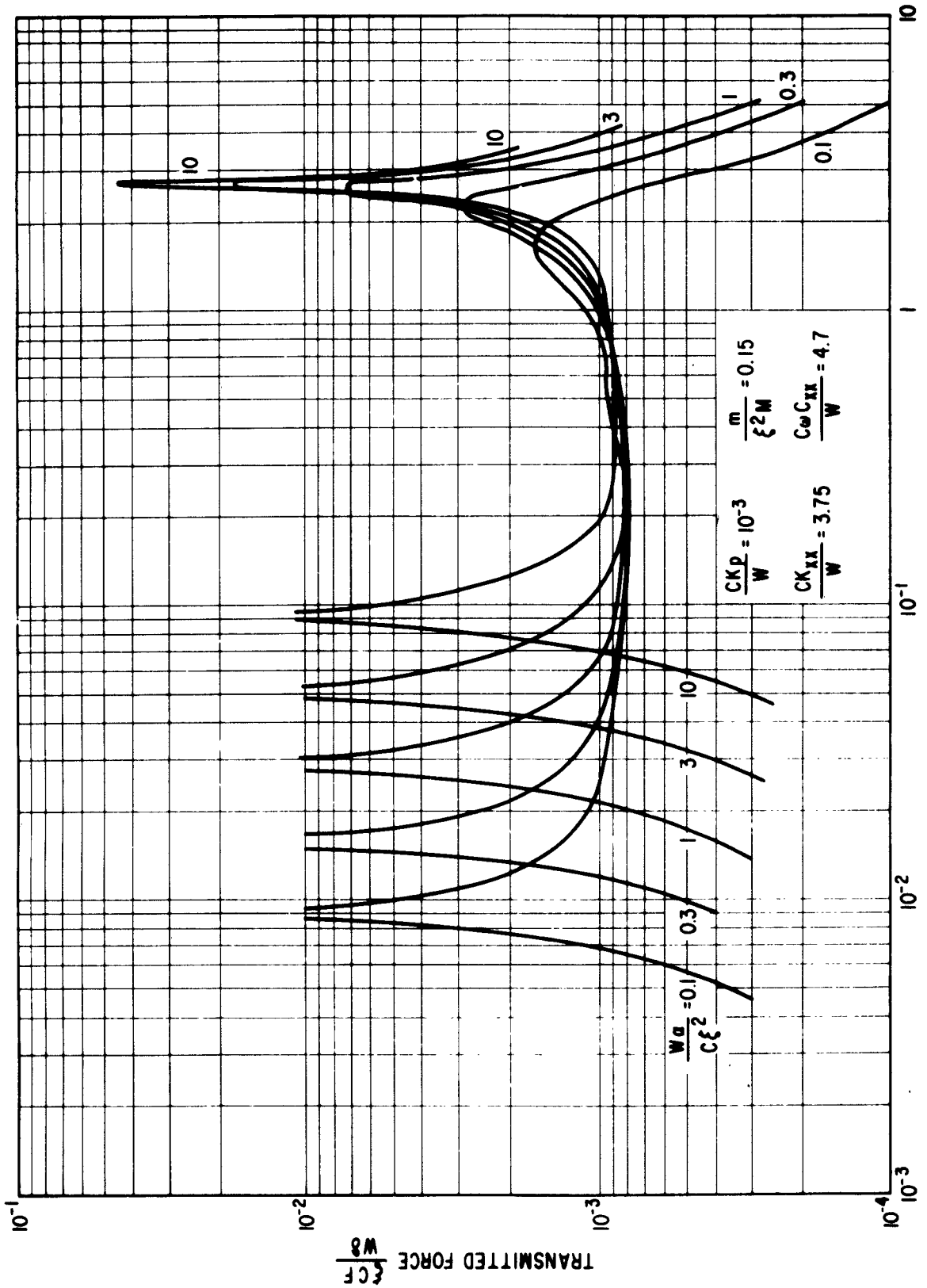

Fig. 3 Dimensionless Transmitted Force vs Rotor Speed Ratio
Dimensionless Support Stiffness = 10^{-3}
Dimensionless Bearing Mass = 0.15

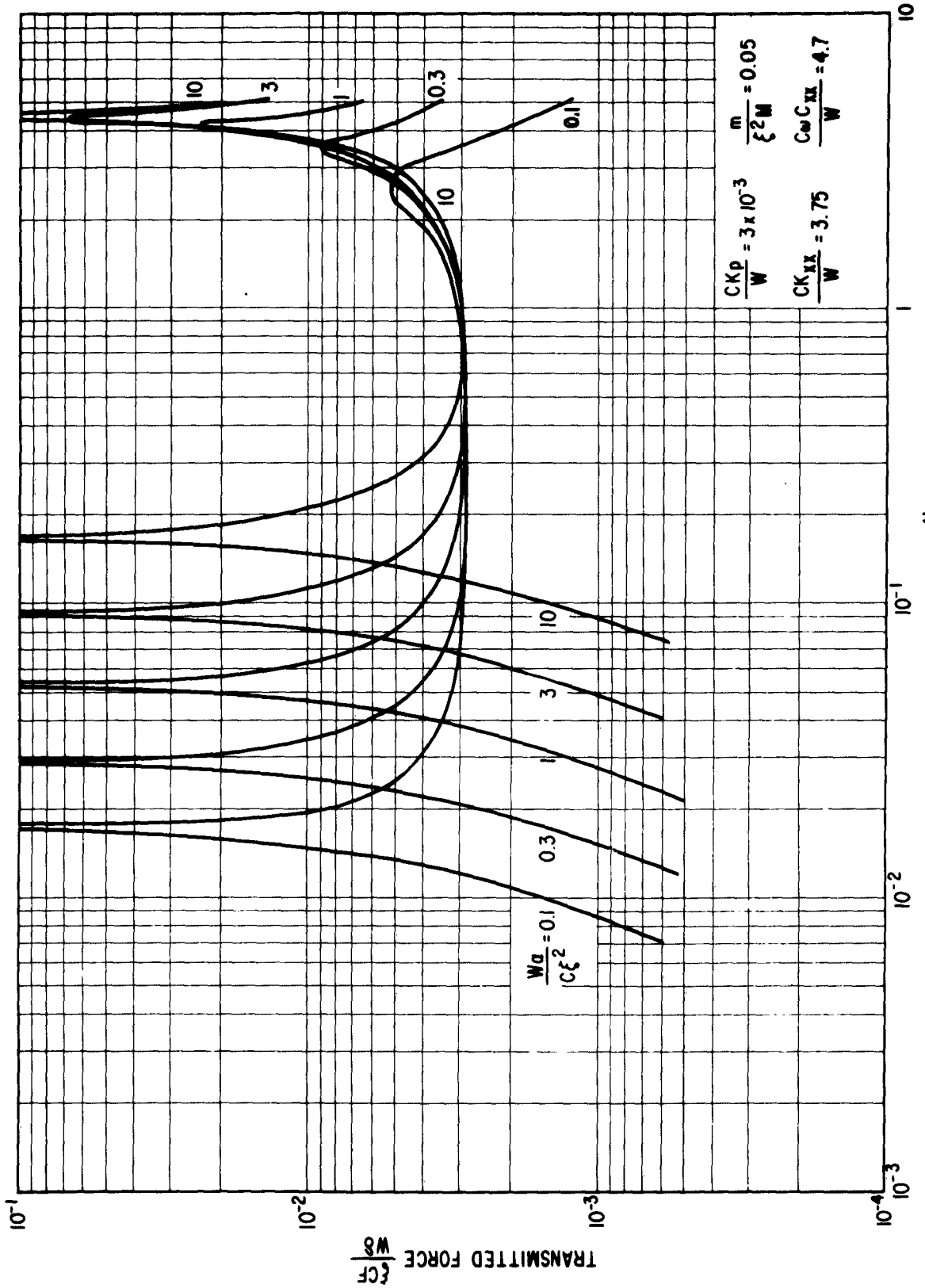

Fig. 4 Dimensionless Transmitted Force vs Rotor Speed Ratio
Dimensionless Support Stiffness = $3 \cdot 10^{-3}$
Dimensionless Bearing Mass = 0.05

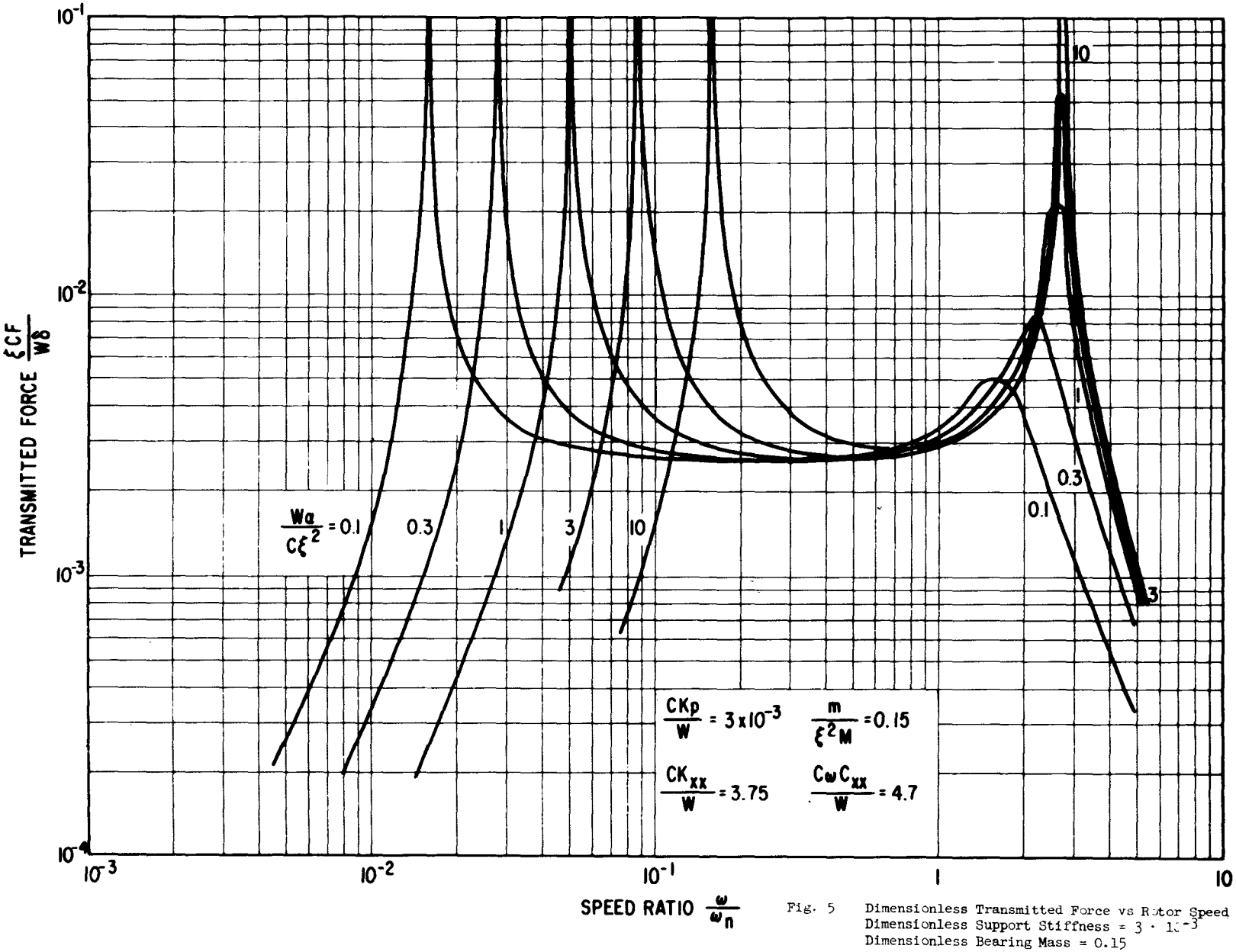

Fig. 5 Dimensionless Transmitted Force vs Rotor Speed Ratio
Dimensionless Support Stiffness = $3 \cdot 10^{-3}$
Dimensionless Bearing Mass = 0.15

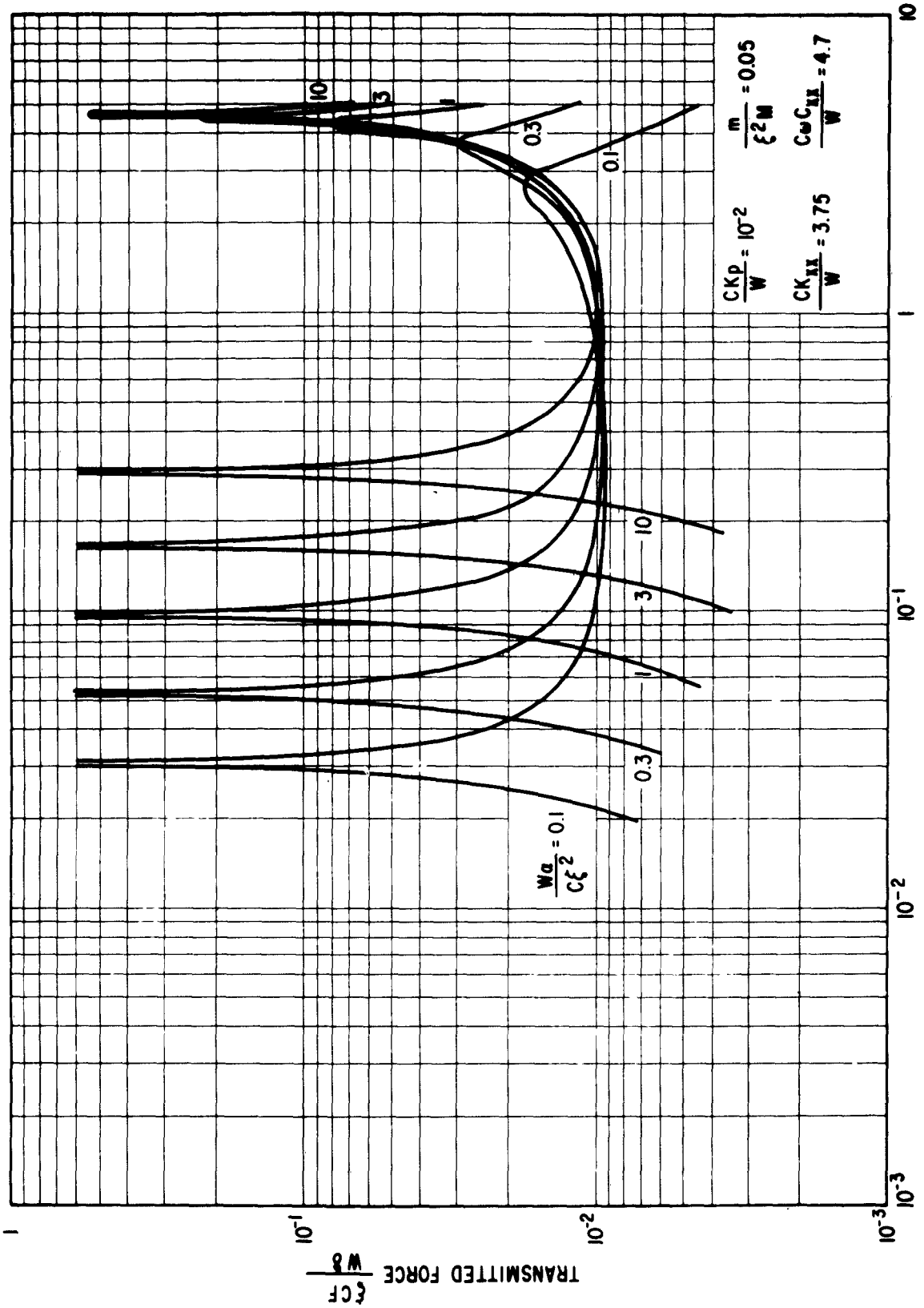

Fig. 6 Dimensionless Transmitted Force vs Rotor Speed Ratio
Dimensionless Support Stiffness = 10^{-2}
Dimensionless Bearing Mass = 0.05

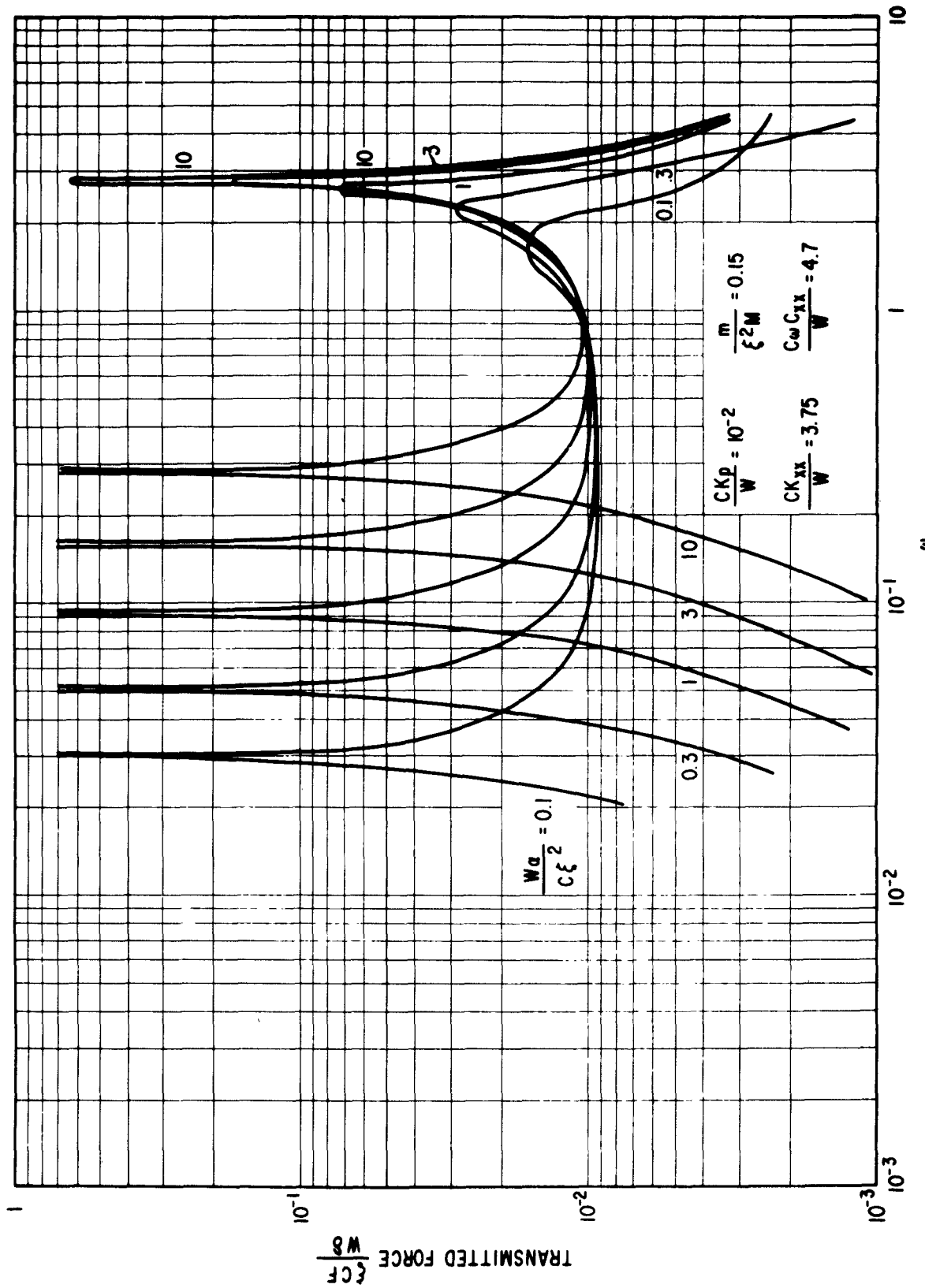

Fig. 7 Dimensionless Transmitted Force vs Rotor Speed Ratio
Dimensionless Support Stiffness = 10^{-2}
Dimensionless Bearing Mass = 0.15

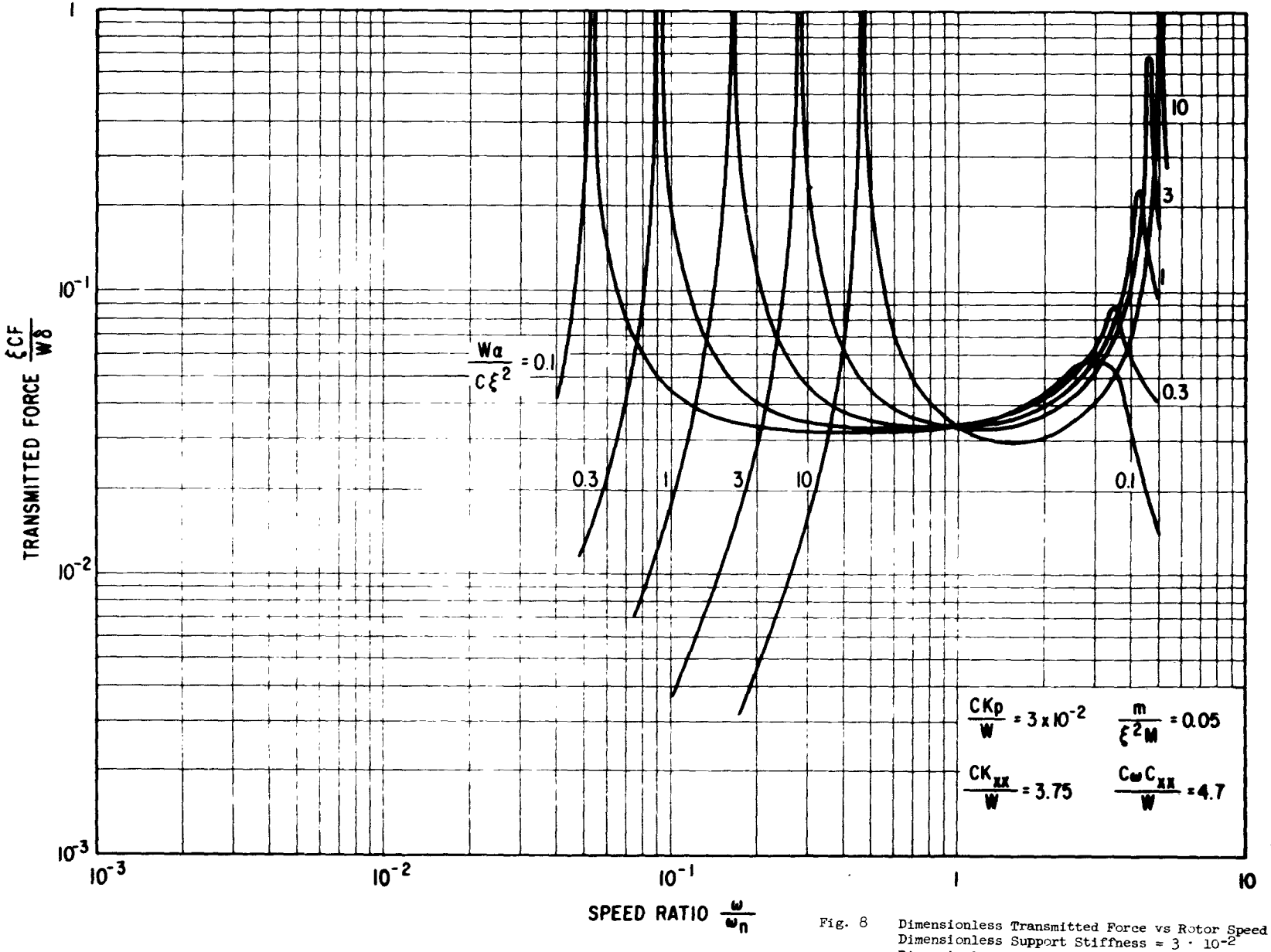

Fig. 8 Dimensionless Transmitted Force vs Rotor Speed Ratio
Dimensionless Support Stiffness = $3 \cdot 10^{-2}$
Dimensionless Bearing Mass = 0.05

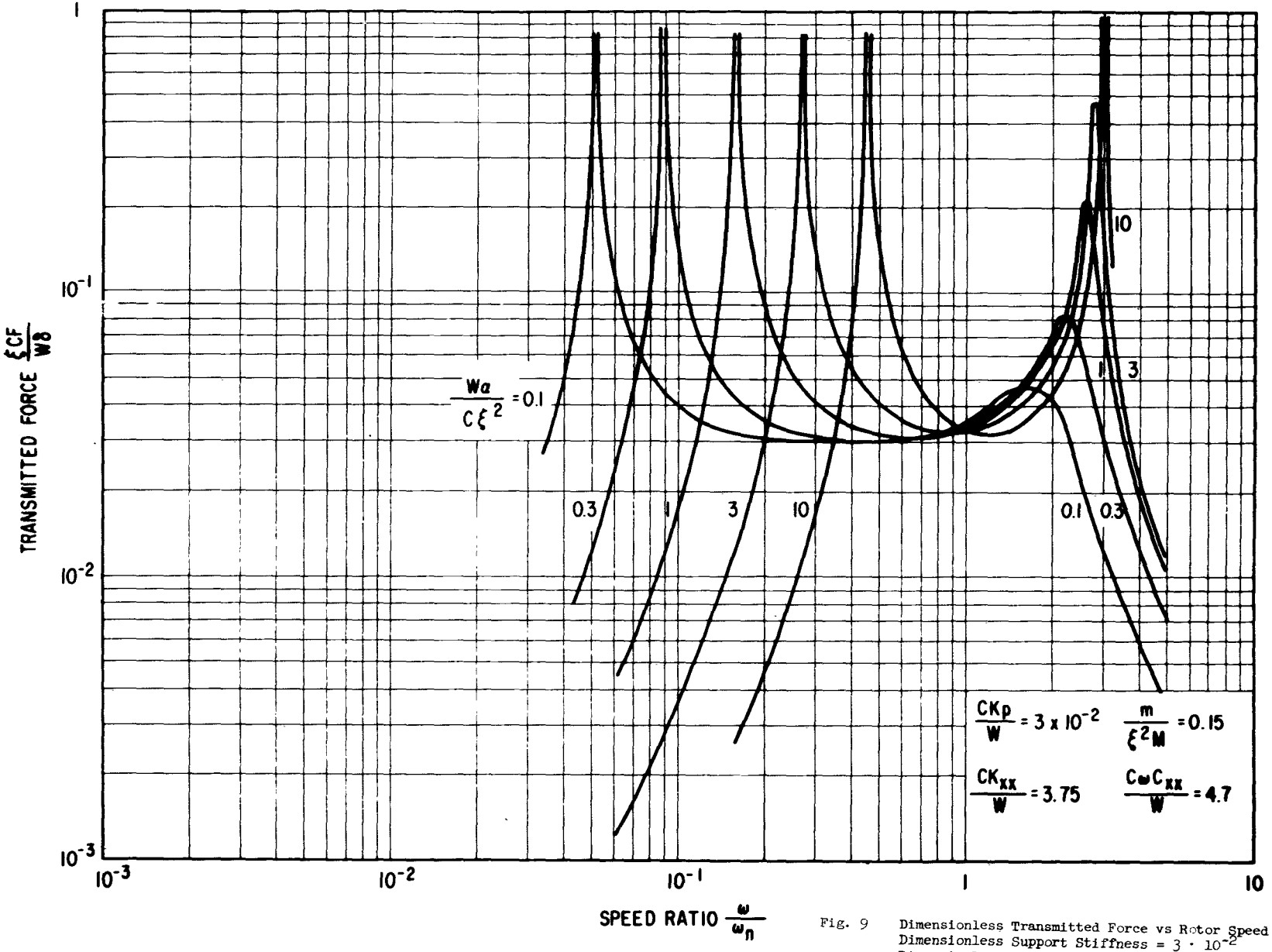

Fig. 9 Dimensionless Transmitted Force vs Rotor Speed Ratio
Dimensionless Support Stiffness = $3 \cdot 10^{-2}$
Dimensionless Bearing Mass = 0.15

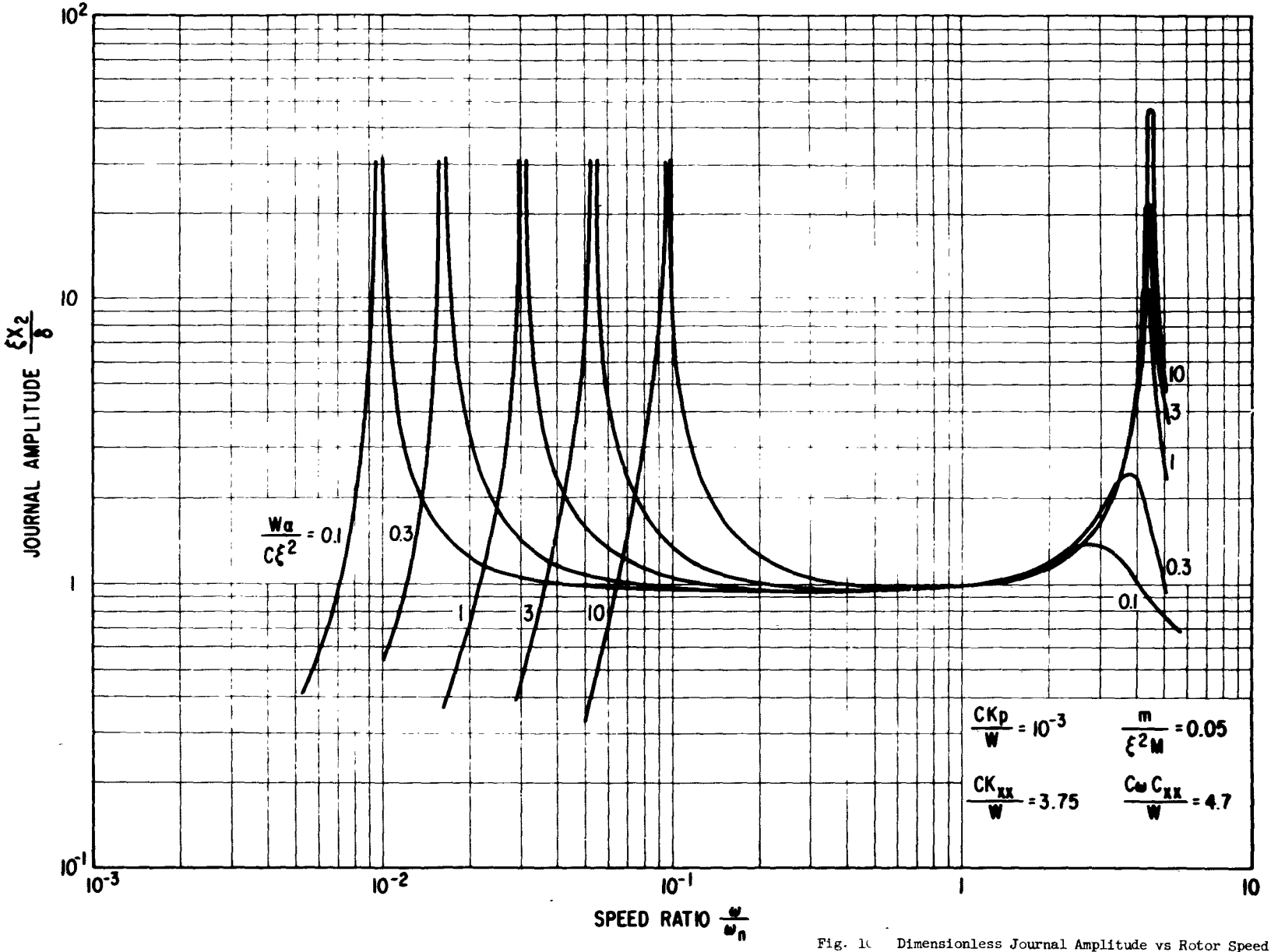

Fig. 1(Dimensionless Journal Amplitude vs Rotor Speed Ratio
Dimensionless Support Stiffness = 10^{-3}
Dimensionless Bearing Mass = 0.05

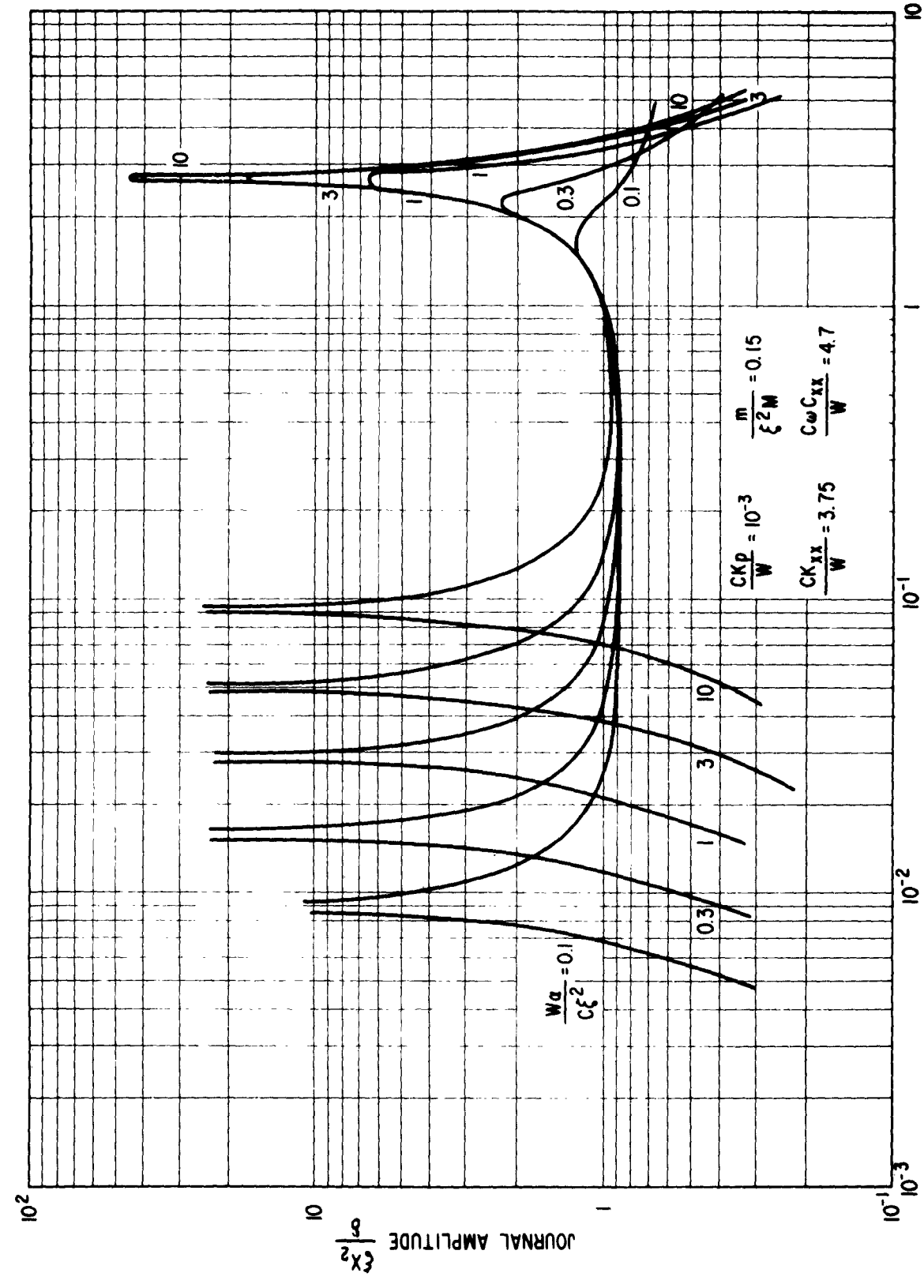

Fig. 11 Dimensionless Journal Amplitude vs Rotor Speed Ratio
Dimensionless Support Stiffness = 10^{-3}
Dimensionless Bearing Mass = 0.15

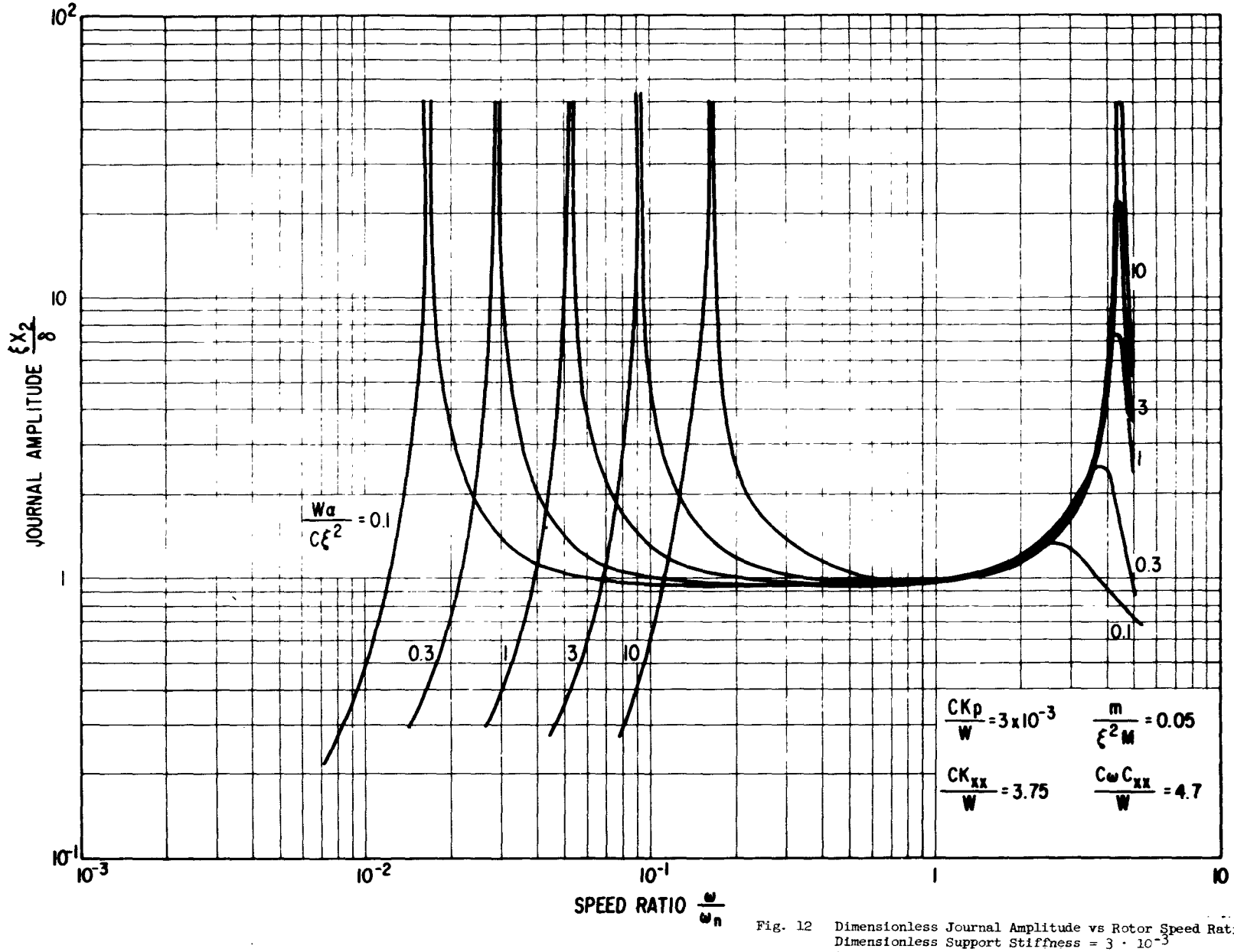

Fig. 12 Dimensionless Journal Amplitude vs Rotor Speed Ratio
Dimensionless Support Stiffness = $3 \cdot 10^{-3}$
Dimensionless Bearing Mass = 0.05

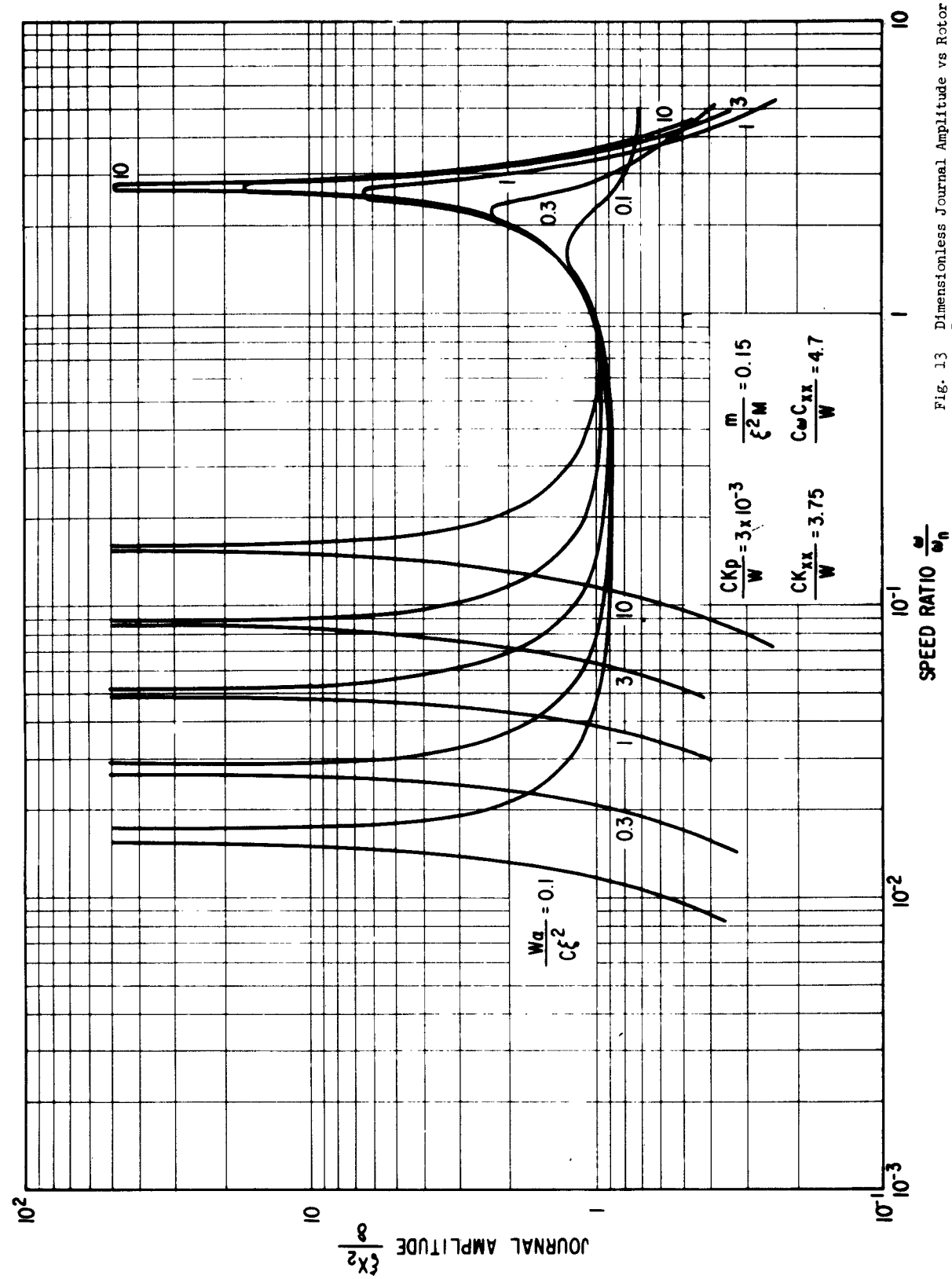

Fig. 13 Dimensionless Journal Amplitude vs Rotor Speed Ratio
Dimensionless Support Stiffness = $3 \cdot 10^{-3}$
Dimensionless Bearing Mass = 0.15

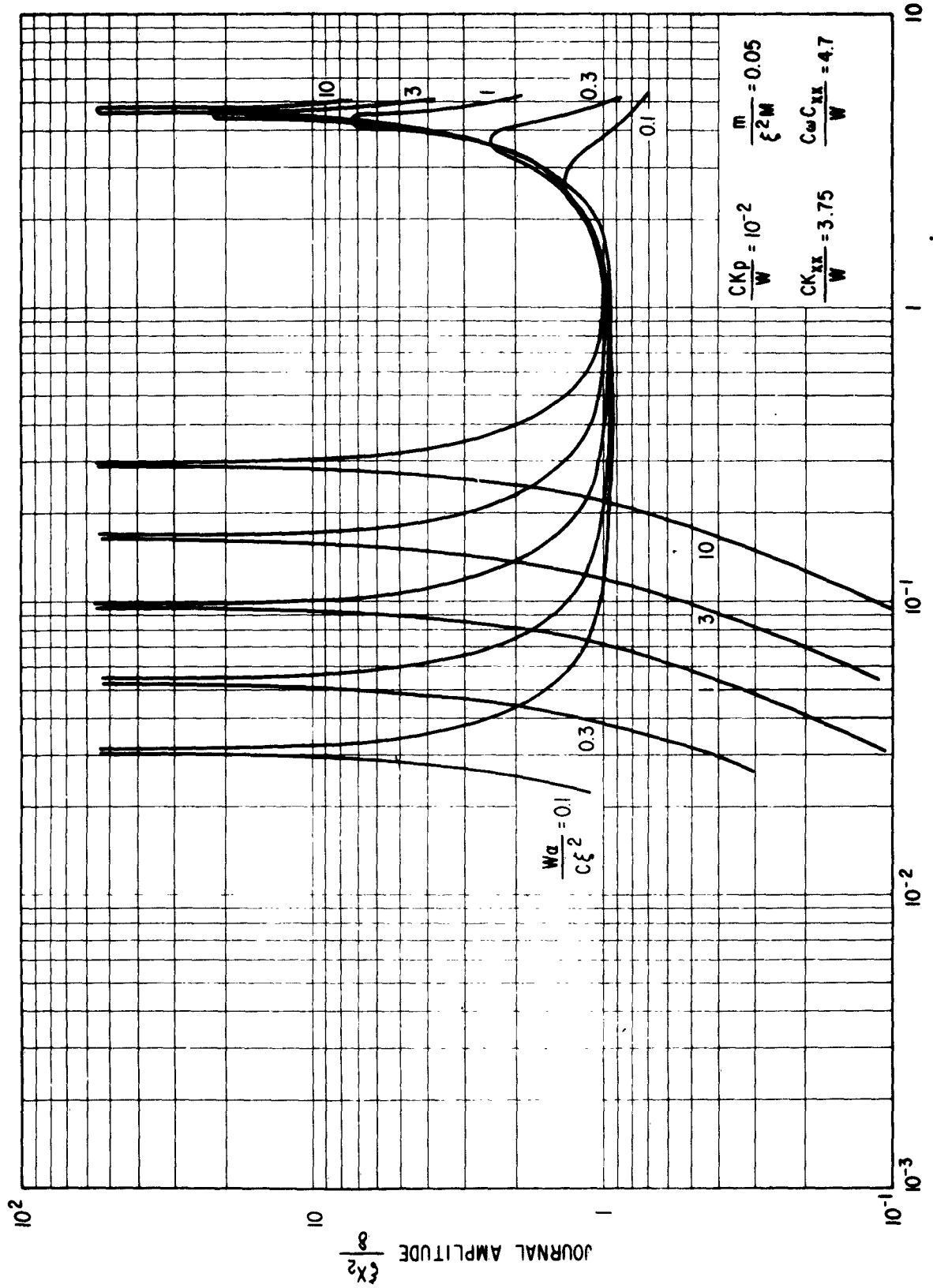

Fig. 14 Dimensionless Journal Amplitude vs Rotor Speed Ratio
Dimensionless Support Stiffness = 10^{-2}
Dimensionless Bearing Mass = 0.05

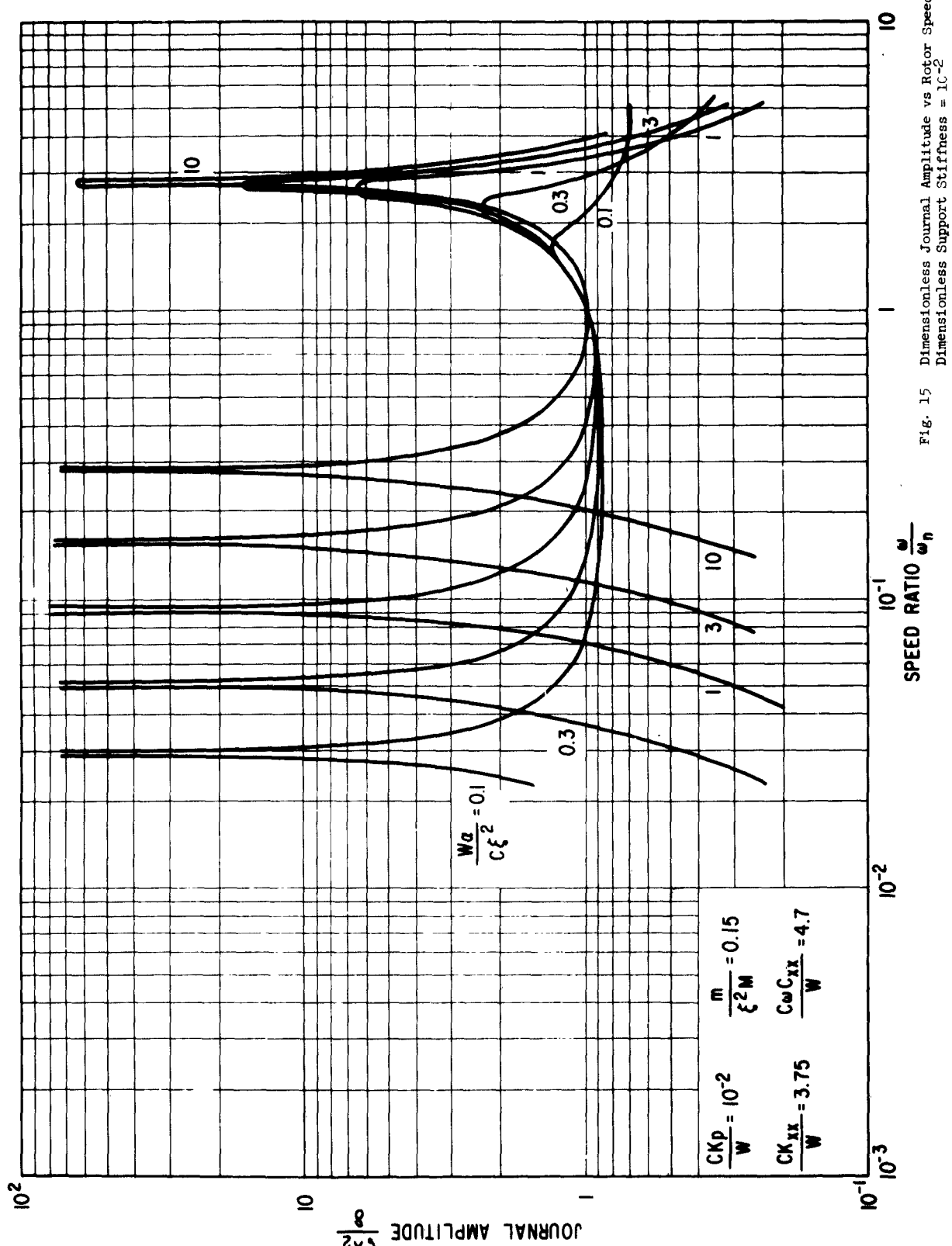

Fig. 15 Dimensionless Journal Amplitude vs Rotor Speed Ratio
Dimensionless Support Stiffness = $1C^{-2}$
Dimensionless Bearing Mass = 0.15

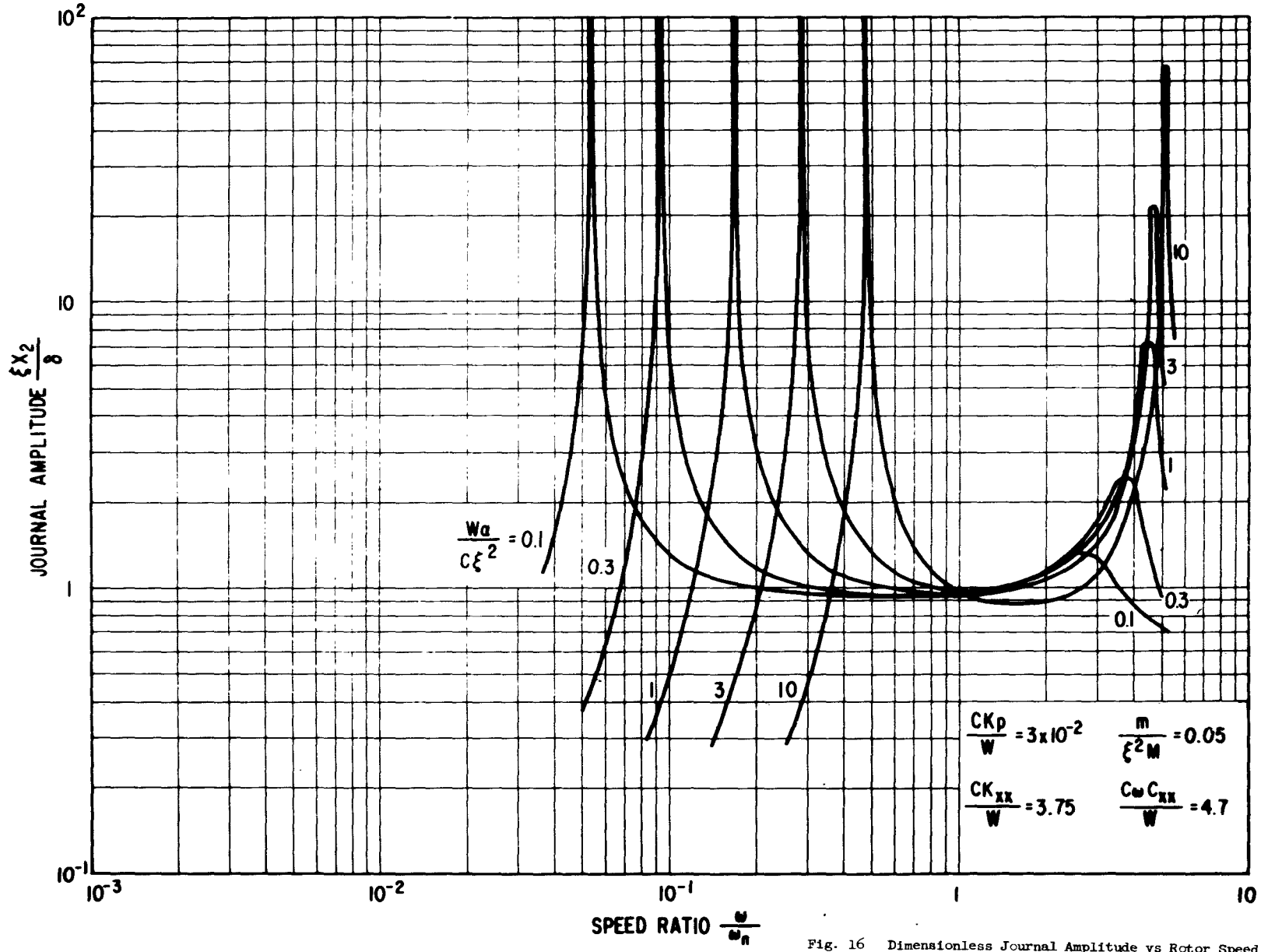

Fig. 16 Dimensionless Journal Amplitude vs Rotor Speed Ratio
Dimensionless Support Stiffness = $3 \cdot 10^{-2}$
Dimensionless Bearing Mass = 0.05

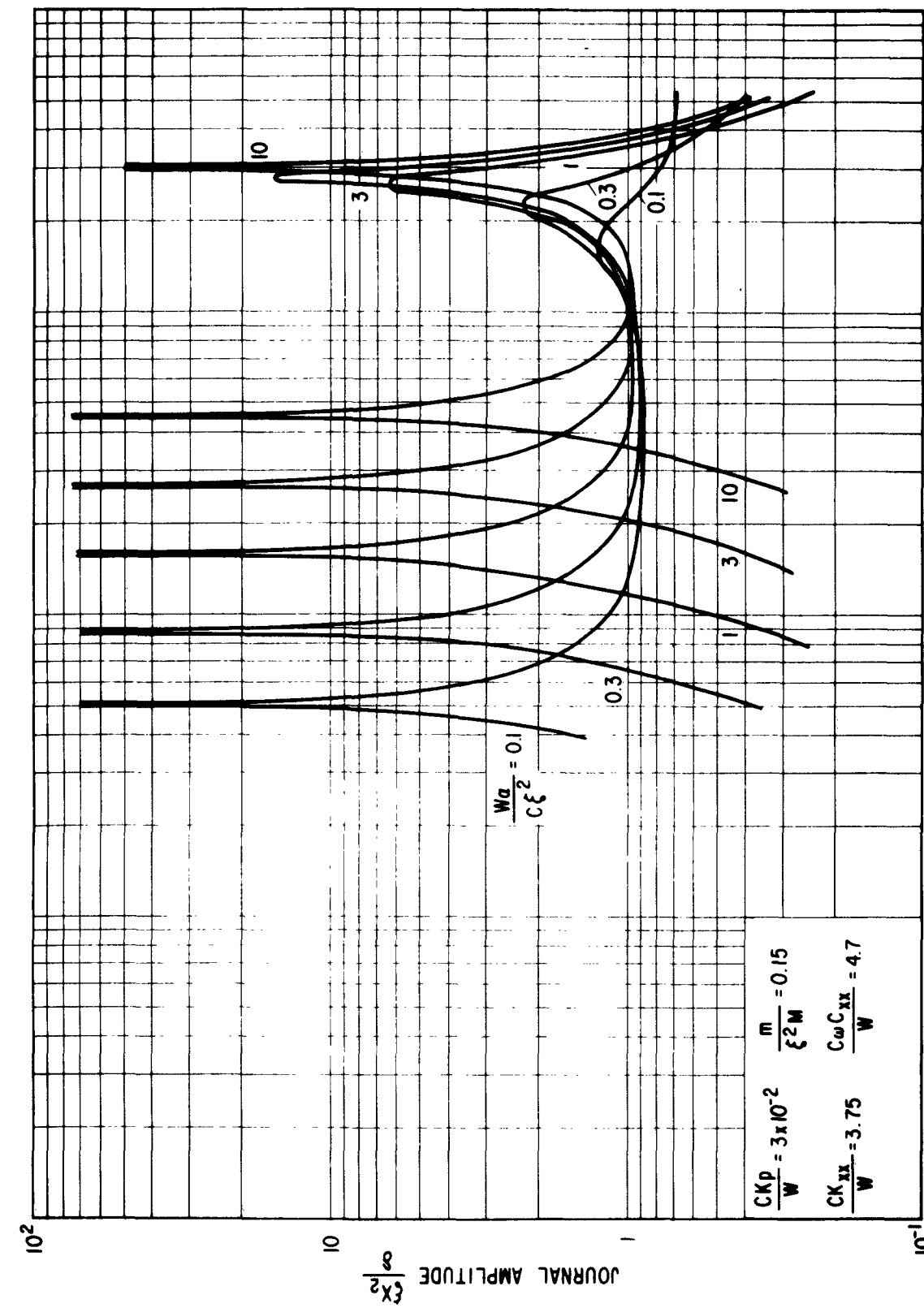

Fig. 17 Dimensionless Journal Amplitude vs Rotor Speed Ratio
Dimensionless Support Stiffness = $3 \cdot 10^{-2}$
Dimensionless Bearing Mass = 0.15

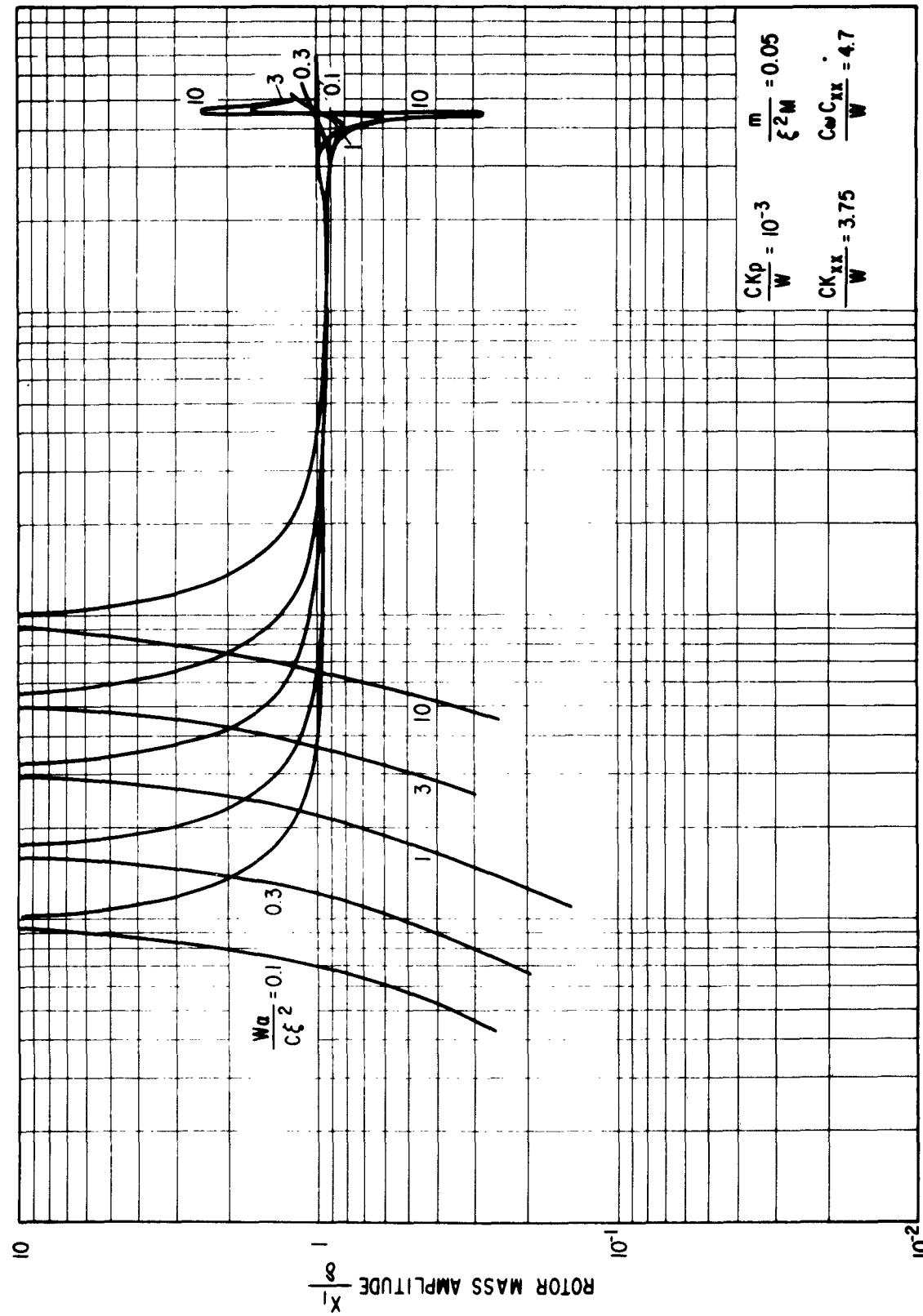

Fig. 18 Dimensionless Rotor Mass Amplitude vs Rotor Speed Ratio
Dimensionless Support Stiffness = 10^{-3}
Dimensionless Bearing Mass = 0.05

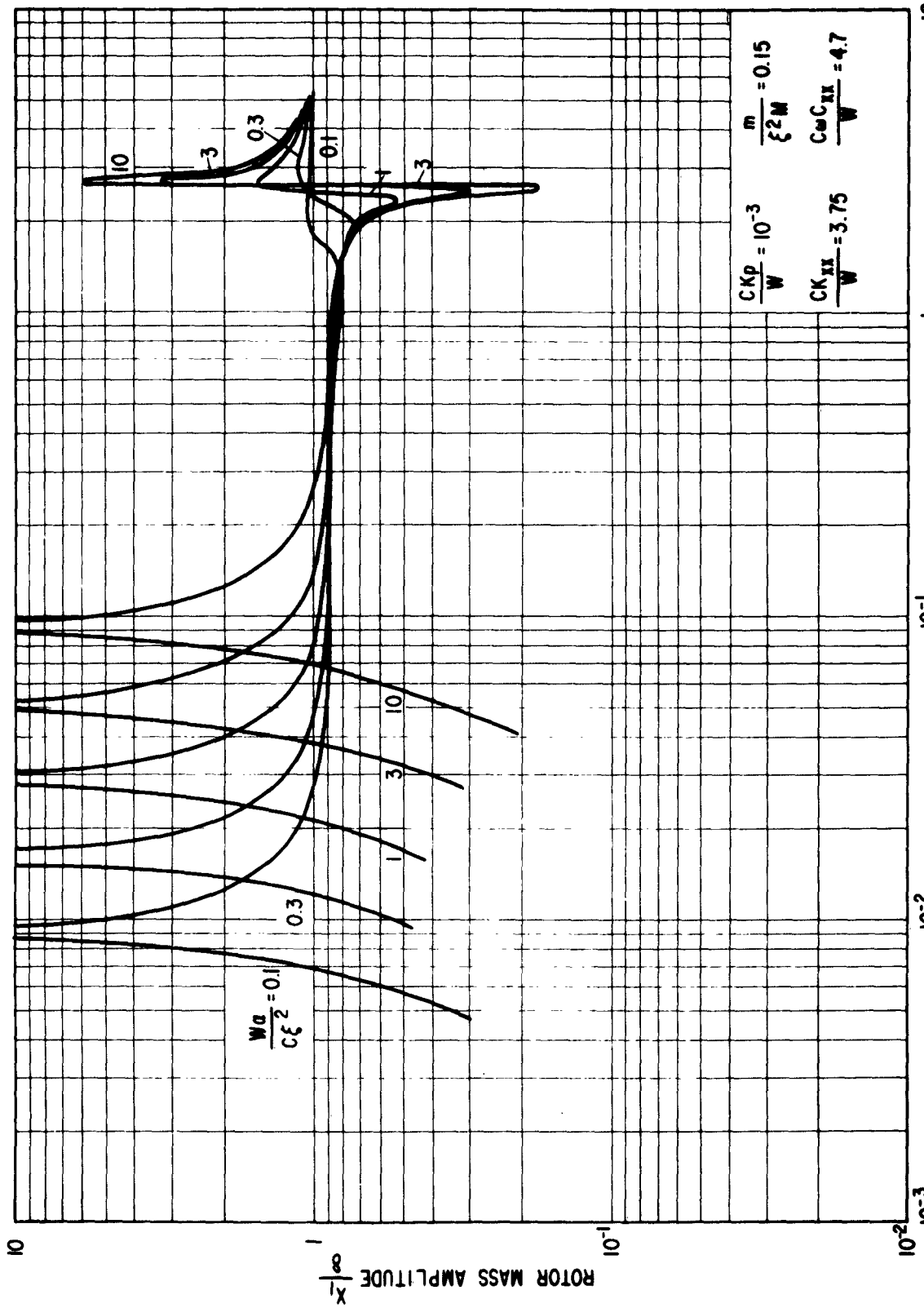

Fig. 19 Dimensionless Rotor Mass Amplitude vs Rotor Speed Ratio
Dimensionless Support Stiffness = 10^{-3}
Dimensionless Bearing Mass = 0.15

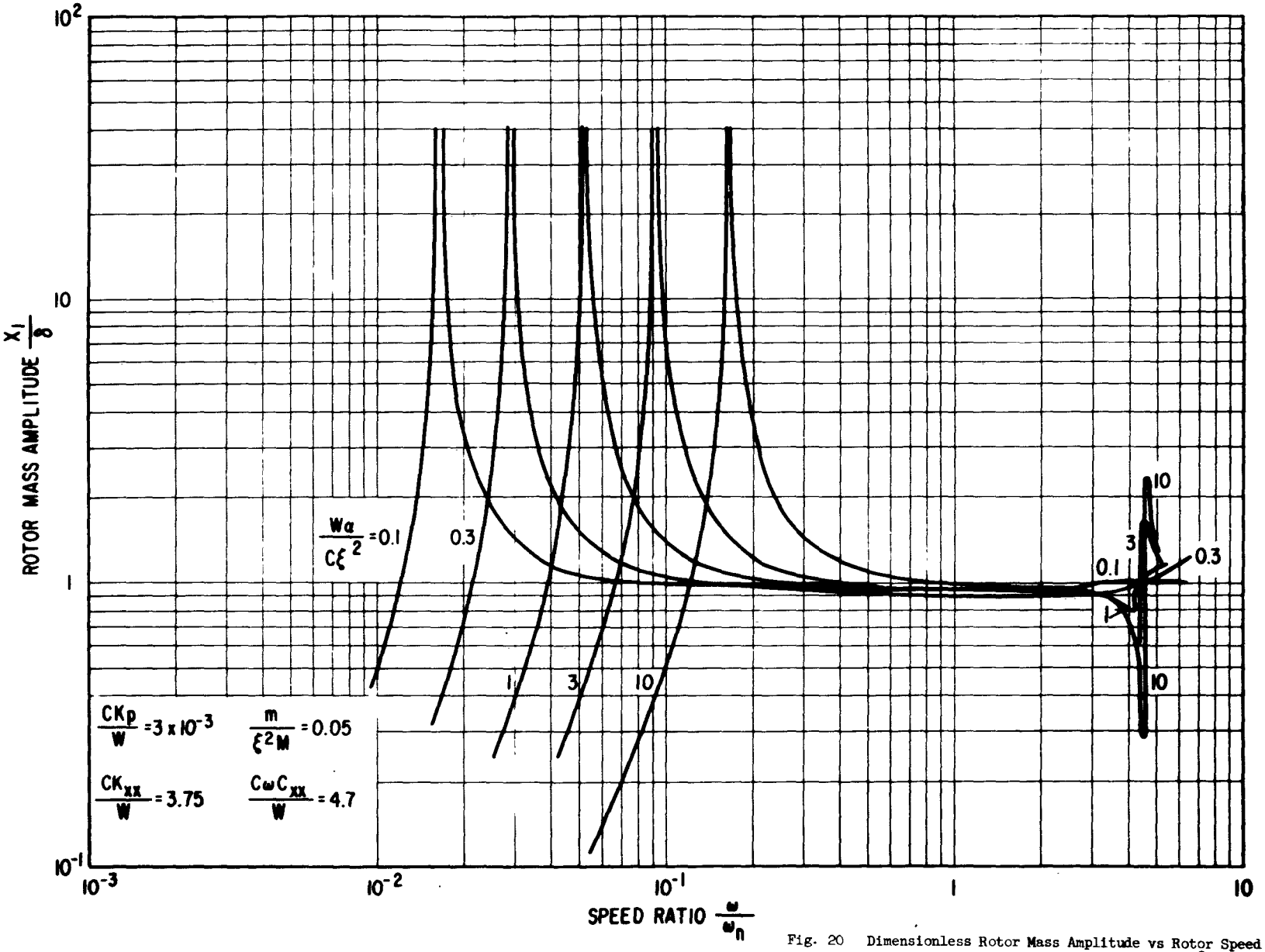

Fig. 20 Dimensionless Rotor Mass Amplitude vs Rotor Speed Ratio
Dimensionless Support Stiffness = $3 \cdot 10^{-3}$
Dimensionless Bearing Mass = 0.05

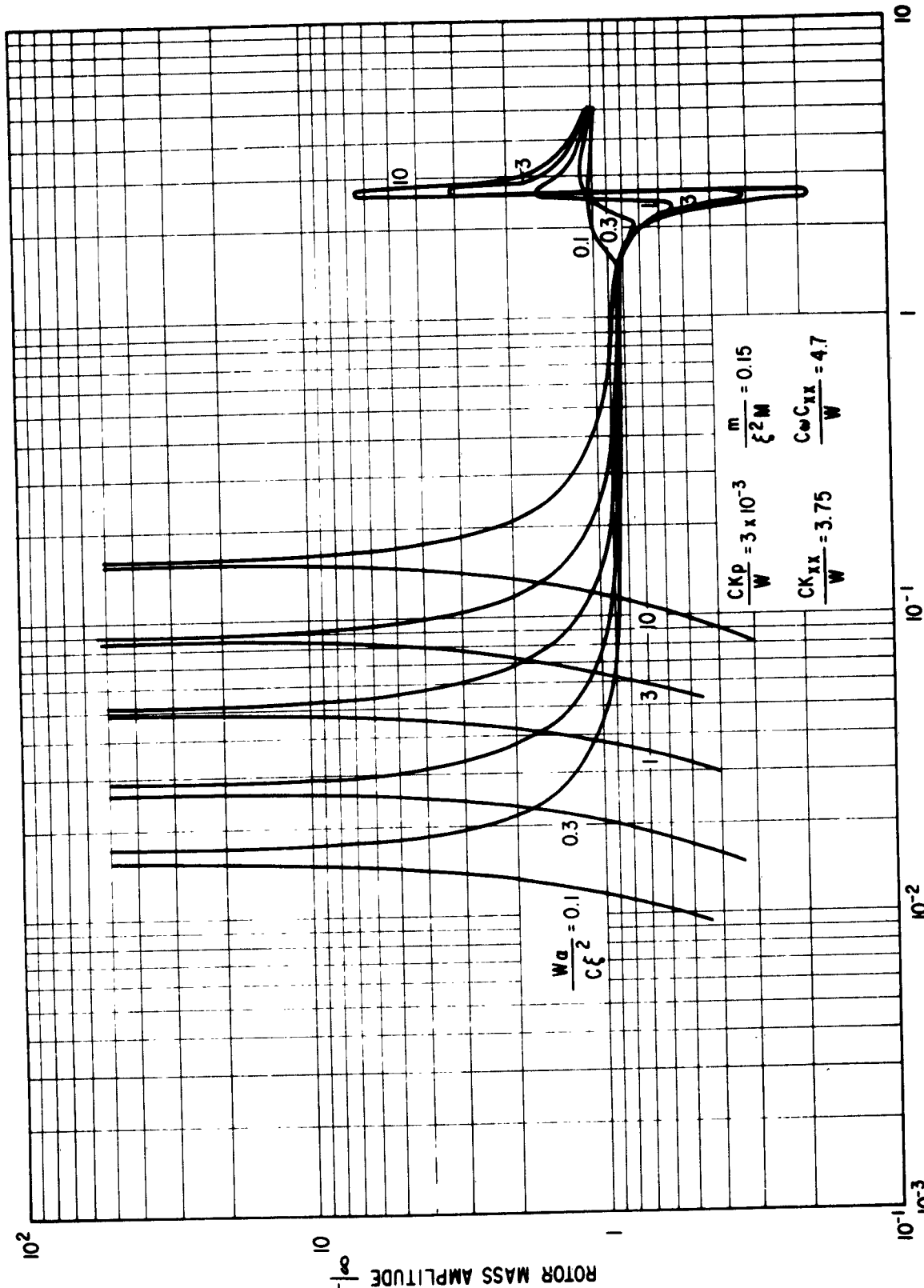

Fig. 21 Dimensionless Rotor Mass Amplitude vs Rotor Speed Ratio
Dimensionless Support Stiffness = $3 \cdot 10^{-3}$
Dimensionless Bearing Mass = 0.15

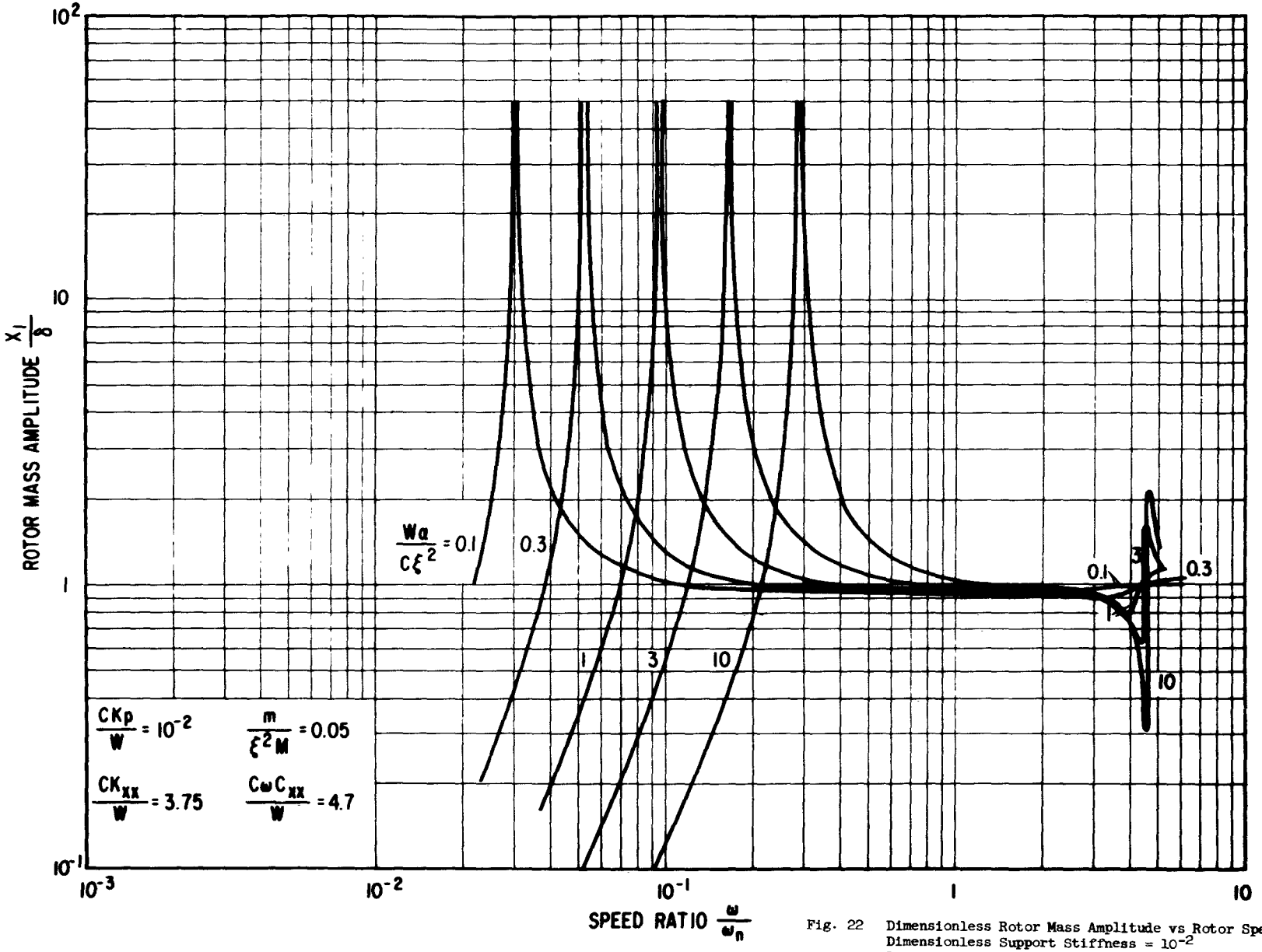

Fig. 22 Dimensionless Rotor Mass Amplitude vs Rotor Speed Ratio
Dimensionless Support Stiffness = 10^{-2}
Dimensionless Bearing Mass = 0.05

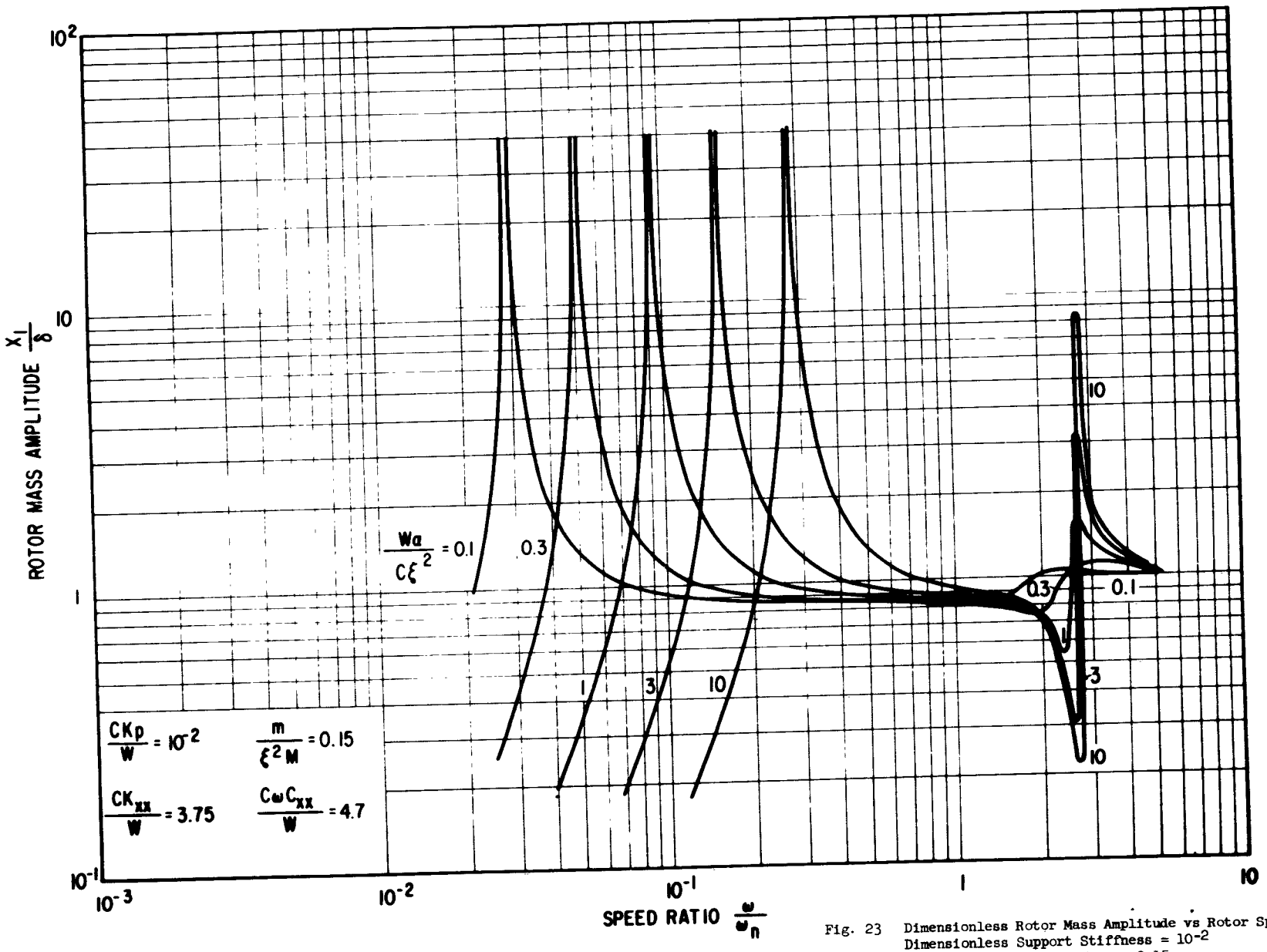

Fig. 23 Dimensionless Rotor Mass Amplitude vs Rotor Speed Ratio
Dimensionless Support Stiffness = 10^{-2}
Dimensionless Bearing Mass = 0.15

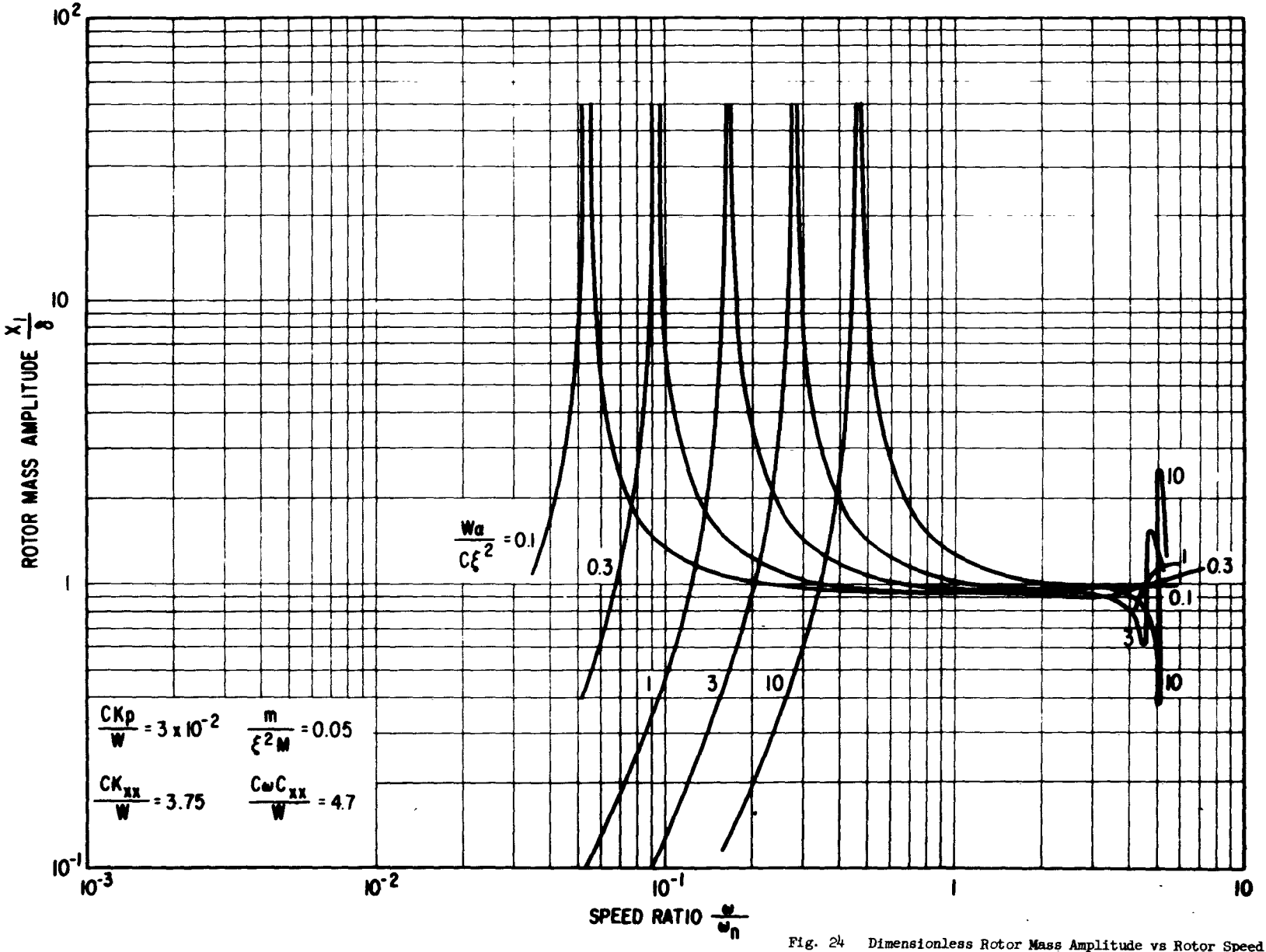

Fig. 24 Dimensionless Rotor Mass Amplitude vs Rotor Speed Ratio
Dimensionless Support Stiffness = $3 \cdot 10^{-2}$
Dimensionless Bearing Mass = 0.05

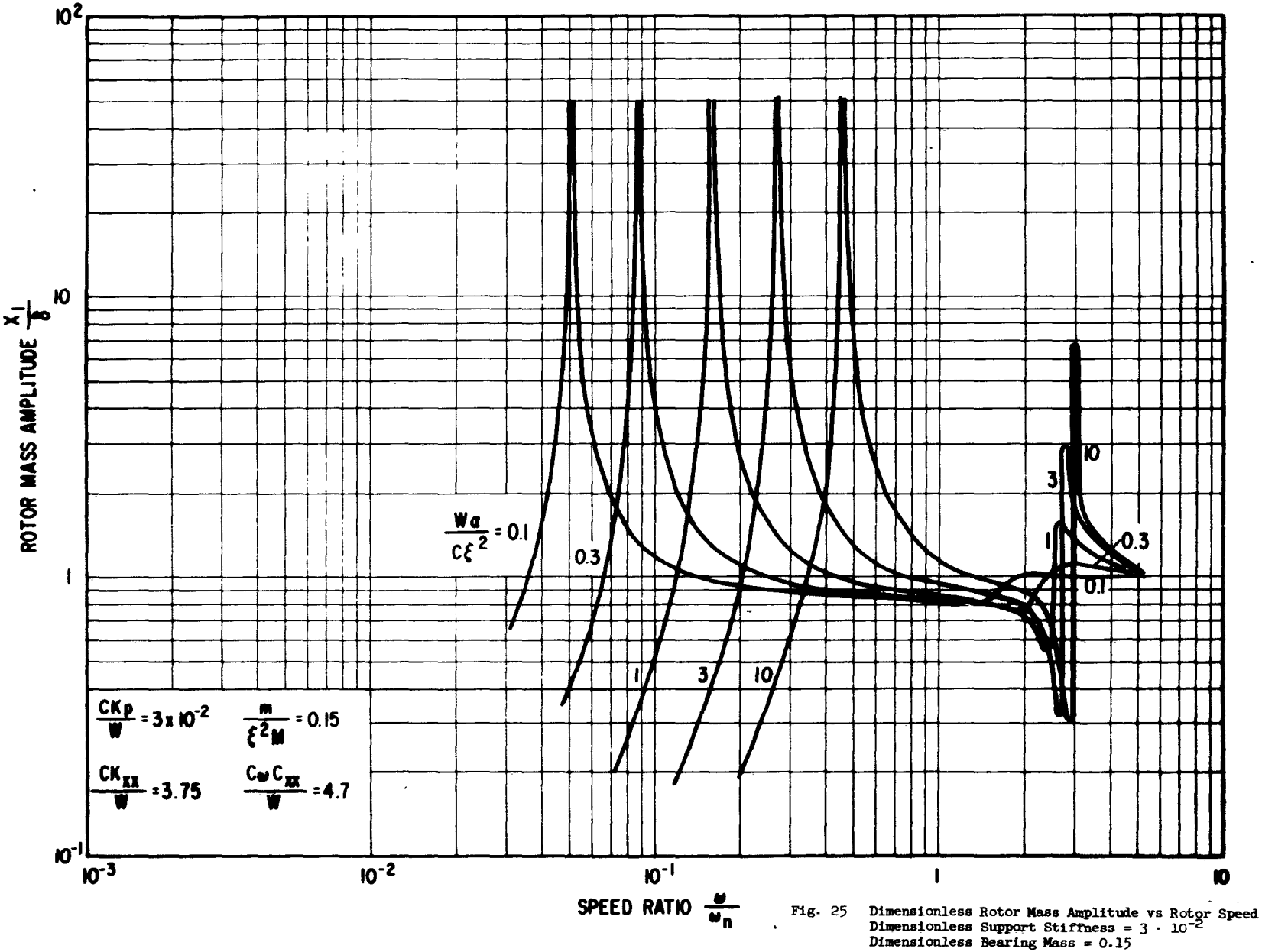

Fig. 25 Dimensionless Rotor Mass Amplitude vs Rotor Speed Ratio
Dimensionless Support Stiffness = $3 \cdot 10^{-2}$
Dimensionless Bearing Mass = 0.15

NOMENCLATURE

C	Radial bearing clearance, inch
$\bar{C}_{xx}, \bar{C}_{xy}, \bar{C}_{yx}, \bar{C}_{yy}$	Bearing damping coefficients, lbs-sec/inch
ωC_{xx}	$= \frac{C \omega \bar{C}_{xx}}{W}$, dimensionless bearing damping coefficient. Similar for $\omega C_{xy}, \omega C_{yx}, \omega C_{yy}$
C_p	Pedestal damping coefficient, lbs-sec/inch
D	Bearing diameter, inch
$\omega_n d$	$= \frac{C \omega_n C_p}{W}$, dimensionless pedestal damping coefficient
E	Real part of eigenvalue of homogenous equations
F	Imaginary part of eigenvalue of homogenous equations
F	Transmitted force, lbs.
F_x, F_y	x and y-components of transmitted force, lbs.
$\bar{K}_{xx}, \bar{K}_{xy}, \bar{K}_{yx}, \bar{K}_{yy}$	Bearing spring coefficients, lbs/in.
K_{xx}	$= \frac{C \bar{K}_{xx}}{W}$ dimensionless bearing spring coefficient. Similar for K_{xy}, K_{yx}, K_{yy}
K_p	Pedestal spring coefficient, lbs/in.
k	$= \frac{C K_p}{W}$, dimensionless pedestal spring coefficient
L	Bearing Length, inch
l	Rotor span between bearing centers, inch
M	Half the rotor mass, lbs-sec^2/in.
m	Mass of bearing housing, lbs-sec^2/in.
N	Rotational speed of rotor, RPS
R	Bearing radius, inch
S	$= \frac{\mu N D L}{W} \left(\frac{R}{C}\right)^2$, Sommerfeld number
s	$= \frac{\omega}{\omega_n}$, Ratio of speed at instability and rotor critical speed
t	Time, seconds

W	Bearing reaction, lbs.
$\bar{X}_1, \bar{Y}_1$	Amplitude of rotor mass, inch
$\bar{X}_2, \bar{Y}_2$	Amplitude of journal center, inch
$\bar{X}_3, \bar{Y}_3$	Amplitude of bearing housing, inch
X_1, Y_1	$= \frac{\bar{X}_1}{\delta}, = \frac{\bar{Y}_1}{\delta}$, Dimensionless amplitude of rotor mass
X_2, Y_2	$= \frac{\xi \bar{X}_2}{\delta}, = \frac{\xi \bar{Y}_2}{\delta}$, Dimensionless amplitude of journal center
X_3, Y_3	$= \frac{\xi \bar{X}_3}{\delta}, = \frac{\xi \bar{Y}_3}{\delta}$, Dimensionless amplitude of bearing housing.
α_{aa}, α_{ab}	Rotor influence coefficient, first index: amplitude, second index: force, in/lbs.
α	$= (\alpha_{aa}+\alpha_{ab})$ for static unbalance, $= (\alpha_{aa}-\alpha_{ab})$ for dynamic unbalance, in/lbs.
β	$= \frac{C\omega C_p}{W}$ Dimensionless pedestal damping coefficient
γ	$= \frac{\nu}{\omega}$, Ratio of instability frequency and rotor speed
δ	Unbalance eccentricity of rotor masses, inch
$\varkappa$	$= \frac{1}{\xi}\left(\frac{\omega}{\omega_n}\right)^2 / \left[1-\left(\frac{\omega}{\omega_n}\right)^2\right]$, parameter
μ	Lubricant viscosity, lbs-sec/in^2
μ	$= \frac{m}{\xi^2 M}$, Dimensionless bearing housing mass
ε	Journal eccentricity ratio in bearing
ν	Instability frequency, rad/sec
ξ	= 1 for static unbalance, = ratio of distance between rotor masses and total rotor length ℓ for dynamic unbalance.
ϱ	$= \frac{W\alpha}{\xi^2 C}$, rotor flexibility parameter
σ	$= \frac{Cm\omega^2}{W}$, dimensionless bearing housing mass
$\sigma_{xx}, \sigma_{xy}, \sigma_{yx}, \sigma_{yy}$	Parameters defined by Eqs. (28) to (31)
ω	Angular speed of rotor, rad/sec.
ω_n	$= \sqrt{\frac{1}{M\alpha}}$, critical speed of rotor on rigid supports, rad/sec.

Volume 2

Part II

Unbalance Response of a Uniform Elastic Rotor Supported In Damped Flexible Bearings

by

Neville F. Rieger

Mechanical Technology Incorporated

TABLE OF CONTENTS

	Page
LIST OF FIGURES	iii
SUMMARY	iiv
INTRODUCTION	1
General	1
Scope of Present Investigation	1
DISCUSSION	3
Non-dimensional Parameters	3
Bearing Properties	5
Maximum Response Values	5
THEORETICAL ANALYSIS OF ROTOR MOTIONS	7
General	7
Basic Equations and Solutions	8
Evaluation of Constants	9
Calculation of Rotor Displacements	14
Calculation of Transmitted Force	16
RESULTS	18
General Features of the Results	18
Influence of Unbalance on Rotor Dynamic Performance	20
Comparison with Other Results	25
Mode Shapes	27
CONCLUSIONS	29
REFERENCES	30
APPENDICES	
A. Notation for Spring and Damping Coefficients	30
B. Program Details and Listing	33
FIGURES	50
NOTATION	76

LIST OF FIGURES

1. Coordinates and Displacements
2. Positive Displacement, Force, Moment and Shear Convention
3. Fluid-Film Forces on Journal at $Z_1 = 0$ and $Z_2 = L_2$
4. Unbalance Acting at $Z_1 = L_1$
5. Force and Displacement Relationships for Whirl Ellipse at Unbalance
6. Rotor Amplitude versus Speed. Axially Symmetrical Unbalance
7. Rotor Amplitude versus Speed. Axially Symmetrical Unbalance
8. Rotor Amplitude versus Speed. Axially Symmetrical Unbalance
9. Rotor Amplitude versus Speed. Axially Symmetrical Unbalance
10. Rotor Amplitude versus Speed, Axially Symmetrical Unbalance
11. Rotor Amplitude versus Speed. Axially Symmetrical Unbalance
12. Rotor Amplitude versus Speed. Axially Asymmetrical Unbalance
13. Rotor Amplitude versus Speed. Axially Asymmetrical Unbalance
14. Rotor Amplitude versus Speed. Axially Asymmetrical Unbalance
15. Rotor Amplitude versus Speed. Axially Asymmetrical Unbalance
16. Rotor Amplitude versus Speed. Axially Asymmetrical Unbalance
17. Rotor Amplitude versus Speed. Axially Asymmetrical Unbalance
18. Rotor Amplitude versus Speed. Axially Asymmetrical Unbalance
19. Maximum Transmitted Force versus Speed. Axially Symmetrical Unbalance
20. Maximum Transmitted Force versus Speed. Axially Symmetrical Unbalance
21. Maximum Transmitted Force versus Speed. Axially Symmetrical Unbalance
22. Maximum Transmitted Force versus Speed. Axially Asymmetrical Unbalance
23. Maximum Transmitted Force versus Speed. Axially Asymmetrical Unbalance
24. Maximum Transmitted Force versus Speed. Axially Asymmetrical Unbalance
25. Sommerfeld Number versus Eccentricity for L/D = 0.5, 1.0
26. Mode Shapes for Symmetrical Unbalance
27. Mode Shapes for Asymmetrical Unbalance
28. Comparison between Results of Present Analysis and Discreet -Mass Rotor Calculations

SUMMARY

The dynamic response of an unbalanced elastic rotor which operates in damped fluid-film bearings has been investigated. The influence of speed, bearing operating eccentricity, and of relative stiffness between the rotor and its bearings have been determined. Results are expressed in terms of rotor maximum whirl amplitude at several locations on the rotor; and in terms of bearing transmitted force. Particular attention has been given to the influence of system parameters on critical speeds, and on the attenuation of bearing transmitted force.

The results are presented as charts which facilitate the design of high-speed rotors by allowing performance characteristics up to and including the fourth system critical to be determined directly. The analysis is exact, and the influence of higher modes is included under all operating conditions. Both static and dynamic unbalance conditions have been considered.

INTRODUCTION

General

A heavy elastic rotor has an infinite number of critical speeds, but, in practice, the operating speed range rarely includes more than three or four of these criticals. These critical speeds and the vibratory form assumed by the rotor are both directly influenced by the stiffness and damping properties of the supporting structure, as well as by the distribution of mass, elasticity, unbalance and damping within the rotor itself.

Little information is presently available on the dynamic response of rotor systems to unbalance in the higher modes. The major studies which have been made to date have been concerned with optimising the rotor-bearing system to achieve maximum attenuation of transmitted force and rotor amplitude in the lower modes. Lund and Sternlicht (Ref. 1) used a simple rotor in fluid-film bearings to investigate force attenuation in the fundamental mode for a variety of bearing types. Warner and Thoman (Ref. 2) extended this work using a two-mass rotor in partial-arc bearings. This rotor included the influence of the second mode in the fundamental rotor motions, and, also, provided data on operation at speeds including the second critical.

In both cases, the simplicity of the rotor precludes any direct extension of this work to higher modes. However, such information is desirable in order to optimise the steady-state performance of high-speed rotors which operate beyond the second bending critical, and to optimise the system run-up and run-down characteristics. Also, the influence of the higher modes on rotor response in the lower modes and throughout the speed range is not indicated in presently available data. Such information is required to enable the most efficient attenuation to be determined. This information is obtained in the present analysis. Finally, the parametric conditions under which stable rotor motions may occur during operation in the higher modes have not been defined up to the present. A simple extension of the results given herein would allow this to be done.

Scope of Present Investigation

In the present analysis, the motions of an unbalanced flexible rotor which is

supported in fluid-film bearings are considered. The rotor is assumed to be of prismatic shape, and to have its mass and elasticity distributed uniformly along its length. This distribution makes it possible for the solutions to the resulting equations of motion of the system to include the influence of all modes directly. Rotor internal damping is assumed to be negligible compared with the damping in the fluid-film bearings. A simple uniform shaft was chosen because it permits a direct analytical solution to be obtained for all required dynamic properties of the system including the higher modes. This rotor-bearing system is not intended to simulate any practical case, but it does indicate certain dynamic characteristics which are common to all cases.

The motions of the rotor are considered to arise from the action of an unbalance $W \frac{1}{g} e$ which is due to the weight of the rotor, W, acting at an eccentricity e, from the rotor geometric centerline. The unbalance is located at a specified point along the length of the rotor, and its distance from the left-hand bearing is included as a variable in the analysis. This is a "static" unbalance. Any desired condition of dynamic unbalance may also be investigated by suitably superposing two sets of static unbalance results to represent the dynamic unbalance couple. This superposition has been included in the analysis, and dynamic unbalance results have been obtained. The point at which the desired amplitude or force response occurs is also included as a variable.

The rotor is supported in a hydrodynamic cylindrical fluid-film journal bearing at either end. The dynamic properties of these bearings are given in Table I. This bearing type is commonly used in practice. It is considered in the analysis by Lund and Sternlicht (Ref. 1), and its characteristics are similar to those of the partial-arc bearing. Thus, this choice of bearing allows a comparison to be made between the present and previous work.

The analysis presented here has been programmed and the following results have been obtained:

1. a. Rotor amplitude at specified stations for a speed range which includes the fourth rigid bearing critical.
   b. Bearing transmitted force for the same speed range.
2. Rotor mode shape in terms of an optional number of rotor stations for selected speeds.

DISCUSSION

Non-Dimensional Parameters

All parameters in the results, Figures 6 through 24, have been made non-dimensional for generality. The parameters and dimensionless ratios used are defined as follows:

1. Notation. Listed at the end of this report
2. Distance ratio, $L_1/L = \mathscr{L}$. Defines the axial location of the unbalance $W \cdot e$ from the L.H. bearing, with respect to shaft length. Figure 1.
3. Position ratio, Z_1/L_1. Defines the axial position of any displacement measurement within Region 1, measured from the L.H. bearing. Figure 1.
4. Position ratio, Z_2/L_2. Defines the axial position of any displacement measurement within Region 2, measured from the unbalance position. Figure 1.
5. Speed ratio, ω/ω_c. Ratio of rotor speed ω to the fundamental bending critical speed ω_c of a uniform rotor in simple rigid end supports. The speed range covered by the analysis extends to $\omega/\omega_c = 24.0$. This includes the first four rigid bearing criticals.

   For the present rotor system $\omega = \frac{(\lambda L)^2}{L^2} \left[\frac{EI}{\rho A}\right]^{\frac{1}{2}}$

   where λL is the system characteristic frequency number.

   For a rigid bearing uniform rotor $\omega_c = \frac{\pi^2}{L^2} \left[\frac{EI}{\rho A}\right]^{\frac{1}{2}}$

   Speed ratio $\left(\frac{\omega}{\omega_c}\right) = \left(\frac{\lambda L}{\pi}\right)^2$ At the rigid bearing critical $\omega/\omega_c = 1.0$.

   Characteristic number $\lambda L = \pi \left(\frac{\omega}{\omega_c}\right)^{\frac{1}{2}}$

   and $\lambda L_1 = \mathscr{L} \pi \left(\frac{\omega}{\omega_c}\right)^2$

   $\lambda L_2 = (1-\mathscr{L}) \pi \left(\frac{\omega}{\omega_c}\right)^2$

6. Flexibility ratio, $\frac{C}{\delta}$. Ratio of the bearing clearance C to the central deflection of a uniformly loaded simply-supported shaft, δ.

7. Stiffness parameter, $\nu = EI\lambda^3 \frac{C}{W}$. Occurs non-dimensionally in the equations of motion. The relationship between ν and $\frac{C}{\delta}$ is as follows:

Central deflection of simply-supported uniform shaft $\delta = \frac{5}{384} \frac{WAL^4}{EI}$

Static load per bearing $W_1 = \frac{WAL}{2}$

Characteristic number $\lambda L = \pi \left(\frac{\omega}{\omega_c}\right)^{\frac{1}{2}}$

Therefore $\nu = EI\lambda^3 \cdot \frac{C}{W} = \left(\frac{5\pi^3}{192}\right)\left(\frac{C}{\delta}\right)\left(\frac{\omega}{\omega_c}\right)^{3/2}$

Stiffness parameter is therefore a dynamic deflection ratio, as shaft stiffness depends on rotor speed. The range of flexibility ratio required for the analysis was established as follows:

Case	Bearing Clearance C, in.	Fundamental Rotor Critical Speed, rpm	Shaft Lateral Deflection, in.	$\frac{C}{\delta}$
Maximum	0.0050	14,000	0.002	30
Minimum	0.0005	4,000	0.015	0.3

The fundamental rotor critical speeds were chosen high in order to apply to a simply-supported shaft in rigid bearings. Flexible bearing system criticals will be considerably lower. The $\frac{C}{\delta}$ values therefore will apply to the range for rotor-bearing system fundamental critical speeds. The above maximum $\frac{C}{\delta}$ value therefore applies to a fairly rigid shaft in flexible bearings. The lowest critical speed will tend towards a rigid-body critical and will be determined mainly by bearing flexibility and rotor mass. The minimum value $\frac{C}{\delta} = 0.3$ corresponds to a flexible shaft in rigid bearings. The lowest critical speed will tend to occur at $\omega/\omega_c = 1.0$, determined by shaft flexibility. These facts are of use in analyzing the results given in Figures 6 through 24

8. Displacement amplitude ratio, $\frac{x}{e}$. Ratio of the maximum rotor displacement x at a specified station to the unbalance eccentricity e.

9. Dimensionless transmitted force, $\frac{CF}{We}$. Ratio of the maximum transmitted force F to the unbalance W · e, normalized by the inclusion of the bearing clearance C.

Bearing Properties

The bearing used in the present analysis is a cylindrical journal bearing. Dynamic stiffness and damping characteristics are given below in Table I, derived from Reference 1 in Appendix A of this report.

TABLE I

Spring and Damping Properties for Cylindrical Journal Bearing, L/D = 1

η	0.2	0.5	0.7
K_{xx}	1.283	2.060	3.59
K_{xy}	5.492	3.230	3.38
K_{yx}	-4.610	-1.070	0.02
K_{yy}	2.220	2.040	1.99
C_{xx}	10.72	6.02	6.23
C_{xy}	1.950	2.00	1.95
C_{yx}	2.290	2.17	2.13
C_{yy}	9.770	3.40	2.00
S	0.665	0.189	0.081
θ_1	76.8	57.5	43.3

The cylindrical journal bearing is similar to the partial-arc bearing in operation because of the presence of cavitation in the film. Thus, the results obtained for the system characteristics are representative for a wide range of common applications. For systems which employ bearing types with important differences, such as a tilting-pad bearing, the qualitative aspects of the results still apply as a guide even though they are not then numerically correct.

Maximum Response Values

Response amplitude and transmitted force results are both given for the maximum values for these parameters. The method of calculation for both maxima types is given in the theoretical analysis, Section 3, and a diagrammatic representation of the component relationships which go to make up the force and displacement maximum values is given in Figure 25.

Both static and dynamic unbalance characteristics are included in the above results. Details for Program 1 are given in Figures 6 through 24, and for Program 2 in Figures 26 and 27. All major system variables are expressed in terms of dimensionless parameters.

The results of the present investigation have been compared with those obtained using a proven discrete-mass rotor-bearing program. Correlation was good in all cases. The results are shown in Figure 28.

THEORETICAL ANALYSIS OF ROTOR MOTIONS

General

The rotor-bearing system shown in Fig. 1 consists of a heavy elastic shaft of uniform circular cross-section along its length, supported at its ends in fluid-film bearings. The bearings have stiffness and damping properties in both x- and y- directions, and also cross-coupling stiffness and damping between these directions. Dimensionless values of the bearing stiffness and damping properties with eccentricity are given in Table 1 for a cylindrical journal bearing.

The shaft considered has an unbalance W·e situated at distance L_1 from $Z_1 = 0$. During rotation, this gives rise to an unbalance force $Me\omega^2$ which rotates in synchronism with the shaft, causing it to whirl about its stationary equilibrium position. Shaft motions are restrained by its own inertia and elasticity, distributed uniformly along its length; and by the bearings at either end. The bearing fluid film forces consist of a linear spring force which opposed displacements, and a viscous damping force due to velocity. Any externally impressed journal motion in a given direction gives rise to fluid-film forces which oppose the motion, both in the direction of the displacement and at right angles to it. The coordinate bearing forces arising from journal motion are written as

y-direction: $$F(Y) = K_{YY}\,Y + C_{YY}\,\dot{Y} + K_{XY}\,X + C_{XY}\,\dot{X}$$

x-direction: $$F(X) = K_{XX}\,X + C_{XX}\,\dot{X} + K_{YX}\,Y + C_{YX}\,\dot{Y}$$

The unbalance force may also be resolved into the x- and y- directions. This allows the usual equations for plane motions to be written for rotor displacements. The solutions to these equations may be combined to yield the maximum displacements and forces acting on the rotor.

The purpose of this investigation is to examine the nature of shaft displacements and transmitted bearing forces which result from shaft unbalance in the system described, over a wide range of speed.

Basic Equations and Solutions

Considering motion in the y-direction of Figure (1), the equilibrium of an elemental length of shaft dz subject only to internal forces is governed by the well-known equation

$$EI\frac{\partial^4 Y}{\partial z^4} + \frac{wA}{g}\frac{\partial^2 Y}{\partial t^2} = 0 \tag{1}$$

The solution to Equation (1) is

$$Y = y(z)\,e^{i\omega t} \tag{2}$$

where y(z) is a function of z and independent of t. For the section $0 \leq z_1 \leq L_1$ substitution gives

$$Y_1 = \left[A_1 \cos \lambda z_1 + B_1 \sin \lambda z_1 + C_1 \cosh \lambda z_1 + D_1 \sinh \lambda z_1\right] e^{i\omega t} \tag{3}$$

where

$$\lambda^4 = \frac{wA\omega^2}{gEI}$$

and A_1, B_1 C_1 and D_1 are constants of integration to be determined from the end conditions of the section. For the section $0 \leq z_2 \leq L_2$ the solution is

$$Y_2 = \left[A_2 \cos \lambda z_2 + B_2 \sin \lambda z_2 + C_2 \cosh \lambda z_2 + D_2 \sinh \lambda z_2\right] e^{i\omega t} \tag{4}$$

where A_2, B_2, C_2 and D_2 are constants of integration.

Similarly, for motion in the x-direction, the governing equation is

$$EI\frac{\partial^4 X}{\partial z^4} + \frac{wA}{g}\frac{\partial^2 X}{\partial t^2} = 0 \tag{5}$$

For $0 \leq z_1 \leq L_1$ the solution is

$$X_1 = \left[E_1 \cos \lambda z_1 + F_1 \sin \lambda z_1 + G_1 \cosh \lambda z_1 + H_1 \sinh \lambda z_1\right] e^{i\omega t} \tag{6}$$

where E_1, F_1 G_1 and H_1 are constants of integration and λ is as defined above.

For $0 \leq z_2 \leq L_2$ the solution is

$$X_2 = \left[E_2 \cos \lambda z_2 + F_2 \sin \lambda z_2 + G_2 \cosh \lambda z_2 + H_2 \sinh \lambda z_2\right] e^{i\omega t} \tag{7}$$

where E_2, F_2, G_2, and H_2 are constants of integration.

Evaluation of Constants

The 16 constants of integration may be evaluated by introducing the solutions containing them into the boundary conditions of the system. Adopting the conventions of Figure 2 allows the boundary conditions to be expressed as follows:

$z_1 = 0$; y-z plane

$$M(Y_1)(0) = 0 \tag{8}$$

$$V(Y_1)(0) = 0 \tag{9}$$

where $$F(Y_1)(0) = K_{yy} Y_1(0) + C_{yy} \dot{Y}_1(0) + K_{xy} X_1(0) + C_{xy} \dot{X}_1(0) \tag{10}$$

$z_1 = 0$; x-z plane

$$M(X_1)(0) = 0 \tag{11}$$

$$V(X_1)(0) = 0 \tag{12}$$

where $$F(X_1)(0) = K_{xx} X_1(0) + C_{xx} \dot{X}_1(0) + K_{yx} Y_1(0) + C_{yx} \dot{Y}_1(0) \tag{13}$$

$z_2 = L_2$; y-z plane.

$$M(Y_2)(L_2) = 0 \tag{14}$$

$$V(Y_2)(L_2) + F(Y_2)(L_2) = 0 \tag{15}$$

where $$F(Y_2)(L_2) = K_{yy} Y_2(L_2) + C_{yy} \dot{Y}_2(L_2) + K_{xy} X_2(L_2) + C_{xy} \dot{X}_2(L_2) \tag{16}$$

$z_2 = L_2$; x-z plane.

$$M(X_2)(L_2) = 0 \tag{17}$$

$$V(X_2)(L_2) + F(X_2)(L_2) = 0 \tag{18}$$

where $$F(X_2)(L_2) = K_{xx} X_2(L_2) + C_{xx} \dot{X}_2(L_2) + K_{yx} Y_2(L_2) + C_{yx} \dot{Y}_2(L_2) \tag{19}$$

$z_1 = L_1$: y-z plane.
$z_2 = 0$:

$$Y_1(L_1) = Y_2(0) \tag{20}$$

$$\frac{d}{dz_1}(Y_1)(L_1) = \frac{d}{dz_2}(Y_2)(0) \tag{21}$$

$$M(Y_1)(L_1) = M(Y_2)(0) \tag{22}$$

$$-V(Y_1)(L_1) + Me\omega^2[-ie^{i\omega t}] + V(Y_2)(0) = 0 \tag{23}$$

where $Me\omega^2[-ie^{i\omega t}]$ is the y- component of the unbalance force acting at L_1.

$z_1 = L_1$: x-z plane.
$z_2 = 0$:

$$X_1(L_1) = X_2(0) \tag{24}$$

$$\frac{d}{dz_1}(X_1)(L_1) = \frac{d}{dz_2}(X_2)(0) \tag{25}$$

$$M(X_1)(L_1) = M(X_2)(0) \tag{26}$$

$$-V(X_1)(L_1) + Me\omega^2 \cdot e^{i\omega t} + V(X_2)(0) = 0 \tag{27}$$

where $Me\omega^2 \cdot e^{i\omega t}$ is the x- component of the unbalance force acting at L_1. Substituting eqs. (3)-(7) int eqs. (8)-(27), and utilizing the moment and shear relations

$$M(Y) = -EI\frac{d^2Y}{dZ^2} \qquad M(X) = -EI\frac{d^2X}{dZ^2}$$

and

$$V(Y) = -EI\frac{d^3Y}{dZ^3} \qquad V(X) = -EI\frac{d^3X}{dZ^3}$$

allows the 16 basic equations of motion to be obtained.
Expressed in dimensionless form in terms of the integration constants, these equations are as follows:

$$\frac{A_1}{e} - \frac{C_1}{e} = 0$$

$$\alpha_1\left(\frac{A_1}{e} + \frac{C_1}{e}\right) - \nu\left(\frac{B_1}{e} - \frac{D_1}{e}\right) + \alpha_2\left(\frac{E_1}{e} + \frac{G_1}{e}\right) = 0$$

$$\left(\frac{E_1}{e} - \frac{G_1}{e}\right) = 0$$

$$\alpha_3\left(\frac{A_1}{e} + \frac{C_1}{e}\right) + \alpha_4\left(\frac{E_1}{e} + \frac{G_1}{e}\right) - \nu\left(\frac{F_1}{e} - \frac{H_1}{e}\right) = 0$$

$$\frac{A_2}{e}\cos\lambda L_2 + \frac{B_2}{e}\sin\lambda L_2 - \frac{C_2}{e}\cosh\lambda L_2 - \frac{D_2}{e}\sinh\lambda L_2 = 0$$

$$\frac{A_2}{e}\alpha_5 + \frac{B_2}{e}\alpha_6 + \frac{C_2}{e}\alpha_7 + \frac{D_2}{e}\alpha_8 + \alpha_2\left[\frac{E_2}{e}\cos\lambda L_2 + \frac{F_2}{e}\sin\lambda L_2 + \frac{G_2}{e}\cosh\lambda L_2 + \frac{H_2}{e}\sinh\lambda L_2\right] = 0$$

$$\frac{E_2}{e}\cos\lambda L_2 + \frac{F_2}{e}\sin\lambda L_2 - \frac{G_2}{e}\cosh\lambda L_2 - \frac{H_2}{e}\sinh\lambda L_2 = 0$$

$$\alpha_3\left[\frac{A_2}{e}\cos\lambda L_2 + \frac{B_2}{e}\sin\lambda L_2 + \frac{C_2}{e}\cosh\lambda L_2 + \frac{D_2}{e}\sinh\lambda L_2\right] + \frac{E_2}{e}\alpha_9 + \frac{F_2}{e}\alpha_{10} + \frac{G_2}{e}\alpha_{11} + \frac{H_2}{e}\alpha_{12} = 0$$

$$\frac{A_1}{e}\cos\lambda L_1 + \frac{B_1}{e}\sin\lambda L_1 + \frac{C_1}{e}\cosh\lambda L_1 + \frac{D_1}{e}\sinh\lambda L_1 - \frac{A_2}{e} - \frac{C_2}{e} = 0$$

$$
\begin{aligned}
&-\frac{A_1}{e}\sin\lambda L_1 + \frac{B_1}{e}\cos\lambda L_1 + \frac{C_1}{e}\sinh\lambda L_1 + \frac{D_1}{e}\cosh\lambda L_1 \\
&\qquad - \frac{B_2}{e} - \frac{D_2}{e} = 0
\end{aligned}
$$

$$
\begin{aligned}
&-\frac{A_1}{e}\cos\lambda L_1 - \frac{B_1}{e}\sin\lambda L_1 + \frac{C_1}{e}\cosh\lambda L_1 + \frac{D_1}{e}\sinh\lambda L_1 \\
&\qquad + \frac{A_2}{e} - \frac{C_1}{e} = 0
\end{aligned}
$$

$$
\begin{aligned}
&\frac{A_1}{e}\sin\lambda L_1 - \frac{B_1}{e}\cos\lambda L_1 + \frac{C_1}{e}\sinh\lambda L_1 + \frac{D_1}{e}\cosh\lambda L_1 \\
&\qquad + \frac{B_2}{e} - \frac{D_2}{e} = i\lambda L
\end{aligned}
$$

$$
\begin{aligned}
&\frac{E_1}{e}\cos\lambda L_1 + \frac{F_1}{e}\sin\lambda L_1 + \frac{G_1}{e}\cosh\lambda L_1 + \frac{H_1}{e}\sinh\lambda L_1 \\
&\qquad - \frac{E_2}{e} - \frac{G_2}{e} = 0
\end{aligned}
$$

$$
\begin{aligned}
&-\frac{E_1}{e}\sin\lambda L_1 + \frac{F_1}{e}\cos\lambda L_1 + \frac{G_1}{e}\sinh\lambda L_1 + \frac{H_1}{e}\cosh\lambda L_1 \\
&\qquad - \frac{F_2}{e} - \frac{H_2}{e} = 0
\end{aligned}
$$

$$
\begin{aligned}
&-\frac{E_1}{e}\cos\lambda L_1 - \frac{F_1}{e}\sin\lambda L_1 + \frac{G_1}{e}\cosh\lambda L_1 + \frac{H_1}{e}\sinh\lambda L_1 \\
&\qquad + \frac{E_2}{e} - \frac{G_2}{e} = 0
\end{aligned}
$$

$$
\begin{aligned}
&\frac{E_1}{e}\sin\lambda L_1 - \frac{F_1}{e}\cos\lambda L_1 + \frac{G_1}{e}\sinh\lambda L_1 + \frac{H_1}{e}\cosh\lambda L_1 \\
&\qquad + \frac{E_2}{e} - \frac{H_2}{e} = -\lambda L
\end{aligned}
$$

(28)

in which

$$\lambda L = \pi\left(\frac{\omega}{\omega_c}\right)^{\frac{1}{2}}, = \left\{\frac{Me\omega^2}{EIg\cdot e}\right\}^{\frac{1}{4}}\cdot L$$

$$\lambda L_1 = \mathcal{L}\,\pi\left(\frac{\omega}{\omega_c}\right)^{\frac{1}{2}}$$

$$\lambda L_2 = (1-\mathcal{L})\,\pi\left(\frac{\omega}{\omega_c}\right)^{\frac{1}{2}}$$

$$\nu = \left(\frac{5\pi^3}{192}\right)\left(\frac{c}{\delta}\right)\left(\frac{\omega}{\omega_c}\right)^{\frac{3}{2}} = \frac{EI\lambda^3 C}{W}$$

$$\alpha_1 = \left[\frac{K_{yy} C}{W} + \frac{i C \omega C_{yy}}{W} \right]$$

$$\alpha_2 = \left[\frac{K_{xy} C}{W} + \frac{i C \omega C_{xy}}{W} \right]$$

$$\alpha_3 = \left[\frac{K_{yx} C}{W} + \frac{i C \omega C_{yx}}{W} \right]$$

$$\alpha_4 = \left[\frac{K_{xx} C}{W} + \frac{i C \omega C_{xx}}{W} \right]$$

$$\alpha_5 = \left[-\nu \sin \lambda L_2 + \alpha_1 \cos \lambda L_2 \right]$$

$$\alpha_6 = \left[\nu \cos \lambda L_2 + \alpha_1 \sin \lambda L_2 \right]$$

$$\alpha_7 = \left[-\nu \sinh \lambda L_2 + \alpha_1 \cosh \lambda L_2 \right]$$

$$\alpha_8 = \left[-\nu \cosh \lambda L_2 + \alpha_1 \sinh \lambda L_2 \right]$$

$$\alpha_9 = \left[-\nu \sin \lambda L_2 + \alpha_4 \cos \lambda L_2 \right]$$

$$\alpha_{10} = \left[\nu \cos \lambda L_2 + \alpha_4 \sin \lambda L_2 \right]$$

$$\alpha_{11} = \left[-\nu \sinh \lambda L_2 + \alpha_4 \cosh \lambda L_2 \right]$$

$$\alpha_{12} = \left[-\nu \cosh \lambda L_2 + \alpha_4 \sinh \lambda L_2 \right]$$

It is convenient to reduce the preceding equations to a set of 6 simultaneous equations in A_1 B_1 C_1 D_1 E_1 F_1 H_1 to facilitate the computer solution which is to follow. After reducing and simplifying the equations become:

$$\frac{A_1}{e}\cdot 2\alpha_1 - \frac{B_1}{e}\cdot\nu + \frac{D_1}{e}\cdot\nu + \frac{E_1}{e}\cdot 2\alpha_2 = 0$$

$$\frac{A_1}{e}\cdot 2\alpha_3 + \frac{E_1}{e}\cdot 2\alpha_4 - \frac{F_1}{e}\cdot\nu + \frac{H_1}{e}\cdot\nu = 0$$

$$\frac{A_1}{e}\left[\cos\lambda L - \cosh\lambda L\right] + \frac{B_1}{e}\sin\lambda L - \frac{D_1}{e}\sinh\lambda L + i\left(\frac{\lambda L}{2}\right)\left[\sin\lambda L_2 + \sinh\lambda L_2\right] = 0$$

$$\frac{E_1}{e}\left[\cos\lambda L - \cosh\lambda L\right] + \frac{F_1}{e}\sin\lambda L - \frac{H_1}{e}\sinh\lambda L - \left(\frac{\lambda L}{2}\right)\left[\sin\lambda L_2 + \sinh\lambda L_2\right] = 0$$

$$\frac{A_1}{e}\left[\alpha_5\cos\lambda L_1 - \alpha_6\sin\lambda L_1 + \alpha_7\cosh\lambda L_1 + \alpha_8\sinh\lambda L_1\right] + \frac{B_1}{e}\left[\alpha_5\sin\lambda L_1 + \alpha_6\cos\lambda L_1\right]$$
$$+ \frac{D_1}{e}\left[\alpha_7\sinh\lambda L_1 + \alpha_8\cosh\lambda L_1\right] + \frac{E_1}{e}\alpha_2\left[\cos\lambda L + \cosh\lambda L\right] + \frac{F_1}{e}\alpha_2\sin\lambda L + \frac{H_1}{e}\alpha_2\sinh\lambda$$
$$= \left(\frac{\lambda L}{2}\right)\left[\alpha_2(\sin\lambda L_2 - \sinh\lambda L_2) - i(\alpha_6 - \alpha_8)\right.$$

$$\frac{A_1}{e}\alpha_3\left[\sin\lambda L + \sinh\lambda L\right] + \frac{B_1}{e}\alpha_3\sin\lambda L + \frac{D_1}{e}\alpha_3\sinh\lambda L$$
$$+ \frac{E_1}{e}\left[\alpha_9\cos\lambda L_1 - \alpha_{10}\sin\lambda L_1 + \alpha_{11}\cosh\lambda L_1 + \alpha_{12}\sinh\lambda L_1\right] + \frac{F_1}{e}\left[\alpha_9\sin\lambda L_1 + \alpha_{10}\cos\lambda L_1\right]$$
$$+ \frac{H_1}{e}\left[\alpha_{11}\sinh\lambda L_1 + \alpha_{12}\cosh\lambda L_1\right] = \left(\frac{\lambda L}{2}\right)\left[(\alpha_{10} - \alpha_{12}) - i\,\alpha_3(\sin\lambda L_2 - \sinh\lambda L_2)\right] \quad (29)$$

The following expressions exist for the remaining constants in terms of the above unknowns.

$$\frac{A_1}{e} = \frac{C_1}{e}$$

$$\frac{E_1}{e} = \frac{G_1}{e}$$

$$\frac{A_2}{e} = \frac{A_1}{e}\cos\lambda L_1 + \frac{B_1}{e}\sin\lambda L_1$$

$$\frac{B_2}{e} = -\frac{A_1}{e}\sin\lambda L_1 + \frac{B_1}{e}\cos\lambda L_1 + i\left(\frac{\lambda L}{2}\right)$$

$$\frac{C_2}{e} = \frac{A_1}{e}\cosh\lambda L_1 + \frac{D_1}{e}\sinh\lambda L_1$$

$$\frac{D_2}{e} = \frac{A_1}{e}\sinh\lambda L_1 + \frac{D_1}{e}\cosh\lambda L_1 - i\left(\frac{\lambda L}{2}\right)$$

$$\frac{E_2}{e} = \frac{E_1}{e}\cos\lambda L_1 + \frac{F_1}{e}\sin\lambda L_1$$

$$\frac{F_2}{e} = -\frac{E_1}{e}\sin\lambda L_1 + \frac{F_1}{e}\cos\lambda L_1 - \left(\frac{\lambda L}{2}\right)$$

$$\frac{G_2}{e} = \frac{E_1}{e}\cosh\lambda L_1 + \frac{H_1}{e}\sinh\lambda L_1$$

$$\frac{H_2}{e} = \frac{E_1}{e}\sinh\lambda L_1 + \frac{H_1}{e}\cosh\lambda L_1 + \left(\frac{\lambda L}{2}\right) \qquad (30)$$

Calculation of Rotor Displacements

In the region $0 \le z_1 \le L_1$, the respective coordinate displacements are given by Eqs. (3) and (6). In order to determine the maximum and minimum values of whirl amplitude, as shown in Figure 5, these equations must be expressed as follows:

Eq. 3: $$Y_1 = \left[A_1\cos\lambda z_1 + B_1\sin\lambda z_1 + C_1\cosh\lambda z_1 + D_1\sinh\lambda z_1\right]e^{i\omega t}$$

Expanding the integration constants in terms of their real and imaginary parts

$$A_1 = A_1^r + iA_1^i \quad ; \quad B_1 = \ldots\ldots \text{ etc.}$$

Thus, $$Y_1 = A\cos\omega t - B\sin\omega t$$

where $$A = A_1^r\cos\lambda z_1 + B_1^r\sin\lambda z_1 + C_1^r\cosh\lambda z_1 + D_1^r\sinh\lambda z_1$$

$$B = A_1^i\cos\lambda z_1 + B_1^i\sin\lambda z_1 + C_1^i\cosh\lambda z_1 + D_1^i\sinh\lambda z_1 \qquad (31)$$

Rejecting the imaginary components gives the above Equations (31)

Similarly, for the other coordinate deflexions:

Eq. 6: $$X_1 = \left[E_1 \cos \lambda z_1 + F_1 \sin \lambda z_1 + G_1 \cosh \lambda z_1 + H_1 \sinh \lambda z_1\right] e^{i\omega t}$$

$$E_1 = E_1^r + iE_1^i \quad ; \quad F_1 = \text{----} \text{ etc.}$$

Thus $$X_1 = E \cos \omega t - F \sin \omega t$$

where

$$E = E_1^r \cos \lambda z_1 + F_1^r \sin \lambda z_1 + G_1^r \cosh \lambda z_1 + H_1^r \sinh \lambda z_1$$

$$F = E_1^i \cos \lambda z_1 + F_1^i \sin \lambda z_1 + G_1^i \cosh \lambda z_1 + \tag{32}$$

The axes of the whirl amplitude ellipse may be calculated as follows:

Major axis: $$a = \sqrt{\tfrac{1}{2}\left[A^2+B^2+E^2+F^2\right] + \tfrac{1}{2}\sqrt{\left[A^2+B^2+E^2+F^2\right]-4\left[-AF+BE\right]^2}} \tag{33}$$

Minor axis: $$b = \sqrt{\tfrac{1}{2}\left[A^2+B^2+E^2+F^2\right] - \tfrac{1}{2}\sqrt{\left[A^2+B^2+E^2+F^2\right]-4\left[-AF+BE\right]^2}} \tag{34}$$

Angle between x- axis and major axis of ellipse:

$$\alpha = \tfrac{1}{2} \operatorname{artan}\left[\frac{2(AE+BF)}{(A^2+B^2-E^2-F^2)}\right] \tag{35}$$

Angle between major axis and unbalance force:

$$\beta = \tfrac{1}{2} \operatorname{artan}\left[\frac{2(AB+EF)}{(A^2-B^2+E^2-F^2)}\right] \tag{36}$$

In the region $0 \leq z_2 \leq L_2$, rotor displacement amplitudes are given by Eqs. (4) and (7). Operating on these in a similar manner to the above gives:

$$Y_2 = A \cos \omega t - B \sin \omega t$$

where

$$A = A_2^r \cos \lambda z_2 + B_2^r \sin \lambda z_2 + C_2^r \cosh \lambda z_2 + D_2^r \sinh \lambda z_2$$

$$B = A_2^i \cos \lambda z_2 + B_2^i \sin \lambda z_2 + C_2^i \cosh \lambda z_2 + D_2^i \sinh \lambda z_2 \tag{37}$$

$$X_2 = E \cos \omega t - F \sin \omega t$$

$$E = E_2^r \cos \lambda z_2 + F_2^r \sin \lambda z_2 + G_2^r \cosh \lambda z_2 + H_2^r \sinh \lambda z_2$$

$$F = E_2^i \cos \lambda z_2 + F_2^i \sin \lambda z_2 + G_2^i \cosh \lambda z_2 + H_2^i \sinh \lambda z_2 \tag{38}$$

The major axis a, minor axis b, position angle α and phase angle β may again be calculated by using Eqs. (33), (34), (35) and (36).

Calculation of Transmitted Force

The force transmitted from the rotor to the bearings due to its motion may be calculated by evaluating the end shear force acting on the rotor, as this force is made up of the resultant spring and damping acting at that point. For the left-hand bearing $z_1 = o$, from Eq. (3),

$$V(Y_1)(o) - F(Y_1)(o) = o$$

where

$$V(Y_1)(o) = -EI\frac{d^3Y_1(o)}{dz_1^3} = -EI\lambda^3\left[A_1\sin\lambda z_1 - B_1\cos\lambda z_1 + C_1\sinh\lambda z_1 + D_1\cosh\lambda z_1\right]e^{i\omega t}$$

Rejecting the imaginary components, the dimensionless force in the y-direction is given by

$$\frac{F_y c}{W\cdot e} = A\cos\omega t - B\sin\omega t$$

where

$$\begin{aligned} A &= -\nu\left[A_1^r\sin\lambda z_1 - B_1^r\cos\lambda z_1 + C_1^r\sinh\lambda z_1 + D_1^r\cosh\lambda z_1\right] \\ B &= -\nu\left[A_1^i\sin\lambda z_1 - B_1^i\cos\lambda z_1 + C_1^i\sinh\lambda z_1 + D_1^i\cosh\lambda z_1\right] \end{aligned} \qquad (39)$$

Similarly, the force in the x- direction is given by

$$\frac{F_x c}{W\cdot e} = E\cos\omega t - F\sin\omega t$$

where

$$\begin{aligned} E &= -\nu\left[E_1^r\sin\lambda z_1 - F_1^r\cos\lambda z_1 + G_1^r\sinh\lambda z_1 + H_1^r\cosh\lambda z_1\right] \\ F &= -\nu\left[E_1^i\sin\lambda z_1 - F_1^i\cos\lambda z_1 + G_1^i\sinh\lambda z_1 + H_1^i\cosh\lambda z_1\right] \end{aligned} \qquad (40)$$

Maximum and minimum values of the transmitted force at the left-hand bearing may also be obtained from the properties of the transmitted force ellipse, described by Eqs. (34) and (34) as follows:

$$F_1(max) = \sqrt{\tfrac{1}{2}\left[A^2+B^2+E^2+F^2\right] + \tfrac{1}{2}\sqrt{\left[A^2+B^2+E^2+F^2\right]-4\left[-AF+BE\right]^2}}$$

$$F_1(min) = \sqrt{\tfrac{1}{2}\left[A^2+B^2+E^2+F^2\right] - \tfrac{1}{2}\sqrt{\left[A^2+B^2+E^2+F^2\right]-4\left[-AF+BE\right]^2}}$$

For the right-hand bearing $Z_2 = L_2$, the transmitted force in the y- direction is found from Eq. (18)

$$V(Y_2)(L_2) + F(Y_2)(L_2) = 0$$

Thus $$\frac{F_y c}{We} = A\cos\omega t - B\sin\omega t$$

where $$A = \nu\left[A_2^r \sin\lambda Z_2 - B_2^r \cos\lambda Z_2 + C_2^r \sinh\lambda Z_2 + D_2^r \cosh\lambda Z_2\right]$$

$$B = \nu\left[A_2^i \sin\lambda Z_2 - B_2^i \cos\lambda Z_2 + C_2^i \sinh\lambda Z_2 + D_2^i \cosh\lambda Z_2\right] \quad (41)$$

Similarly, in the x- direction,

$$\frac{F_x c}{We} = E\cos\omega t - F\sin\omega t$$

where $$E = \nu\left[E_2^r \sin\lambda Z_2 - F_2^r \cos\lambda Z_2 + G^r \sinh\lambda Z_2 + H^r \cosh\lambda Z_2\right]$$

$$F = \nu\left[E_2^i \sin\lambda Z_2 - F_2^i \cos\lambda Z_2 + G^i \sinh\lambda Z_2 + H^i \cosh\lambda Z_2\right] \quad (42)$$

Maximum and minimum values of the transmitted force and of the phase angle may now be obtained using the above constants, by the previously described method. The above equations have been programmed for computer solution. The program is given in Appendix B. Computed results for maximum amplitude and maximum transmitted force are shown graphically in Figures (6) to (24).

RESULTS

General Features of the Results

The results obtained apply to ranges of parameters which identify the performance characteristics of a high-speed rotor in fluid-film bearings. Also provided is a maximum of design information. The location of the rotor unbalance on the shaft determines the modes which may be excited in the motion. The speed, stiffness ratio and bearing eccentricity govern the rotor amplitude and the transmitted force. Table II, page 19 , lists the unbalance location and amplitude position or transmitted force location for each of Figures 6 through 23. Two particular cases have been examined in detail: (a) Midspan (static) unbalance $L_1 = 0.50$ L and (b) unbalance at $L_1 = 0.45$ L and 0 55 L superimposed 180 degrees apart to give the dynamic unbalance condition. The charts show:

(a) Variation of maximum rotor amplitude at a given station with speed, due to rotor unbalance

(b) Variation of maximum transmitted force between rotor and bearing with speed, due to rotor unbalance.

Using the charts and principles discussed in this section, a preliminary high-speed rotor design may be established. Final design behavior may be examined by use of the computer program listed in Appendix 2. The following is a discussion of certain features.

Unbalance at Midspan

Due to symmetry of the system, only symmetrical rotor modes may be excited. Examples of these mode shapes are given in Figs. 26. Amplitude at this unbalance position is large in all modes. Amplitude at the unbalance position is shown in Figs. 6 through 8, for eccentricity ratios of 0.2, 0.5 and 0.7 respectively. Amplitude at the bearings is shown in Figs. 9 through 11. Transmitted force at the bearings is indicated in Figs. 19 through 21.

Unbalance at $L_1 = 0.45$ L and 0.55 L, Superimposed

This unbalance condition is also associated with large rotor displacements in the lowest mode. Although the unbalance forces are symmetrically arranged about the half-span point, the 180 degree phase difference between the forces causes a

TABLE II

Details of System for Unbalance Response Calculations

Fig. No.	Unbalance Position	Amplitude Position	Transmitted Force Position	Bearing Eccentricity Ratio
6	$L_1 = 0.5L$,	$Z_1 = L_1$		0.2
7	Midspan	Midspan		0.5
8				0.7
9	$L_1 = 0.5L$	$Z_1 = 0$		0.2
10	Midspan	Left-hand Bearing		0.5
11				0.7
12	$L_1 = 0.45$ L	$Z_1 = 0.25L_1$		0.2
13				0.5
14				0.7
15	$L_1 = 0.45L$	$Z_1 = 0$		0.2
16		Left Hand Bearing		0.5
17				0.7
18	$L_1 = 0.45L$	$Z_1 = L_1$		0.5
19	$L_1 = 0.5L$		$Z_1 = 0$	0.2
20			Left-hand Bearing	0.5
21				0.7
22	$L_1 = 0.45L$		$Z_1 = 0$	0.2
23			Left-hand Bearing	0.5
24				0.7

moment to act on the rotor which gives rise to both symmetrical and asymmetrical modes of oscillation. These modes are shown in Fig. 27. Amplitude response at $Z_1 = 0.25L_1$ is given in Figs. 12 through 14, close to the left-hand journal but sufficiently on the rotor for the relative response of all modes to be present in the results. Amplitude response at the left-hand bearing is shown in Figs. 15 through 17, and force transmitted at the left-hand bearing is indicated in Figs. 22 through 24. The amplitude versus speed results shown in Fig. 18 indicate the

displacement response at the unbalance position $Z_1 = L_1$ for asymmetrical unbalance. Bearing eccentricity is $\eta = 0.5$. Response for two rotor stiffnesses is shown, $c/\delta = 0.3$ and $c/\delta = 10.0$.

Influence of Eccentricity Ratio η

Each eccentricity value corresponds to a particular Sommerfeld Number $(\frac{\mu NLD}{W_1})(\frac{R}{C})^2 = S$. The relationship for the plain cylindrical bearing is shown in Fig. 25. In calculating any particular rotor-bearing system, it is necessary to first calculate the Sommerfeld Number corresponding to the bearing operating conditions. Using Fig. 25, the eccentricity can be found, corresponding to the bearing L/D ratio. The eccentricity so found allows the appropriate figures to be selected for the determination of amplitude and transmitted force.

Influence of Unbalance on Rotor Dynamic Performance

The rotor-bearing system characteristics may be discussed conveniently in terms of the following seven cases of response results:

1. Midspan amplitude; midspan unbalance. Influence of eccentricity ratio. Figs. 6, 7, 8.
2. Journal Amplitude; midspan unbalance. Influence of eccentricity ratio. Figs. 9, 10, 11.
3. Shaft amplitude at $Z_1/L_1 = 0.25$; unbalance at $L_1/L = 0.45, 0.55$. Influence of eccentricity ratio. Figs. 12, 13, 14.
4. Journal amplitude; unbalance at $L_1/L = 0.45, 0.55$. Influence of eccentricity ratio. Figs 15, 16, 17.
5. Shaft amplitude at $Z_1/L_1 = 1$, unbalance at $L_1/L = 0.45$. Eccentricity ratio $\eta = 0.5$. Fig. 18.
6. Transmitted force; midspan unbalance. Influence of eccentricity ratio. Figs. 19, 20, 21.
7. Transmitted force; unbalance of $L_1/L = 0.45, 0.55$. Influence of eccentricity ratio. Figs. 22, 23, 24.

A number of general conclusions can be drawn from each case, and these are listed below. The terms "low speed range," "medium speed range," and "high speed range,"

are used for convenience and refer approximately to speed ratios, $\frac{\omega}{\omega_c}$, 0 to 1.0, 1.0 to 10.0, and 10.0 to 24.0 respectively. Critical speeds are identified below by reference to these speed ranges, because changes in stiffness parameter and unbalance position influence the modes which may appear in the motion, and make comparison difficult along conventional lines.

Case A: Flexible bearings serve to:

(1) increase shaft amplitude in the low speed range,
(2) attenuate the fundamental critical amplitude,
(3) cause a critical speed with large amplitude in the medium speed range.

Rigid bearings tend to:

(1) limit amplitude in the low speed range,
(2) cause a critical with large amplitudes around $\omega/\omega_c = 1.0$ (Rigid bearing critical)
(3) attenuate amplitude in the medium speed range.

Both bearing types tend to:

(1) cause a large critical in the high speed range, with larger amplitudes in the case of flexible bearings.

The effect of increased journal eccentricity is:

(1) increased amplitude in the low speed range for flexible bearing case.
(2) increased the medium speed amplitude peak for flexible bearings.
(3) increased the number of small amplitude peaks throughout the speed range, for both bearing types.

Case B: Flexible bearings tend to:

(1) increase journal amplitude in the low speed range,
(2) cause a large amplitude critical in the medium speed range,

Rigid bearings tend to:

(1) limit amplitude in the low speed range,

(2) attenuate amplitudes in the medium speed range.

Both bearing types tend to:

(1) give similar amplitudes around $\omega/\omega_c = 1.0$,
(2) give a critical in the same area in the high-speed range, with larger amplitudes in the case of flexible bearings.

The effect of increased journal eccentricity is:

(1), (2), (3) same general effect as in Case A.
(4) decreased the low and medium speed attenuation in the case of rigid bearings.

Case C: Flexible bearings tend to:

(1) increase journal amplitudes in the low speed range,
(2) give a large critical in the medium speed range,
(3) attenuate amplitudes below $\omega/\omega_c = 4.5$.

Rigid bearings tend to:

(1) limit amplitudes in the low speed range,
(2) cause a critical around $\omega/\omega_c = 1.0$

Both bearing types tend to:

(1) create large amplitudes in the medium to high speed range,
(2) create a large critical in the high speed range, with larger amplitudes for flexible bearings.

The effect of increased journal eccentricity is:

(1), (3) as in Case A. No other major effect.

Case D: Similar tendencies to Case B occur.

The effect of increased journal eccentricity is:

(1), (3) as in Case A. No other major effect.

Case E: Similar tendencies occur with bearing transmitted force to those which occur with amplitude in Case B.

The effect of increased journal eccentricity is:

(1) Somewhat increased transmitted force in low speed range for flexible bearings.

Case F: Flexible bearings tend to:

(1) increase transmitted force in the low speed range,
(2) promote an amplitude build-up in the medium speed range,
(3) give higher over-all transmitted forces throughout the speed range.

Rigid bearings tend to:

(1) limit transmitted force in the low-speed range,
(2) attenuate transmitted force in the medium speed range,

Both bearing types tend to:

(1) give similar force values around $\omega/\omega_c = 1.0$,
(2) cause a large increase in transmitted force in the high speed range, with highest values for flexible bearings,
(3) sustained high transmitted forces beyond high speed critical.

The effect of increased journal eccentricity is:

(1) As in case E.

Consideration of the above list reveals certain consistent tendencies which appear in all cases. These may be explained as follows:

(a) increased bearing flexibility tends to limit rotor amplitude in the low speed range. This is due to the normal attenuation which accompanies any system flexibility and more effective use of squeeze-film damping effects in the clearance. The critical speed is decreased because of the added system flexibility. The upper limit of the fundamental critical speed is the rigid bearing case, $\omega/\omega_c = 1.0$.

(b) Attenuation in the medium speed range is a normal condition for operation beyond the rigid bearing critical speed of any elastic rotor. In the flexible bearing case, there is some attenuation beyond the first low-speed critical. This critical is predominantly a bearing flexibility, rigid-body effect. The amplitude peak in the medium speed range is the second system critical. It includes both bearing flexibility effects and shaft flexure effects.

(c) The high speed critical occurs at approximately the same speed ratio for all stiffnesses because here the bearings are effectively rigid and the rotor oscillates as a pinned-pinned beam in the third harmonic mode.

(d) An increase in the number of small amplitude peaks for operation at higher eccentricity ratios occurs because the respective stiffnesses in the x and y directions of both bearings become significantly different with increase in journal eccentricity. This tends to give rise to two critical speeds, each associated with a particular coordinate stiffness.

Bearing Attenuation

Figures 19 through 24 indicate that greater attenuation of transmitted force is achieved by using a flexible rotor in relatively stiff bearings throughout the low and medium speed ranges.

For symmetrical unbalance the transmitted force for a rigid-bearing flexible-rotor system $C/\delta = 0.3$, is often an order of magnitude lower than for a flexible-bearing rigid rotor system. For both systems the transmitted force is of comparable magnitude in the high speed range, except at the high speed critical peak. For unsymmetrical unbalance, the same general result occurs, but to a somewhat lesser degree.

In the low speed range, operation at a bearing eccentricity of 0.5 gives the greatest attenuation of transmitted force, for both unbalance conditions. At this eccentricity the decrease is in the order of 15 to 20 percent over the other eccentricities. For the medium speed range, the attenuation obtained in the flexible bearing rigid-rotor case appears to increase with increase in eccentricity, while in the rigid-bearing flexible-rotor case the attenuation decreases with

increase in eccentricity. In the high speed range, the degree of attenuation obtained depends on both the nature of the unbalance and on the type of system, but the general result is that operation at an eccentricity of 0.5 promotes the most likely condition for obtaining good attenuation of transmitted force. In this case, specific results should be obtained from the curves themselves.

In general, the results indicate that the operating eccentricity at which the maximum attenuation of transmitted force occurs depends on the stiffness ratio of the system, the nature of the unbalance and on the speed of operation. In the low speed range $\eta = 0.5$ gives the greatest attenuation, but for higher speeds this simple rule does not apply, and the curves must be used to select the operating eccentricity, and to examine how the run-up and run-down transmitted force characteristics will be influenced by change in eccentricity with speed.

Comparison With Other Results

The results of the present investigation were verified against those given by a proven existing computer program. This other program was based on the Myklestad-Prohl method of beam analysis, in which the rotor is divided into a specific number of discrete masses, separated from each other by flexible members which represent the rotor elasticity. The program includes the fluid-film bearing properties as spring and damping coefficients in both the x- and y-directions in the same manner as described in this report. The results of this comparison are shown in Figure 28. It will be seen that the agreement is very close in all cases. This existing program could have obtained all the results given herein, but the computing time involved would have become increasingly greater for the higher modes. The present analysis takes the same computing time whatever the mode, and the results obtained are exact and independent of the number of discrete masses into which the rotor is divided.

The results obtained were also compared with those given in the earlier investigation, References 1 and 2. No satisfactory correlation was obtained in either case, for a number of reasons. The single disc rotor of Reference 1 has its mass and unbalance concentrated at a single point. When the mass is 'distributed' across the span for comparison with the present work, the unbalance is, in effect, distributed also. This changes both the magnitude and nature of the disturbing force,

and so changes the rotor response. No meaningful comparison was achieved in this case. A similar condition occurred when a comparison was attempted with Reference 2. Rotor mass and unbalance are again concentrated at discrete points and so the problem of distribution again arises. This instance is more complicated as the properties of the first and second critical speeds are obtained uniquely for either case from the equations, by adjusting the nature of the unbalance and its position. This gives results which are properties of that mode alone. Static and dynamic response results cannot be superimposed into an overall effect. Both types of result arise naturally in the present analysis. Also, the results given herein apply for circular cylindrical bearings, whereas the results of Reference 2 apply to the 150 degree partial arc bearing. In operation the dynamic properties of both bearing types are quite similar due to the presence of cavitation in the cylindrical fluid film. This means that the present results may be used to obtain a fair indication of the performance of an elastic rotor in partial arc bearings as well.

The results of comparison with other data are that excellent correlation was found where the rotor and its operation was simulated exactly, using a computerized discrete-mass approach and that no direct comparison was obtainable with other published work because an adequate numerical comparison between the operating unbalance condition, the rotor mass distribution, and the mechanism of modal excitation could not be made.

Mode Shapes

Symmetrical Unbalance

Figure 26 applies to the operating conditions shown in Fig. 7, $C/\delta = 10.0$ and $\eta = 0.5$. The five mode shapes correspond to major features of that curve. Local amplitude peaks occur at speed ratios of 0.6, 2.25 and 12.0. Local minima occur at 1.50 and 9.0. Figure 26 indicates the rotor form under these conditions.

The damping introduced by the bearings serves to limit the peak amplitudes, and to increase the magnitude of the attenuation which may be realized between critical speeds. This is evident from the amplitude scales shown, and also from Fig. 7. The heavily attenuated low-speed critical at $\omega/\omega_c = 0.60$ is mainly composed of rigid body shaft displacement within the bearings, with a slight amount of bending. At $\omega/\omega_c = 1.50$ the local maximum attenuation occurs, but the increased speed effects plus the high stiffness and damping present hold the amplitude to two-thirds of the first crtical amplitude at midspan, and give rise to amplitudes at the ends which are greater than those of the first critical.

The increased bending associated with higher speeds is clearly shown in the second critical speed mode shape at $\omega/\omega_c = 2.25$. This mode is similar in form to the fundamental free-free vibration of a uniform beam. The results show that flexible shafts tend towards pinned-pinned beam modes, while rigid shafts tend toward free-free modes, because for a flexible shaft the bearings control the motion, whereas in the latter case, the shaft properties alone determine its modal form.

A second attenuation trough occurs at $\omega/\omega_c = 9.00$. Amplitude at midspan is small, but elsewhere it is of moderate size with a maximum at the ends of 4.2. The third critical occurs at $\omega/\omega_c = 12.00$. The motion is almost wholly bending, and the form corresponds to the third mode of a free-free beam. The speed-dependent forcing promotes the large amplitudes which are indicated.

In this instance, the symmetry of the system and its excitation do not allow motions with asymmetrical modes to occur.

Asymmetrical Unbalance

The influence of dynamic moment unbalance on the previously discussed operating

conditions, $c/\delta = 10.0$ and $\eta = 0.5$, is shown in Fig. 27. Figure 13 indicates the amplitude response. The low speed rigid-body critical speed occurs at $\omega/\omega_c = 0.9$. The motion is mainly translation with some rocking and no bending. This speed constitutes a 50 percent rise over the previous unbalance case, but there is significant decrease in amplitude level. There is very little bending present in this mode. At $\omega/\omega_c = 3.0$, an attenuation trough exists. The mode shape here is similar to the free-free beam fundamental. The second critical speed occurs at $\omega/\omega_c = 6.0$. This corresponds to the second free-free beam modal form, and the increased existing force again begins to promote large amplitudes with the higher speeds. This mode is almost wholly bending. The third critical speed occurs at $\omega/\omega_c = 20.0$, accompanied by even higher amplitudes, with a shape corresponding to the fourth free-free beam mode. There is an order of magnitude amplitude decrease within the intervening trough between criticals, which means that between $\omega/\omega_c = 5.0$ and 25.0 midspan amplitudes never decrease below $(x/e) = 1.0$ and are usually much larger for most of this range. Modal form within the amplitude trough was not determined, but is is likely that it would be similar to the third free-free beam mode, considering the above-mentioned sequence of free-free beam forms.

The moment unbalance tends to give rise to even free-free modes more readily than to the odd modes. These latter tend to occur in the amplitude "troughs", which themselves are often associated with large amplitudes, probably because they contain suppressed criticals.

CONCLUSIONS

1. A study has been made of the dynamic behavior of an unbalanced elastic rotor supported in damped fluid-film bearings. Extensive numerical results have been obtained for amplitude response and transmitted force, over wide ranges of speed, system stiffness and bearing operating conditions.

2. The results indicate that rotor motions are largely determined by the interaction between rotor stiffness and bearing stiffness; and by the type of unbalance, force or moment, which is present in the system.

3. A flexible rotor tends to vibrate in modes which are determined by the rigidity of the bearings, i.e., as a pinned-pinned beam. A rigid rotor vibrates as a rigid body at low speeds, but where bending effects predominate, its motions are similar to those of a free-free beam.

4. Symmetrical unbalance excites only those modes which are symmetrical about midspan. Unsymmetrical or moment unbalance excites mainly motions which are unsymmetrical about midspan, and suppresses the symmetrical motions somewhat.

5. The operating eccentricity corresponding to maximum transmitted force attenuation depends on the stiffness ratio of the system, the nature of the unbalance, and on the speed of operation. In the low-speed range $\eta = 0.5$ gives the greatest attenuation, but for higher speeds this simple rule does not apply and the curves given herein must be used to select the condition of optimum operation.

6. The results obtained may be used directly as a guide towards a preliminary design. The performance of the final design may be obtained by using the computer program listed herein.

7. Correlation between the results obtained herein and those given by a comparable computer program of known accuracy has been demonstrated.

REFERENCES

1. Lund, J. W. and Sternlicht, B., "Rotor-Bearing Dynamics with Emphasis on Attenuation," Journal of Basic Engineering, Transactions ASME, Vol. 84, Series D, December, 1962.

2. Warner, P. C. and Thoman, R. J., "The Effect of The 150 Degree Partial Bearings on Rotor-Unbalance Vibration," ASME Transactions., Paper No. 63-Lubs-6 Presented June 2-5, 1963, Boston.

APPENDIX A. Notation for Spring and Damping Coefficients

Reference 1 lists the dimensionless bearing stiffnesses as:

$$\frac{K_{xx}}{\frac{1}{c}\lambda\omega} \qquad \frac{K_{xy}}{\frac{1}{c}\lambda\omega} \qquad \frac{K_{yx}}{\frac{1}{c}\lambda\omega} \qquad \frac{K_{yy}}{\frac{1}{c}\lambda\omega}$$

where K_{xx}, K_{xy}, K_{yx}, K_{yy} are the bearing stiffness coefficients in the xx, xy, yx and yy directions respectively.

c is the bearing clearance and

$\lambda\omega = \frac{SW_l}{\pi}$ where S = Sommerfeld Number

and W_l = bearing load.

Similarly the dimensionless bearing damping is given as

$$\frac{\omega C_{xx}}{\frac{1}{c}\lambda\omega} \qquad \frac{\omega C_{xy}}{\frac{1}{c}\lambda\omega} \qquad \frac{\omega C_{yx}}{\frac{1}{c}\lambda\omega} \qquad \frac{\omega C_{yy}}{\frac{1}{c}\lambda\omega}$$

where C_{xx}, C_{xy}, C_{yx}, C_{yy} are the bearing velocity damping coefficients in the xx, xy, yx and yy direction respectively.

Notation used differs between References 1 and 2 respectively, and in the present report. For ease of comparison the following table has been prepared.

TABLE II

Comparative Listing of Symbols Used for Stiffness and Damping Coefficients

Lund and Sternlicht (1)	Warner and Thoman (2)	Present Work
K_{xx}	CK_y/W	K_{xx}
K_{yy}	CK_x/W	K_{yy}
$-K_{xy}$	CD_y/W	K_{xy}
$-K_{yx}$	$-CD_x/W$	K_{yx}
C_{xx}	$CB_{yy}\omega/W$	C_{xx}
C_{yy}	$CB_{xx}\omega/W$	C_{yy}
$-C_{xy}$	$CB_{yx}\omega/W$	C_{xy}
$-C_{yx}$	$CB_{xy}\omega/W$	C_{yx}

```
C     MECHANICAL TECHNOLOGY INC., LATHAM,N.Y., ST5-0922   J. MICHAUD
C     PN0121   VIBRATION ANALYSIS OF A UNIFORM BEAM
      DIMENSION SPD(100),DEFL(15),DIST(10),A(6,6),B(6,6),C(6),D(6)
      DIMENSION E(12,12),F(12),IPIVO(12),PIVOT(12),ZEE1(10),ZEE2(10)
    1 READ 743
      READ 710, SXX,SXY,SYX,SYY
      READ 710, DXX,DXY,DYX,DYY
    2 READ 720, NSPD,NDEFL,NDIST,NZEE1,NZEE2,INPUT,NDIAG,NZ
      DO 650 JJ=1,NDIST,5
  650 READ 730, DIST(JJ),DIST(JJ+1),DIST(JJ+2),DIST(JJ+3),DIST(JJ+4)
      DO 660 MM=1,NDEFL,5
  660 READ 730, DEFL(MM),DEFL(MM+1),DEFL(MM+2),DEFL(MM+3),DEFL(MM+4)
      DO 670 II=1,NSPD,5
  670 READ 730, SPD(II),SPD(II+1),SPD(II+2),SPD(II+3),SPD(II+4)
      IF (NZ) 687,674,687
  674 IF (NZEE1) 675,675,680
  675 READ 735,ZEE2(1)
      NNN=2
      KFORK=1
      ZEE=ZEE2(1)
      GO TO 690
  680 DO 685 I=1,NZEE1,5
  685 READ 730, ZEE1(I),ZEE1(I+1),ZEE1(I+2),ZEE1(I+3),ZEE1(I+4)
      IF (NZEE2) 688,688,689
  688 NNN=1
      KFORK=1
      ZEE=ZEE1(1)
       GO TO 690
  689 DO 686 I=1,NZEE2,5
  686 READ 730,ZEE2(I),ZEE2(I+1),ZEE2(I+2),ZEE2(I+3),ZEE2(I+4)
      KFORK=2
```

```
      GO TO 690
  687 READ 730, Z1,Z2,ZEE
      KFORK=1
      NNN=1
  690 WRITE OUTPUT TAPE 3, 762
      WRITE OUTPUT TAPE 3, 743
      WRITE OUTPUT TAPE 3, 740, SXX,SXY,SYX,SYY
      WRITE OUTPUT TAPE 3, 741, DXX,DXY,DYX,DYY
      DO 900 JJ=1,NDIST
      DO 910 MM=1,NDEFL
      GO TO (691,692),KFORK
  691 WRITE OUTPUT TAPE 3, 744
      WRITE OUTPUT TAPE 3, 745
      WRITE OUTPUT TAPE 3, 746, DIST(JJ),DEFL(MM),NNN,ZEE
      WRITE OUTPUT TAPE 3, 747
      GO TO 695
  692 WRITE OUTPUT TAPE 3, 751
      WRITE OUTPUT TAPE 3, 745
  695 DO 920 II=1,NSPD
      GO TO (810,805),KFORK
  805 WRITE OUTPUT TAPE 3, 752, SPD(II),DIST(JJ),DEFL(MM)
      WRITE OUTPUT TAPE 3, 780
  810 DIST2=1.0-DIST(JJ)
      VAR1=3.1415927*SQRTF(SPD(II))
      ARG1=DIST(JJ)*VAR1
      ARG2=DIST2*VAR1
      GNU=0.257021*DEFL(MM)*SPD(II)*VAR1
      VAR2=COSF(VAR1)
      VAR3=SINF(VAR1)
      VAR4=COSF(ARG1)
      VAR5=SINF(ARG1)
```

```
VAR6=COSF(ARG2)
VAR7=SINF(ARG2)
VAR9=EXPF(VAR1)
VAR8=(VAR9+1.0/VAR9)/2.0
VAR9=(VAR9-1.0/VAR9)/2.0
VAR11=EXPF(ARG1)
VAR10=(VAR11+1.0/VAR11)/2.0
VAR11=(VAR11-1.0/VAR11)/2.0
VAR13=EXPF(ARG2)
VAR12=(VAR13+1.0/VAR13)/2.0
VAR13=(VAR13-1.0/VAR13)/2.0
AFR5=-GNU*VAR7+SYY*VAR6
AFI5=          DYY*VAR6
AFR6= GNU*VAR6+SYY*VAR7
AFI6=          DYY*VAR7
AFR7=-GNU*VAR13+SYY*VAR12
AFI7=           DYY*VAR12
AFR8=-GNU*VAR12+SYY*VAR13
AFI8=           DYY*VAR13
AFR9=-GNU*VAR7+SXX*VAR6
AFI9=          DXX*VAR6
AFR10=GNU*VAR6+SXX*VAR7
AFI10=         DXX*VAR7
AFR11=-GNU*VAR13+SXX*VAR12
AFI11=          DXX*VAR12
AFR12=-GNU*VAR12+SXX*VAR13
AFI12=          DXX*VAR13
THA4=VAR7+VAR13
THA7=VAR7-VAR13
A(1,1)=2.0*SYY
A(1,2)=-GNU
```

```
A(1,3)=GNU
A(1,4)=2.0*SYX
A(1,5)=0.0
A(1,6)=0.0
A(2,1)=2.0*SXY
A(2,2)=0.0
A(2,3)=0.0
A(2,4)=2.0*SXX
A(2,5)=-GNU
A(2,6)=GNU
A(3,1)=VAR2-VAR8
A(3,2)=VAR3
A(3,3)=-VAR9
A(3,4)=0.0
A(3,5)=0.0
A(3,6)=0.0
A(4,1)=0.0
A(4,2)=0.0
A(4,3)=0.0
A(4,4)=VAR2-VAR8
A(4,5)=VAR3
A(4,6)=-VAR9
A(5,1)=AFR5*VAR4-AFR6*VAR5+AFR7*VAR10+AFR8*VAR11
A(5,2)=AFR5*VAR5+AFR6*VAR4
A(5,3)=AFR7*VAR11+AFR8*VAR10
A(5,4)=SYX*(VAR2+VAR8)
A(5,5)=SYX*VAR3
A(5,6)=SYX*VAR9
A(6,1)=SXY *(VAR2+VAR8)
A(6,2)=SXY *VAR3
A(6,3)=SXY *VAR9
```

```
A(6,4)=AFR9*VAR4-AFR10*VAR5+AFR11*VAR10+AFR12*VAR11
A(6,5)=AFR9*VAR5+AFR10*VAR4
A(6,6)=AFR11*VAR11+AFR12*VAR10
B(1,1)=2.0*DYY
B(1,2)=0.0
B(1,3)=0.0
B(1,4)=2.0*DYX
B(1,5)=0.0
B(1,6)=0.0
B(2,1)=2.0*DXY
B(2,2)=0.0
B(2,3)=0.0
B(2,4)=2.0*DXX
B(2,5)=0.0
B(2,6)=0.0
B(3,1)=0.0
B(3,2)=0.0
B(3,3)=0.0
B(3,4)=0.0
B(3,5)=0.0
B(3,6)=0.0
B(4,1)=0.0
B(4,2)=0.0
B(4,3)=0.0
B(4,4)=0.0
B(4,5)=0.0
B(4,6)=0.0
B(5,1)=AFI5*VAR4-AFI6*VAR5+AFI7*VAR10+AFI8*VAR11
B(5,2)=AFI5*VAR5+AFI6*VAR4
B(5,3)=AFI7*VAR11+AFI8*VAR10
B(5,4)=DYX*(VAR2+VAR8)
```

```
      B(5,5)=DYX*VAR3
      B(5,6)=DYX*VAR9
      B(6,1)=DXY *(VAR2+VAR8)
      B(6,2)=DXY *VAR3
      B(6,3)=DXY *VAR9
      B(6,4)=AFI9*VAR4-AFI10*VAR5+AFI11*VAR10+AFI12*VAR11
      B(6,5)=AFI9*VAR5+AFI10*VAR4
      B(6,6)=AFI11*VAR11+AFI12*VAR10
      C(1)=0.0
      C(2)=0.0
      C(3)=0.0
      C(4)=0.5*VAR1*THA4
      C(5)=0.5*VAR1*(THA7*SYX +(AFI6-AFI8))
      C(6)=0.5*VAR1*((AFR10-AFR12)+THA7*DXY)
      D(1)=0.0
      D(2)=0.0
      D(3)=-0.5*VAR1*THA4
      D(4)=0.0
      D(5)=0.5*VAR1*(THA7*DYX -(AFR6-AFR8))
      D(6)=0.5*VAR1*((AFI10-AFI12)-THA7*SXY)
      IF(NDIAG) 9,15,9
    9 DO 11 I=1,6
   11 WRITE OUTPUT TAPE 3, 791,A(I,1),A(I,2),A(I,3),A(I,4),A(I,5),A(I,6)
      DO 13 I=1,6
   13 WRITE OUTPUT TAPE 3, 791,B(I,1),B(I,2),B(I,3),B(I,4),B(I,5),B(I,6)
      WRITE OUTPUT TAPE 3, 791, C(1),C(2),C(3),C(4),C(5),C(6)
      WRITE OUTPUT TAPE 3, 791, D(1),D(2),D(3),D(4),D(5),D(6)
C       THIS PROGRAM SOLVES A SYSTEM OF LINEAR EQUATIONS  AX=B
C       WHERE THE VARIABLES ARE COMPLEX
C       A=MATRIX OF REAL PART OF THE COMPLEX SYSTEM
C       B=MATRIX OF IMAGINARY PART OF COMPLEX SYSTEM
```

```
C       C=COLUMN VECTOR OF THE REAL PART OF THE RIGHT-HAND VECTORS
C       D=COLUMN MATRIX OF THE IMAGINARY PART OF THE RIGHT-HAND VECTORS
C       THE UNKNOWN COLUMN MATRIX X IS STORED IN C AND D
C       C BEING THE REAL PART AND D THE IMAGINARY PART
   15 N=6
      DO 10 I=1,N
      DO 10 J=1,N
   10 E(I,J)=A(I,J)
      LL=N+1
      LM=2*N
      DO 12 I=1,N
      DO 12 J=LL,LM
      K=J-N
   12 E(I,J)=-B(I,K)
      DO 14 I=LL,LM
      DO 14 J=1,N
      KK=I-N
   14 E(I,J)=B(KK,J)
      DO 16 I=LL,LM
      DO 16 J=LL,LM
      K=J-N
      KK=I-N
   16 E(I,J)=A(KK,K)
      DO 18 J=1,N
   18 F(J)=C(J)
      DO 22 J=LL,LM
      K=J-N
   22 F(J)=D(K)
      N=LM
      DO 20 J=1,N
   20 IPIVO(J)=0
```

```
      DO 550 I=1,N
C                                                                    F4020015
C     SEARCH FOR PIVOT ELEMENT                                       F4020016
C                                                                    F4020017
      AMAX=0.0
      DO 105 J=1,N
      IF (IPIVO(J)-1) 60,105,60
   60 DO 100 K=1,N
      IF (IPIVO(K) -1) 80, 100, 600
   80 IF (AMAX) 62,63,63
   62 AMAX=-AMAX
   63 IF (E(J,K)) 64,65,65
   64 TOOT=-E(J,K)
      GO TO 67
   65 TOOT=E(J,K)
   67 IF (AMAX-TOOT) 85,100,100
   85 IROW=J
      ICOLU =K
      AMAX=E(J,K)
  100 CONTINUE
  105 CONTINUE
      IPIVO(ICOLU)=IPIVO(ICOLU)+1
C                                                                    F4020030
C     INTERCHANGE ROWS TO PUT PIVOT ELEMENT ON DIAGONAL              F4020031
C                                                                    F4020032
      IF (IROW-ICOLU)  140, 260, 140
  140 DO 200 L=1,N
      AMAX=E(IROW,L)
      E(IROW,L)=E(ICOLU,L)
  200 E(ICOLU,L)=AMAX
      AMAX=F(IROW)
```

```
      F(IROW)=F(ICOLU)
      F(ICOLU)=AMAX
  260 PIVOT(I)=E(ICOLU,ICOLU)
C                                                              F4020048
C     DIVIDE PIVOT ROW BY PIVOT ELEMENT                        F4020049
C                                                              F4020050
      E(ICOLU,ICOLU)=1.0
      DO 350 L=1,N
  350 E(ICOLU,L)=E(ICOLU,L)/PIVOT(I)
      F(ICOLU)=F(ICOLU)/PIVOT(I)
C                                                              F4020057
C     REDUCE NON-PIVOT ROWS                                    F4020058
C                                                              F4020059
      DO 550 L1=1,N
      IF(L1-ICOLU)  400, 550, 400
  400 AMAX=E(L1,ICOLU)
      E(L1,ICOLU) =0.0
      DO 450 L=1,N
  450 E(L1,L)=E(L1,L)-E(ICOLU,L)*AMAX
      F(L1)=F(L1)-F(ICOLU)*AMAX
  550 CONTINUE
  600 N=N/2
      DO 641 J=1,N
  641 C(J)=F(J)
      DO 645 J=LL,LM
      K=J-N
  645 D(K)=F(J)
      CSR2=C(1)*VAR10+C(3)*VAR11
      CSI2=D(1)*VAR10+D(3)*VAR11
      GSR2=C(4)*VAR10+C(6)*VAR11
      GSI2=D(4)*VAR10+D(6)*VAR11
```

```
      DSR2=C(1)*VAR11+C(3)*VAR10
      DSI2=D(1)*VAR11+D(3)*VAR10-0.5*VAR1
      HSR2=C(4)*VAR11+C(6)*VAR10+0.5*VAR1
      HSI2=D(4)*VAR11+D(6)*VAR10
      ESR2=C(4)*VAR4+C(5)*VAR5
      ESI2=D(4)*VAR4+D(5)*VAR5
      FSR2=-C(4)*VAR5+C(5)*VAR4-0.5*VAR1
      FSI2=-D(4)*VAR5+D(5)*VAR4
      ASR2=C(1)*VAR4+C(2)*VAR5
      ASI2=D(1)*VAR4+D(2)*VAR5
      BSR2=-C(1)*VAR5+C(2)*VAR4
      BSI2=-D(1)*VAR5+D(2)*VAR4+0.5*VAR1
      IF(NDIAG) 643,644,643
  643 WRITE OUTPUT TAPE 3, 791, C(1),C(2),C(3),C(4),C(5),C(6)
      WRITE OUTPUT TAPE 3, 791, D(1),D(2),D(3),D(4),D(5),D(6)
      WRITE OUTPUT TAPE 3, 791, CSR2,CSI2,GSR2,GSI2,DSR2,DSI2
      WRITE OUTPUT TAPE 3, 791, HSR2,HSI2,ESR2,ESI2,FSR2,FSI2
      WRITE OUTPUT TAPE 3, 791, ASR2,ASI2,BSR2,BSI2
  644 GO TO (810,812), KFORK
  810 IF (NZ) 1500,811,1500
  811 GO TO (812,830),NNN
  812 DO 2000 I=1,NZEE1
      ZAR1=ARG1*ZEE1(I)
      VAR14=COSF(ZAR1)
      VAR15=SINF(ZAR1)
      VAR19=EXPF(ZAR1)
      VAR18=(VAR19+1.0/VAR19)/2.0
      VAR19=(VAR19-1.0/VAR19)/2.0
      FI1=VAR14+VAR18
      AR1=C(1)*(    FI1      )+C(2)*VAR15+C(3)*VAR19
      BI1=D(1)*(     FI1     )+D(2)*VAR15+D(3)*VAR19
```

```
      ER1=C(4)*(      FI1    )+C(5)*VAR15+C(6)*VAR19
      FI1=D(4)*(     FI1     )+D(5)*VAR15+D(6)*VAR19
      SUB11=AR1**2+BI1**2+ER1**2+FI1**2
      SUB12=+ER1*BI1-FI1*AR1
      SUB13=ER1*AR1+FI1*BI1
      SUB14=-ER1**2-FI1**2+AR1**2+BI1**2
      SUB15= ER1*FI1+AR1*BI1
      SUB16=ER1**2-FI1**2+AR1**2-BI1**2
      AMAXX=SQRTF(SUB11**2-4.0*SUB12**2)
      AMAX1=SQRTF(0.5*SUB11+0.5*AMAXX)
      BMIN1=SQRTF(0.5*SUB11-0.5*AMAXX)
      OAL1=0.5*ANG(SUB14,2.0*SUB13)
      OBL1=0.5*ANG(SUB16,2.0*SUB15)
      IF (ZEE1(I)) 911,912,911
  911 AMAX=AMAX1
      BMIN=BMIN1
      OAL=OAL1
      OBL=OBL1
      GO TO 950
  912 FAR1=GNU*(C(2)-C(3))
      FBI1=GNU*(D(2)-D(3))
      FER1=GNU*(C(5)-C(6))
      FFI1=GNU*(D(5)-D(6))
      FS B11=FER1**2+FFI1**2+FAR1**2+FBI1**2
      FS B12=FER1*FBI1-FFI1*FAR1
      FSB13=-FER1**2-FFI1**2+FAR1**2+FBI1**2
      FS B14=FER1*FAR1+FFI1*FBI1
      FMAXX=SQRTF(FSB11**2-4.0*FSB12**2)
      FMAX1=SQRTF(0.5*FSB11+0.5*FMAXX)
      FMIN1=SQRTF(0.5*FSB11-0.5*FMAXX)
      FALF1=0.5*ANG(FSB13,2.0*FSB14)
```

```
      AMAX=AMAX1
      BMIN=BMIN1
      OAL=OAL1
      OBL=OBL1
      FMAX=FMAX1
      FMIN=FMIN1
      FALF=FALF1
      GO TO 960
  950 GO TO (902,909),KFORK
  902 WRITE OUTPUT TAPE 3, 749, SPD(II),AMAX,BMIN,OAL,OBL
      GO TO 2000
  909 WRITE OUTPUT TAPE 3, 768,ZEE1(I),AMAX,BMIN,OAL,OBL
      GO TO 2000
  960 GO TO (922,928), KFORK
  922 WRITE OUTPUT TAPE 3, 770, SPD(II),AMAX,BMIN,OAL,OBL,FMAX,FMIN,FALF
      GO TO 2000
  928 WRITE OUTPUT TAPE 3, 772, ZEE1(I),AMAX,BMIN,OAL,OBL,FMAX,FMIN,FALF
 2000 CONTINUE
      GO TO (920,830), KFORK
  830 DO 3000 I=1,NZEE2
      ZAR2=ARG2*ZEE2(I)
      VAR16=COSF(ZAR2)
      VAR17=SINF(ZAR2)
      VAR21=EXPF(ZAR2)
      VAR20=(VAR21+1.0/VAR21)/2.0
      VAR21=(VAR21-1.0/VAR21)/2.0
      AR2=ASR2*VAR16+BSR2*VAR17+CSR2*VAR20+DSR2*VAR21
      BI2=ASI2*VAR16+BSI2*VAR17+CSI2*VAR20+DSI2*VAR21
      ER2=ESR2*VAR16+FSR2*VAR17+GSR2*VAR20+HSR2*VAR21
      FI2=ESI2*VAR16+FSI2*VAR17+GSI2*VAR20+HSI2*VAR21
      SUB21=AR2**2+BI2**2+ER2**2+FI2**2
```

```
      SUB22=ER2*BI2-FI2*AR2
      SUB23=ER2*AR2+FI2*BI2
      SUB24=-ER2**2-FI2**2+AR2**2+BI2**2
      SUB25= ER2*FI2+AR2*BI2
      SUB26=ER2**2-FI2**2+AR2**2-BI2**2
      AMAXX=SQRTF(SUB21**2-4.0*SUB22**2)
      AMAX2=SQRTF(0.5*SUB21+0.5*AMAXX)
      BMIN2=SQRTF(0.5*SUB21-0.5*AMAXX)
      OAL2=0.5*ANG(SUB24,2.0*SUB23)
      OBL2=0.5*ANG(SUB26,2.0*SUB25)
      IF (ZEE2(I)-1.0) 914,915,914
  914 AMAX=AMAX2
      BMIN=BMIN2
      OAL=OAL2
      OBL=OBL2
      GO TO 970
  915 FAR2= GNU*(ASR2*VAR7-BSR2*VAR6+CSR2*VAR13+DSR2*VAR12)
      FBI2= GNU*(ASI2*VAR7-BSI2*VAR6+CSI2*VAR13+DSI2*VAR12)
      FER2= GNU*(ESR2*VAR7-FSR2*VAR6+GSR2*VAR13+HSR2*VAR12)
      FFI2= GNU*(ESI2*VAR7-FSI2*VAR6+GSI2*VAR13+HSI2*VAR12)
      FS B21=FER2**2+FFI2**2+FAR2**2+FBI2**2
      FS B22=FER2*FBI2-FFI2*FAR2
      FSB23=-FER2**2-FFI2**2+FAR2**2+FBI2**2
      FS B24=FER2*FAR2+FFI2*FBI2
      FMAXX=SQRTF(FSB21**2-4.0*FSB22**2)
      FMAX2=SQRTF(0.5*FSB21+0.5*FMAXX)
      FMIN2=SQRTF(0.5*FSB21-0.5*FMAXX)
      FALF2=0.5*ANG(FSB23,2.0*FSB24)
      AMAX=AMAX2
      BMIN=BMIN2
      OAL=OAL2
```

```
      OBL=OBL2
      FMAX=FMAX2
      FMIN=FMIN2
      FALF=FALF2
      GO TO 980
  970 GO TO (972,978),KFORK
  972 WRITE OUTPUT TAPE 3, 749, SPD(II),AMAX,BMIN,OAL,OBL
      GO TO 3000
  978 WRITE OUTPUT TAPE 3, 765, ZEE2(I),AMAX,BMIN,OAL,OBL
      GO TO 3000
  980 GO TO (982,986), KFORK
  982 WRITE OUTPUT TAPE 3, 770, SPD(II),AMAX,BMIN,OAL,OBL,FMAX,FMIN,FALF
      GO TO 3000
  986 WRITE OUTPUT TAPE 3, 774, ZEE2(I),AMAX,BMIN,OAL,OBL,FMAX,FMIN,FALF
 3000 CONTINUE
      GO TO 920
 1500 ZAR1=ARG1*Z1
      VAR14=COSF(ZAR1)
      VAR15=SINF(ZAR1)
      VAR19=EXPF(ZAR1)
      VAR18=(VAR19+1.0/VAR19)/2.0
      VAR19=(VAR19-1.0/VAR19)/2.0
      FI1=VAR14+VAR18
      AR1=C(1)*(    FI1      )+C(2)*VAR15+C(3)*VAR19
      BI1=D(1)*(     FI1     )+D(2)*VAR15+D(3)*VAR19
      ER1=C(4)*(      FI1    )+C(5)*VAR15+C(6)*VAR19
      FI1=D(4)*(     FI1     )+D(5)*VAR15+D(6)*VAR19
      ZAR2=ARG2*Z2
      VAR16=COSF(ZAR2)
      VAR17=SINF(ZAR2)
      VAR21=EXPF(ZAR2)
```

```
      VAR20=(VAR21+1.0/VAR21)/2.0
      VAR21=(VAR21-1.0/VAR21)/2.0
      AR2=ASR2*VAR16+BSR2*VAR17+CSR2*VAR20+DSR2*VAR21
      BI2=ASI2*VAR16+BSI2*VAR17+CSI2*VAR20+DSI2*VAR21
      ER2=ESR2*VAR16+FSR2*VAR17+GSR2*VAR20+HSR2*VAR21
      FI2=ESI2*VAR16+FSI2*VAR17+GSI2*VAR20+HSI2*VAR21
      YY1=AR1-AR2
      XX1=BI1-BI2
      YY2=ER1-ER2
      XX2=FI1-FI2
      SUB31=YY1**2+XX1**2+YY2**2+XX2**2
      SUB32=YY2*XX1-XX2*YY1
      SUB33=YY2*YY1+XX2*XX1
      SUB34=-YY2**2-XX2**2+YY1**2+XX1**2
      SUB35=YY2*XX2+YY1*XX1
      SUB36=YY2**2-XX2**2+YY1**2-XX1**2
      AMAXX=SQRTF(SUB31**2-4.0*SUB32**2)
      AMAX =SQRTF(0.5*SUB31+0.5*AMAXX)
      BMIN =SQRTF(0.5*SUB31-0.5*AMAXX)
      OAL =0.5*ANG(SUB34,2.0*SUB33)
      OBL =0.5*ANG(SUB36,2.0*SUB35)
      IF (ZEE) 1100,1050,1100
1050  FAR1=GNU*(C(2)-C(3))
      FBI1=GNU*(D(2)-D(3))
      FER1=GNU*(C(5)-C(6))
      FFI1=GNU*(D(5)-D(6))
      FAR2= GNU*(ASR2*VAR7-BSR2*VAR6+CSR2*VAR13+DSR2*VAR12)
      FBI2= GNU*(ASI2*VAR7-BSI2*VAR6+CSI2*VAR13+DSI2*VAR12)
      FER2= GNU*(ESR2*VAR7-FSR2*VAR6+GSR2*VAR13+HSR2*VAR12)
      FFI2= GNU*(ESI2*VAR7-FSI2*VAR6+GSI2*VAR13+HSI2*VAR12)
      FAR= FAR1-FAR2
```

```
      FBI= FBI1-FBI2
      FER= FER1-FER2
      FFI= FFI1-FFI2
      FSB31=FER**2+FFI**2+FAR**2+FBI**2
      FSB32=FER*FBI-FFI*FAR
      FSB33=-FER**2-FFI**2+FAR**2+FBI**2
      FSB34=FER*FAR+FFI*FBI
      FMAXX=SQRTF(FSB31**2-4.0*FSB32**2)
      FMAX3=SQRTF(0.5*FSB31+0.5*FMAXX)
      FMIN3=SQRTF(0.5*FSB31-0.5*FMAXX)
      FALF =0.5*ANG(FSB33,2.0*FSB34)
      WRITE OUTPUT TAPE 3,770,SPD(II),AMAX,BMIN,OAL,OBL,FMAX3,FMIN3,FALF
      GO TO 920
 1100 WRITE OUTPUT TAPE 3,749, SPD(II), AMAX, BMIN, OAL, OBL
  920 CONTINUE
  910 CONTINUE
  900 CONTINUE
      GO TO (1, 2, 3500), INPUT
 3500 CALL ENDJOB
  735 FORMAT (E15.9)
  743 FORMAT(49H                                                )
  710 FORMAT(4E15.9)
  720 FORMAT(8I5)
  730 FORMAT (5E10.4)
  740 FORMAT(5H0SXX=,E11.5,6X4HSXY=,E11.5,6X4HSYX=,E11.5,6X4HSYY=,E11.5)
  741 FORMAT(5H0DXX=,E11.5,6X4HDXY=,E11.5,6X4HDYX=,E11.5,6X4HDYY=E11.5)
  744 FORMAT(1H1,38 X30HUNBALANCE  AMPLITUDE  RESPONSE)
  745 FORMAT(1H0,24X48HALL  VALUES  TABULATED  BELOW  ARE DIMENSIONLESS)
  746 FORMAT(1H0,23X13HUNBAL. L1/L =,F6.3,3X13HSTIFFN RATIO=,E11.5,
     12X3HZEE,I2,1H=,F6.3)
  747 FORMAT(7H0 SPEED,6X4HAMAX,8X4HBMIN,7X5HALPHA,7X4HBETA,9X4HFMAX,
```

```
     18X4HFMIN,7X5HPHASE)
  751 FORMAT(1H1,33X30HMODE  SHAPE  FOR  GIVEN  SPEED)
  762 FORMAT (1H1)
  752 FORMAT(1H021X11HSPD RATIO =,F6.2,4X11HUNBAL L1/L=,F6.3,
     14X14HSTIFFN RATIO =,E11.5)
  780 FORMAT(12H0Z1/L1 Z2/L2,4X4HAMAX,8X4HBMIN,5X5HALPHA,8X4HBETA,8X4HFM
     1AX,8X4HFMIN,8X5HPHASE)
  765 FORMAT(6XF5.2,1XE11.5,1XE11.5,1XE11.5,1XE11.5)
  768 FORMAT(1XF5.2,6XE11.5,1XE11.5,1XE11.5,1XE11.5)
  770 FORMAT(1XF6.2,2XE11.5,1XE11.5,1XE11.5,1XE11.5,1XE11.5,1XE11.5,1XE1
     11.5)
  772 FORMAT(1XF5.2,6XE11.5,1XE11.5,1XE11.5,1XE11.5,1XE11.5,1XE11.5,1XE1
     11.5)
  774 FORMAT(6XF5.2,1XE11.5,1XE11.5,1XE11.5,1XE11.5,1XE11.5,1XE11.5,1XE1
     11.5)
  749 FORMAT(1XF6.2,2XE11.5,1XE11.5,1XE11.5,1XE11.5)
  791 FORMAT(1XE12.6,1XE12.6,1XE12.6,1XE12.6,1XE12.6,1XE12.6)
      END
```

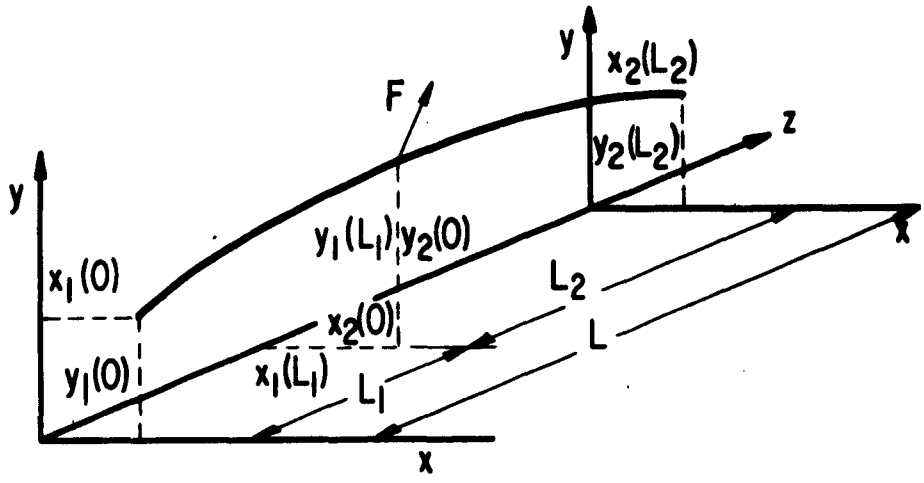

Fig. 1 Coordinates and Displacements

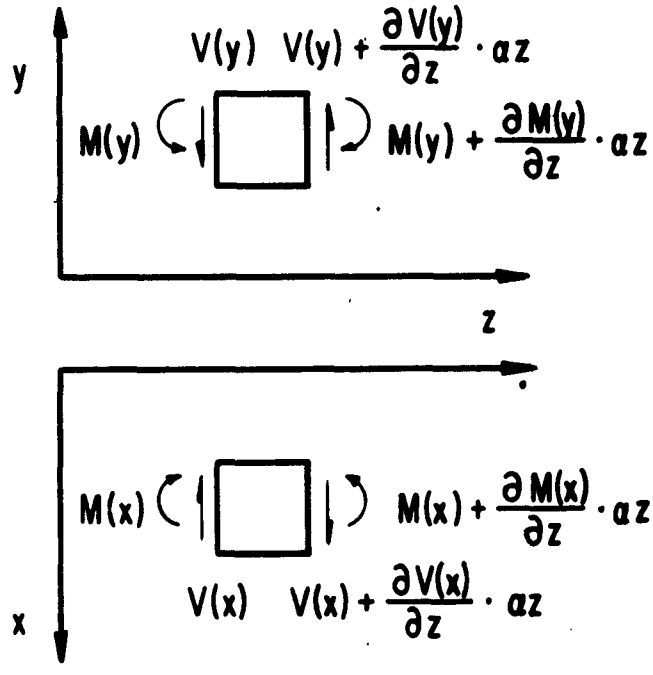

Fig. 2 Positive Displacement, Force, Moment and Shear Convention

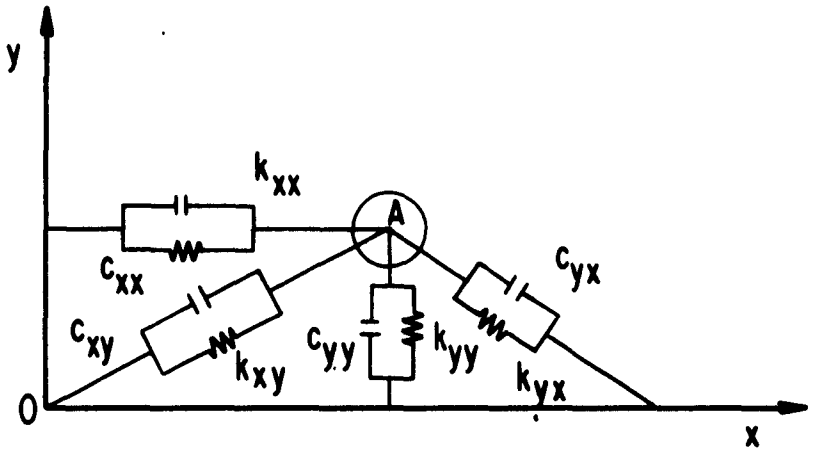

Fig. 3 Fluid-film Forces on Journal at $Z_1 = 0$ and $Z_2 = L_2$

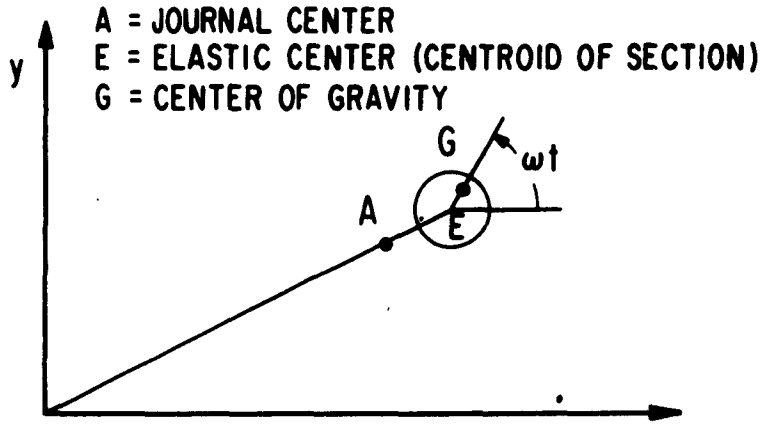

Fig. 4 Unbalance Acting at $Z_1 = L_1$

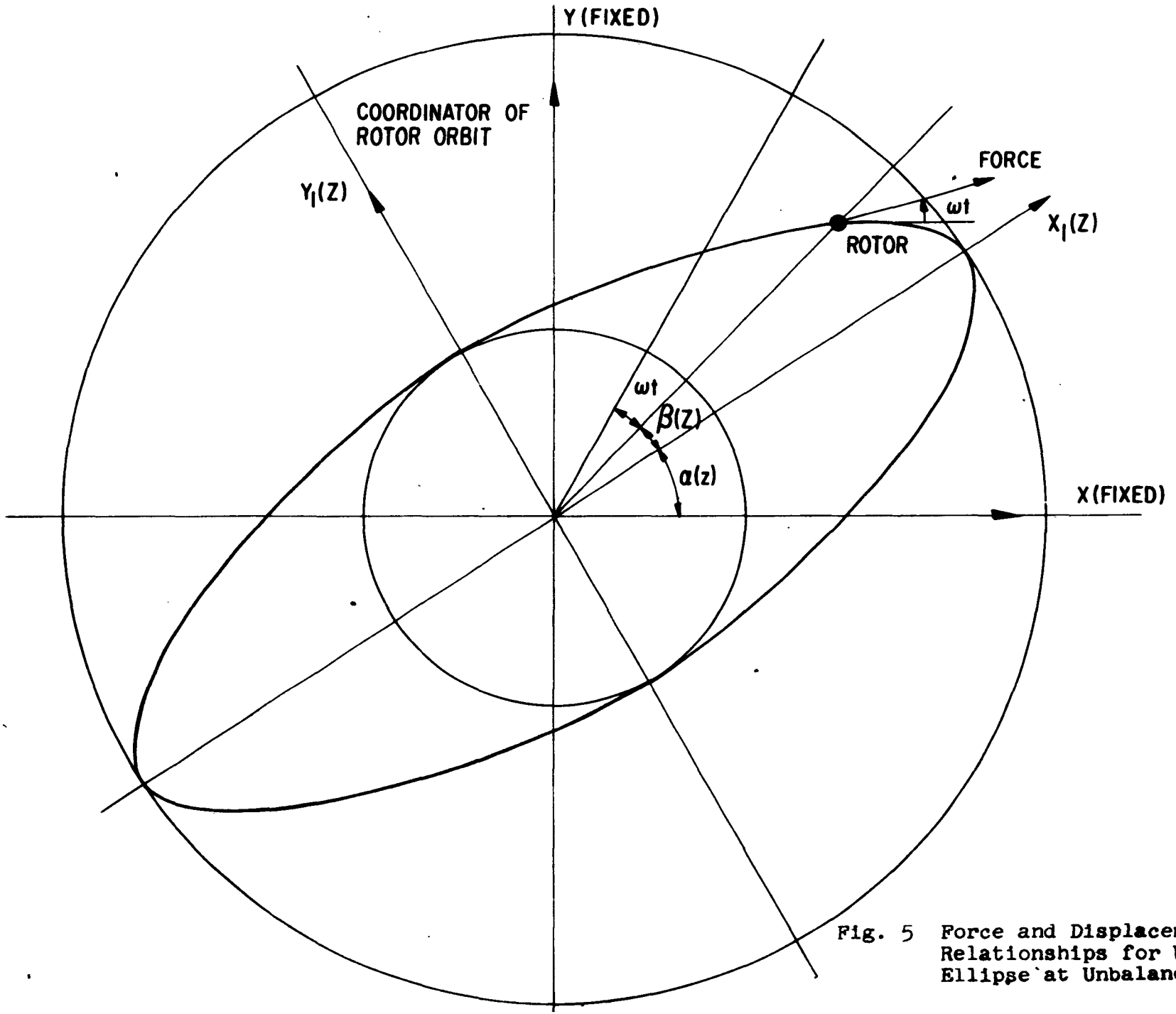

Fig. 5 Force and Displacement Relationships for Whirl Ellipse at Unbalance

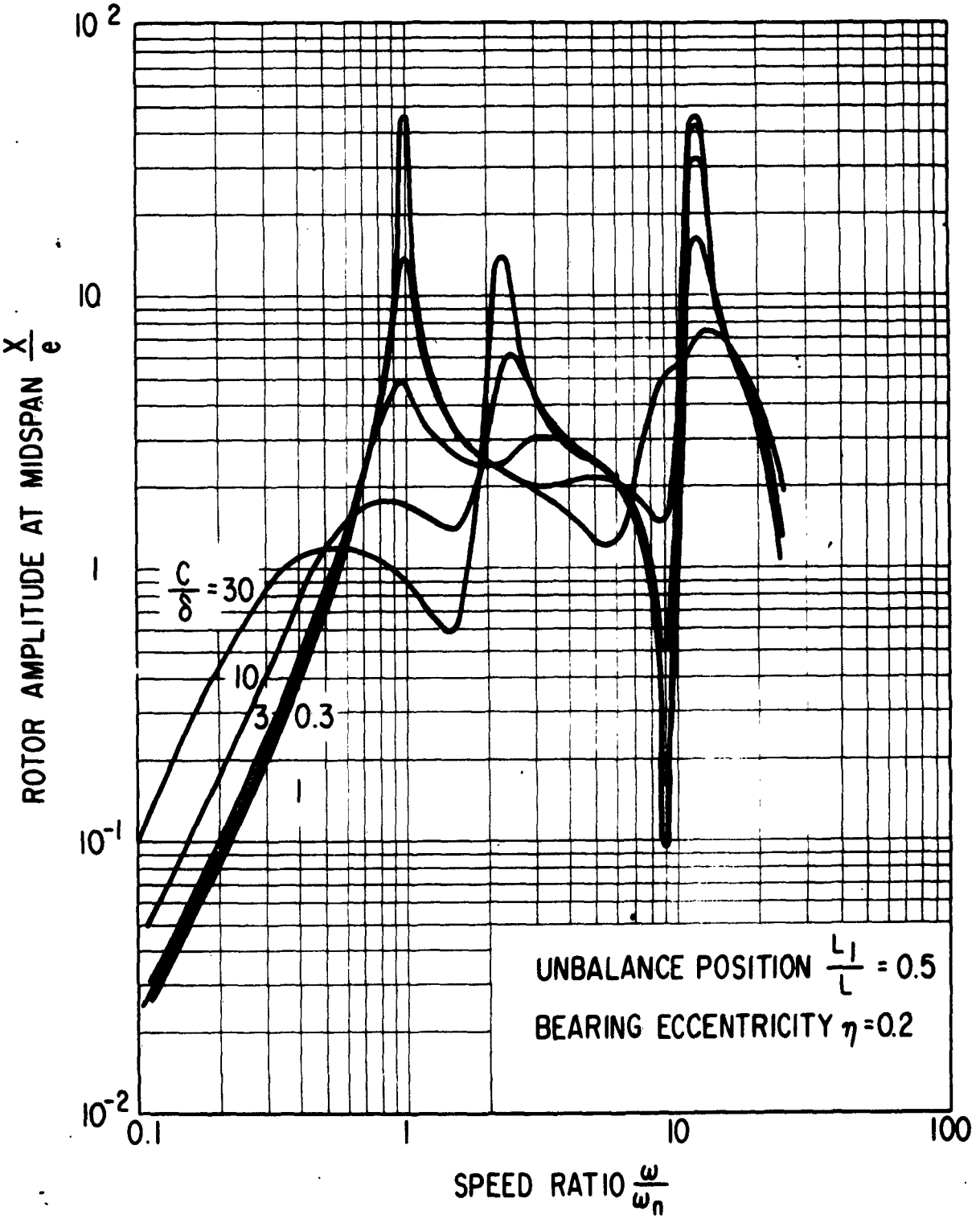

Fig. 6 Rotor Amplitude vs. Speed - Axially Symmetrical Unbalance

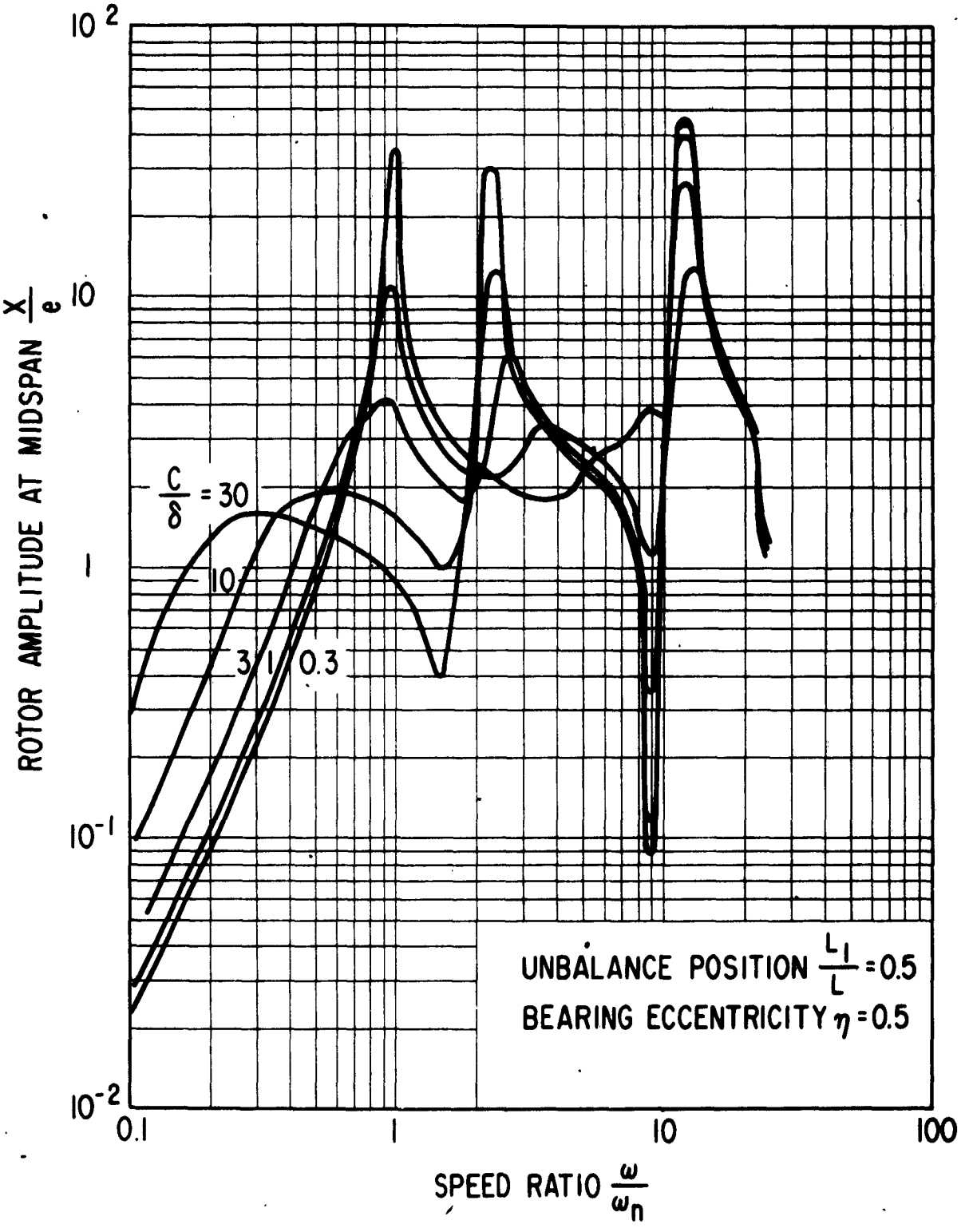

Fig. 7 Rotor Amplitude vs. Speed - Axially Symmetrical Unbalance

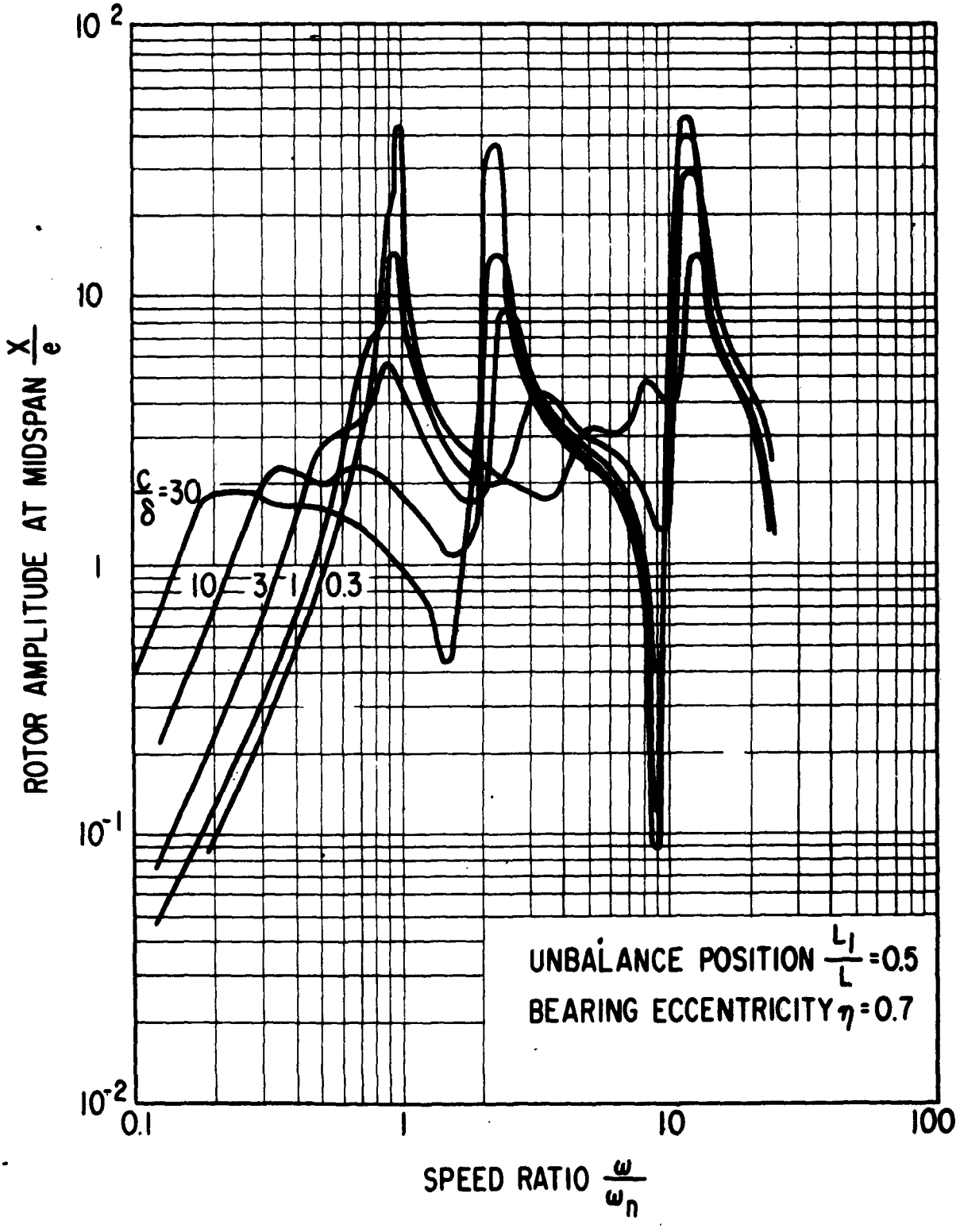

Fig. 8 Rotor Amplitude vs. Speed - Axially Symmetrical Unbalance

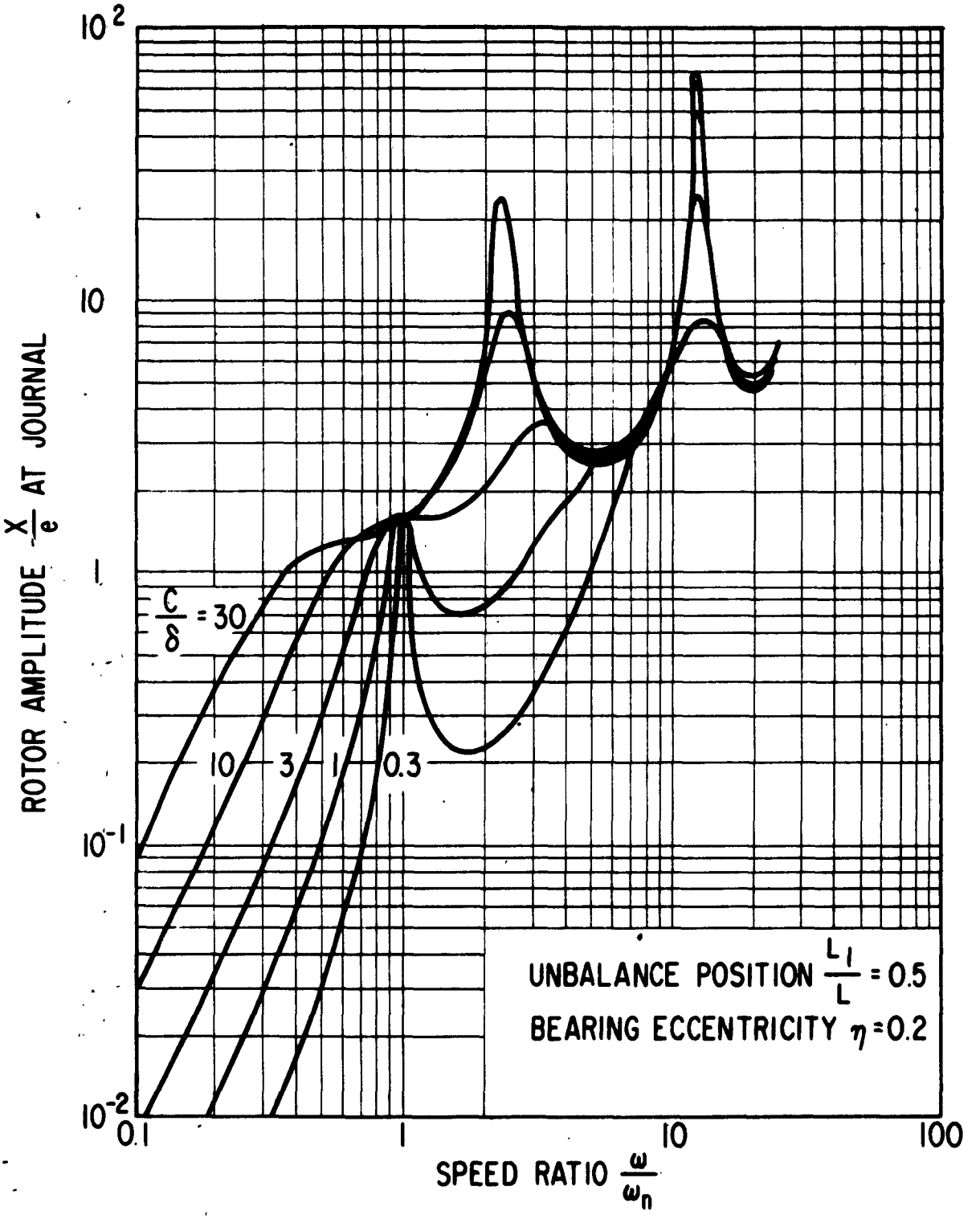

Fig. 9 Rotor Amplitude vs. Speed - Axially Symmetrical Unbalance

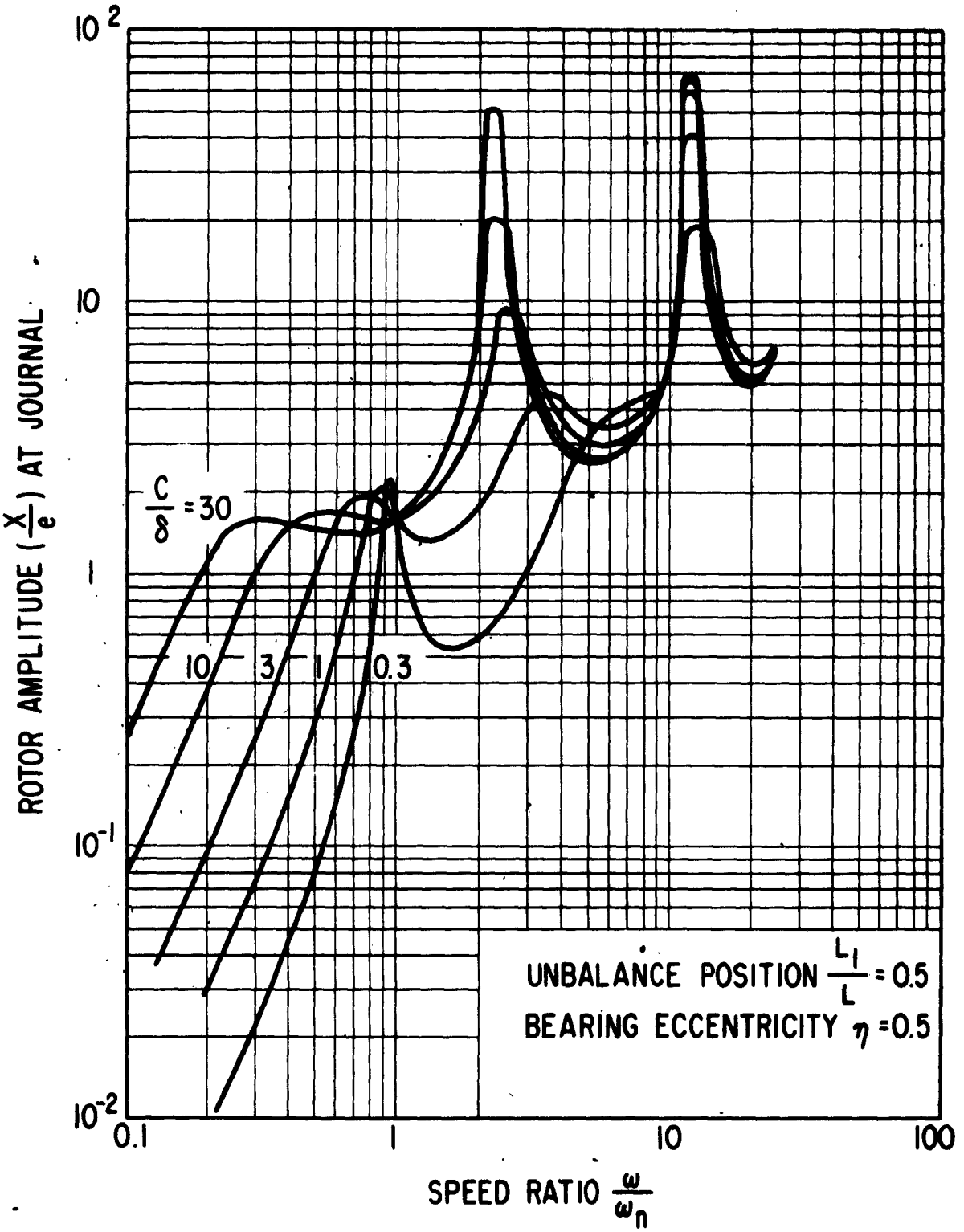

Fig. 10 Rotor Amplitude vs. Speed - Axially Symmetrical Unbalance

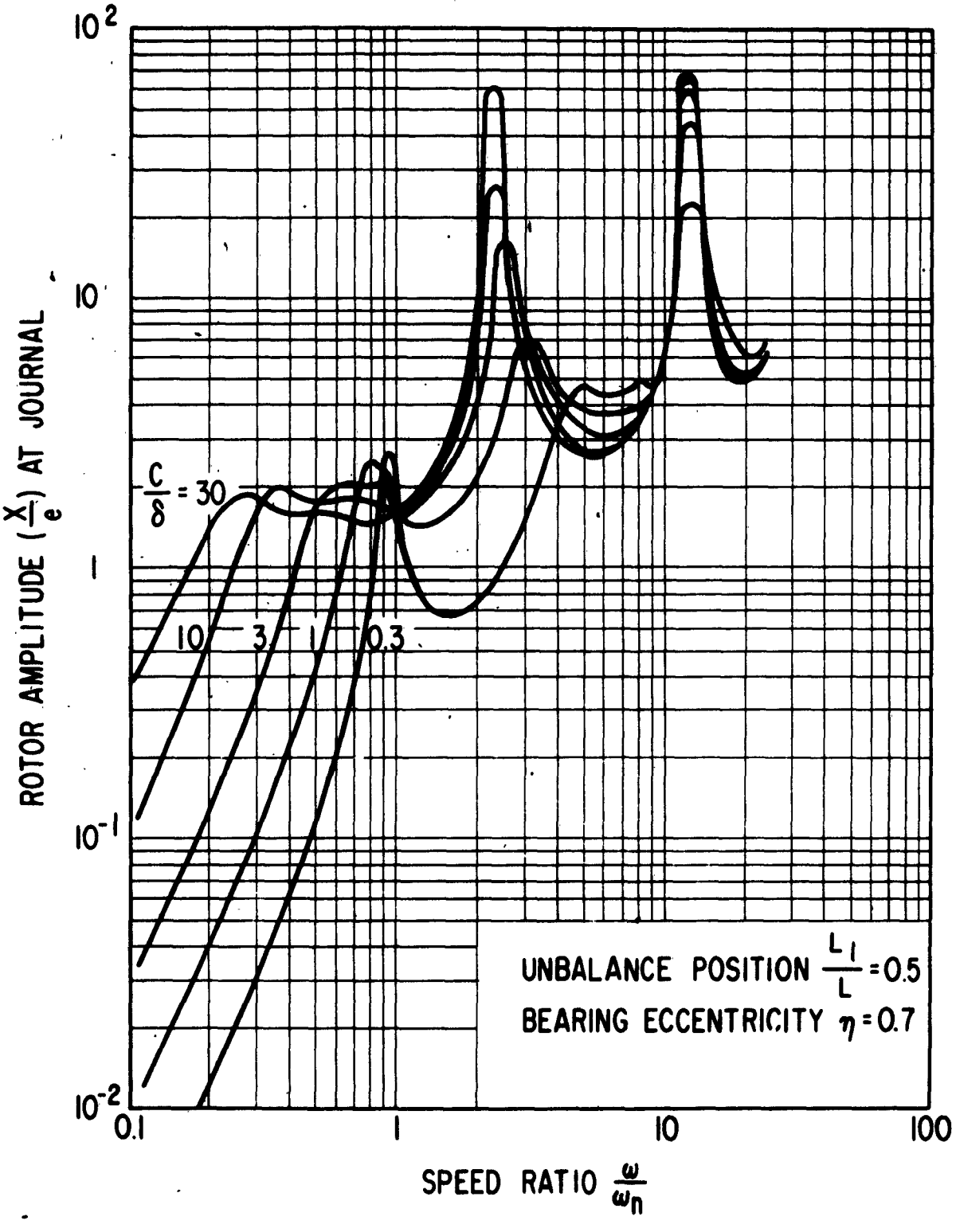

Fig. 11 Rotor Amplitude vs. Speed - Axially Symmetrical Unbalance

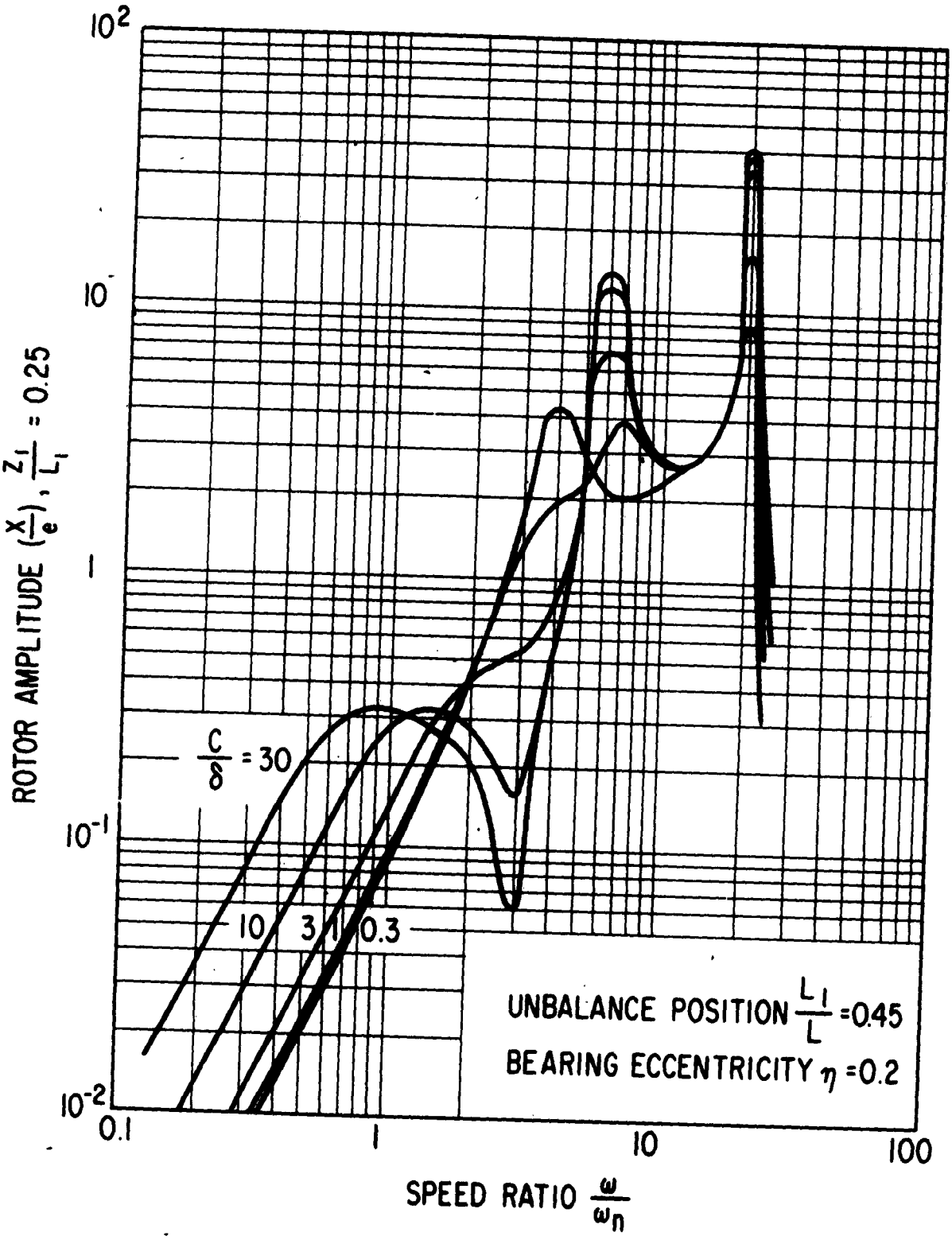

Fig. 12 Rotor Amplitude vs. Speed - Axially Asymmetrical Unbalance

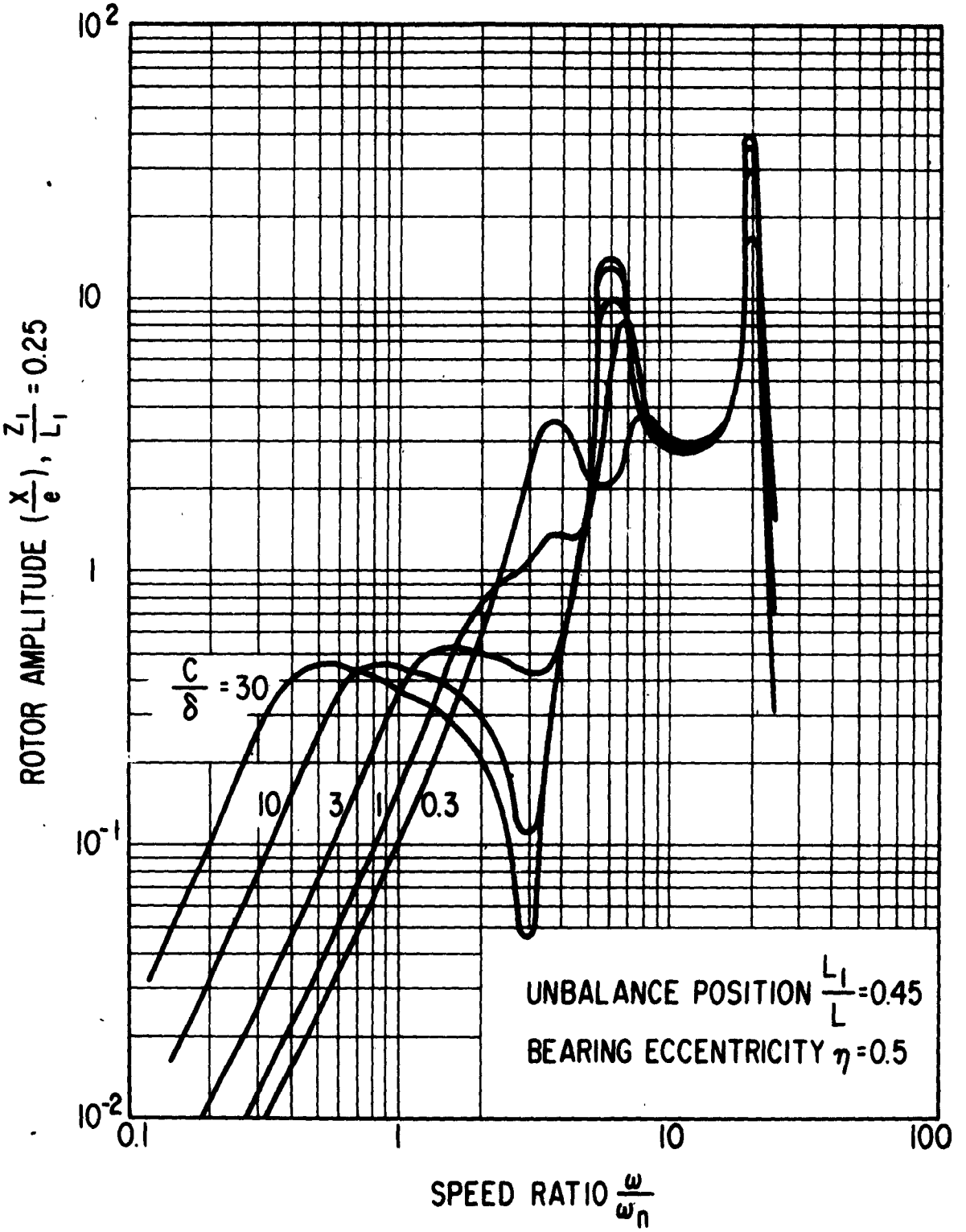

Fig. 13 Rotor Amplitude vs. Speed - Axially Asymmetrical Unbalance

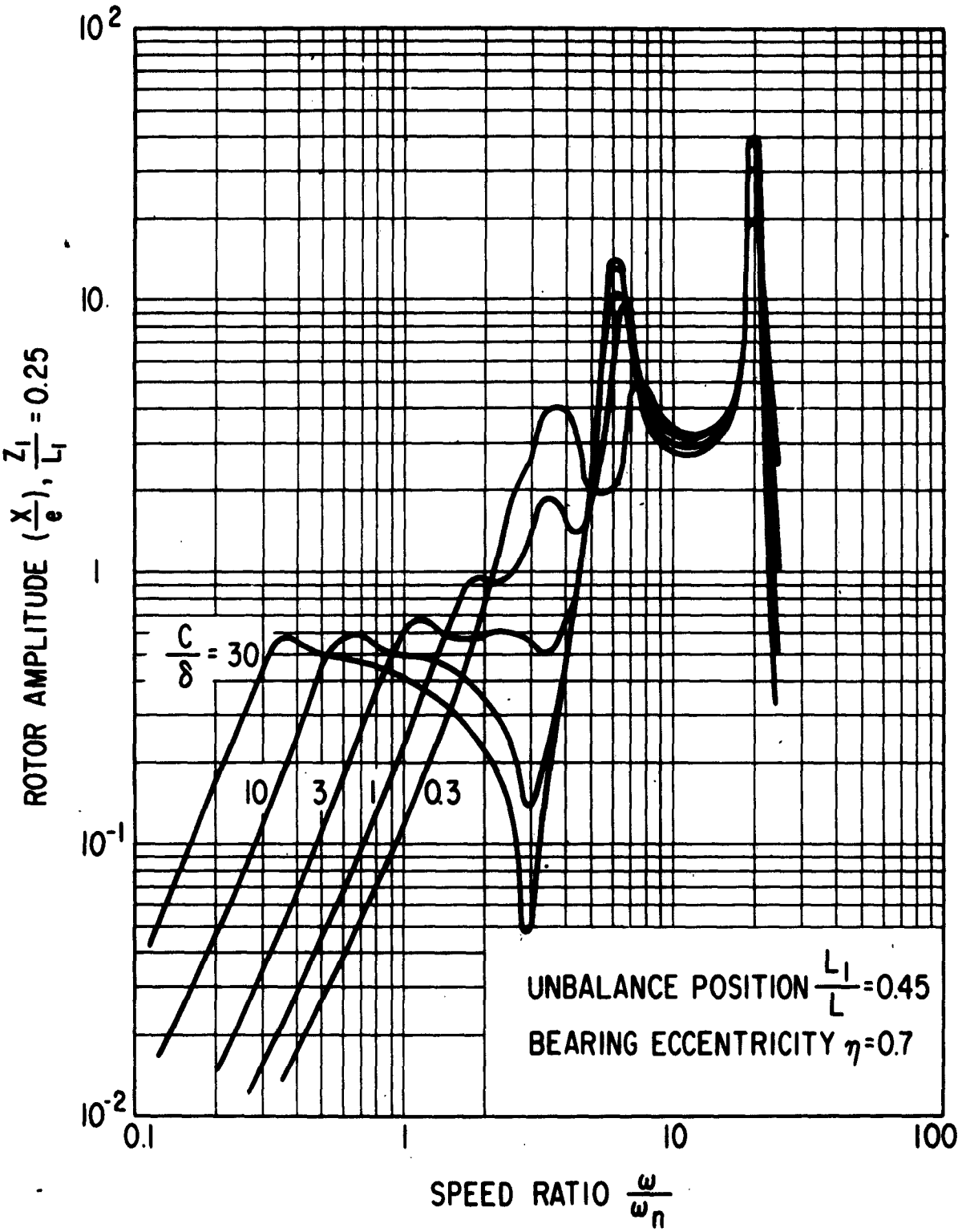

Fig. 14 Rotor Amplitude vs. Speed - Axially Asymmetrical Unbalance

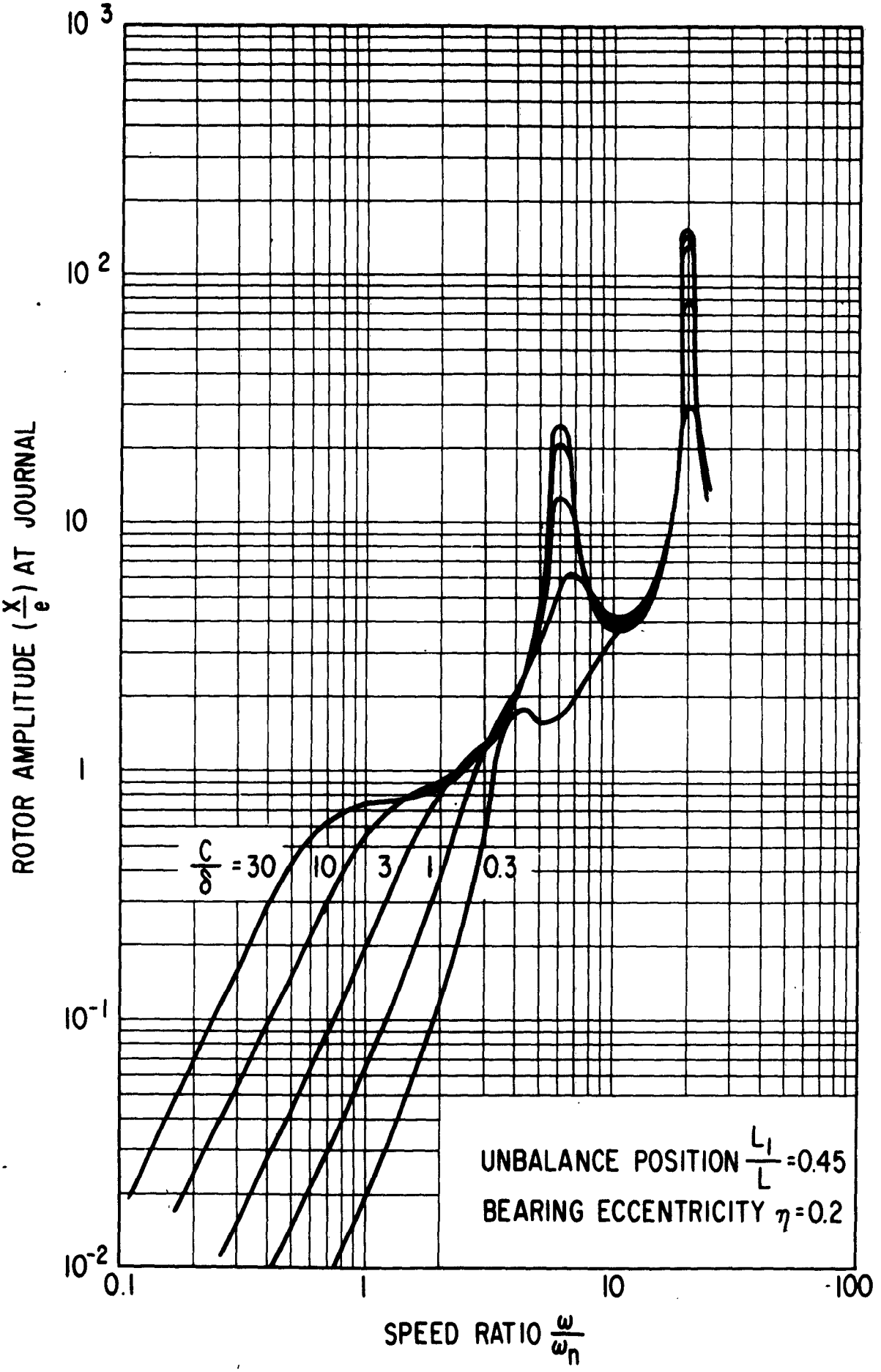

Fig. 15 Rotor Amplitude vs. Speed - Axially Asymmetrical Unbalance

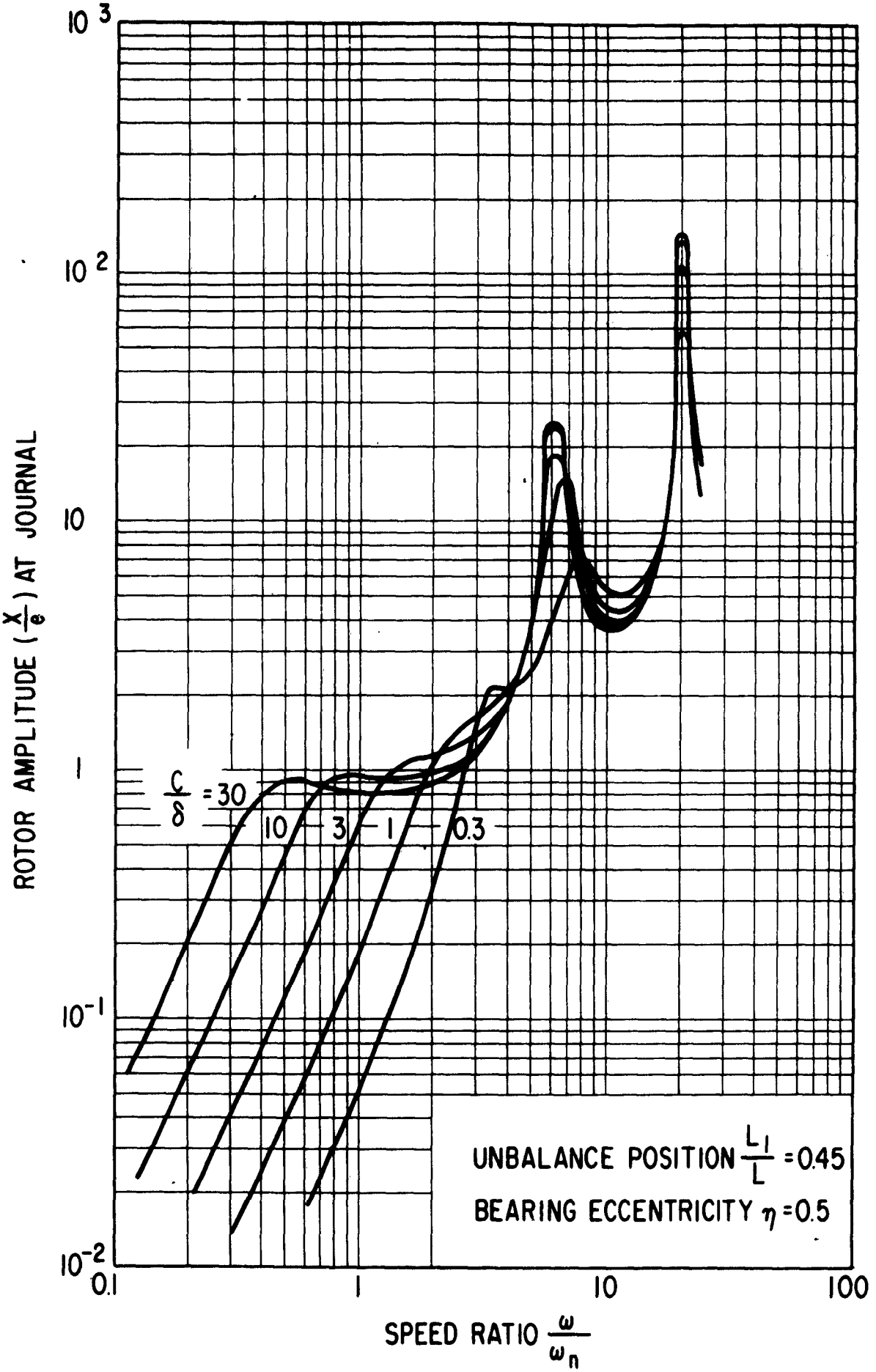

Fig. 16 Rotor Amplitude vs. Speed - Axially Asymmetrical Unbalance

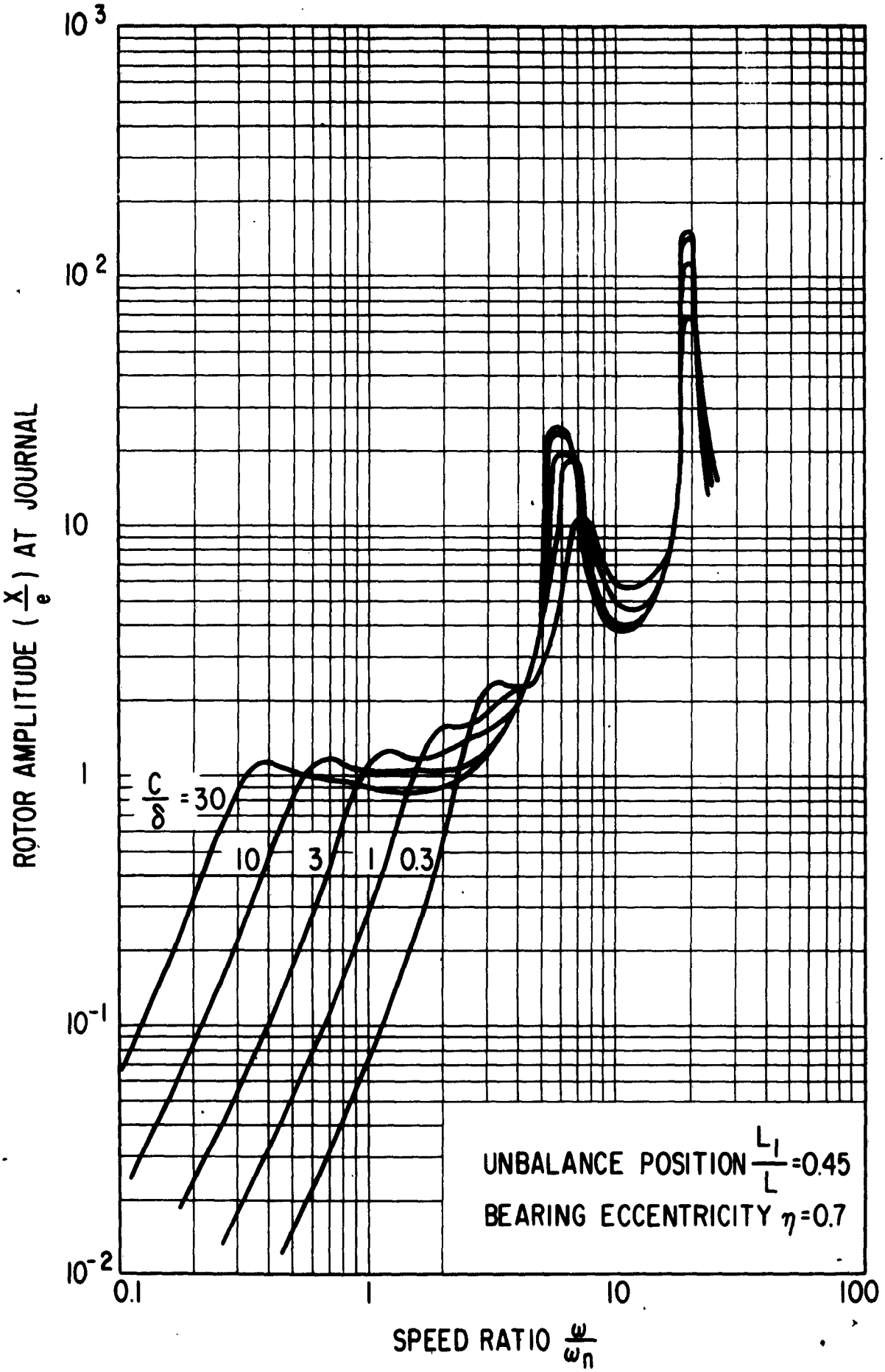

Fig. 17 Rotor Amplitude vs. Speed - Axially Asymmetrical Unbalance

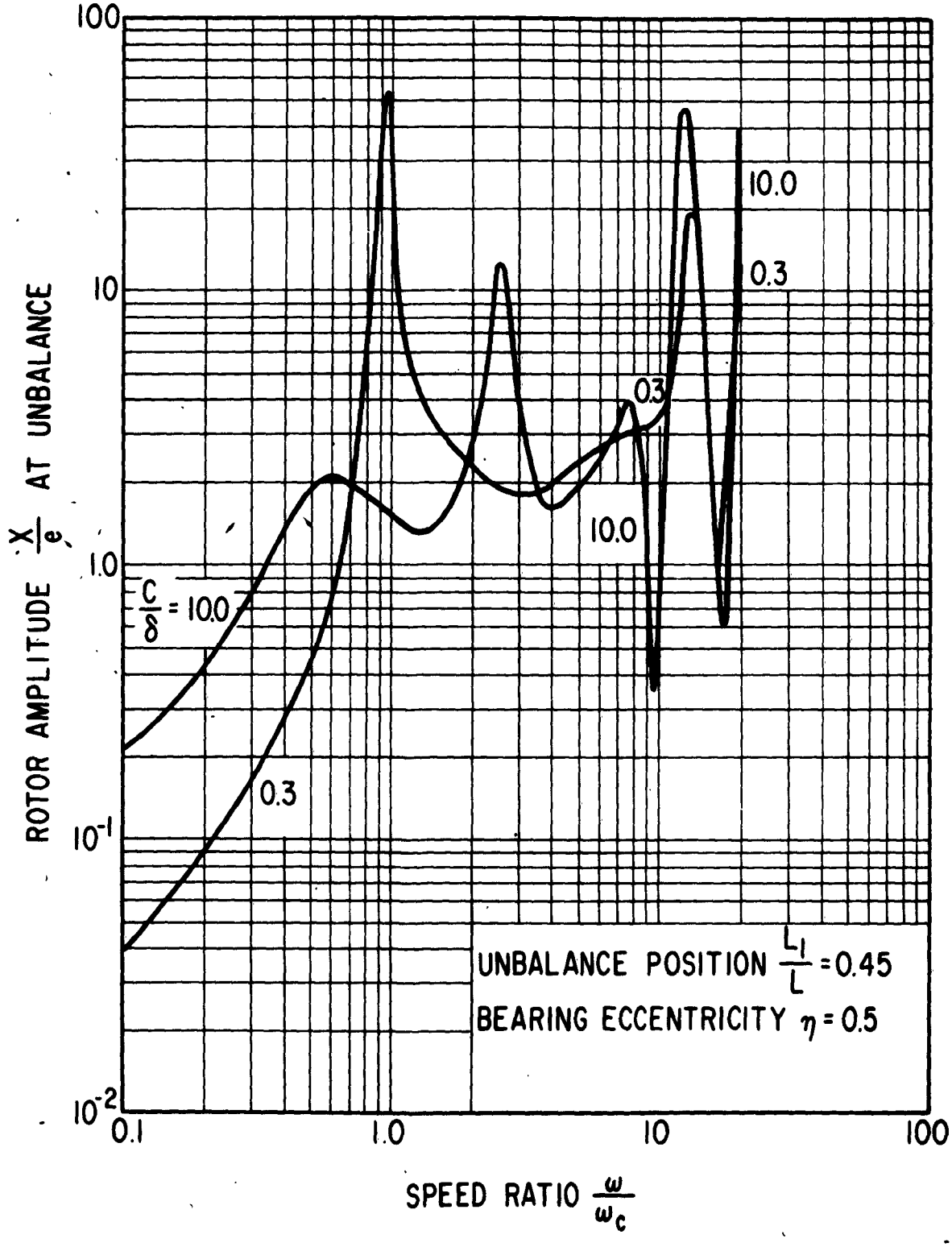

Fig. 18 Rotor Amplitude vs. Speed - Axially Asymmetrical Unbalance

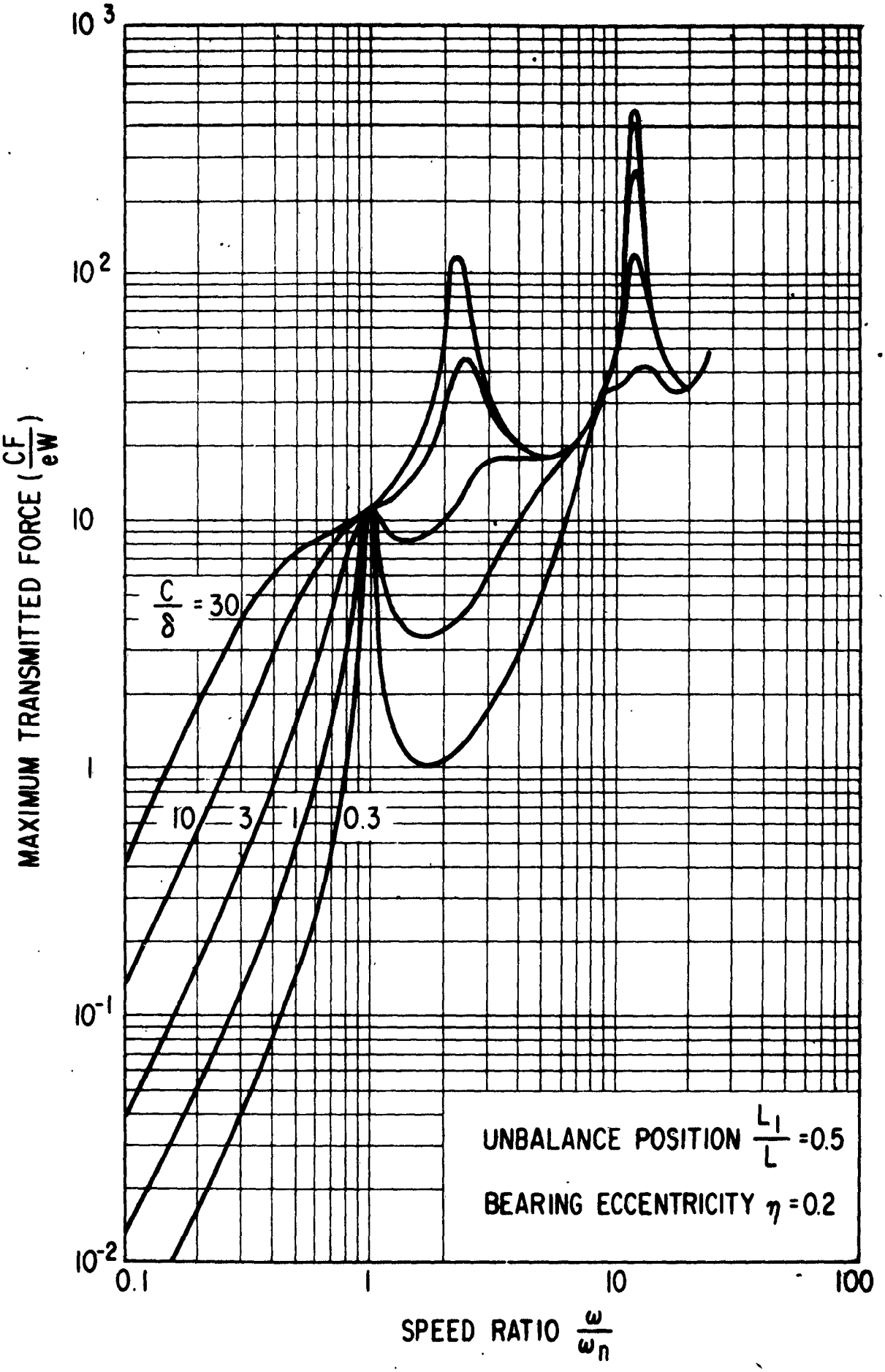

Fig. 19 Maximum Transmitted Force vs. Speed – Axially Symmetrical Unbalance

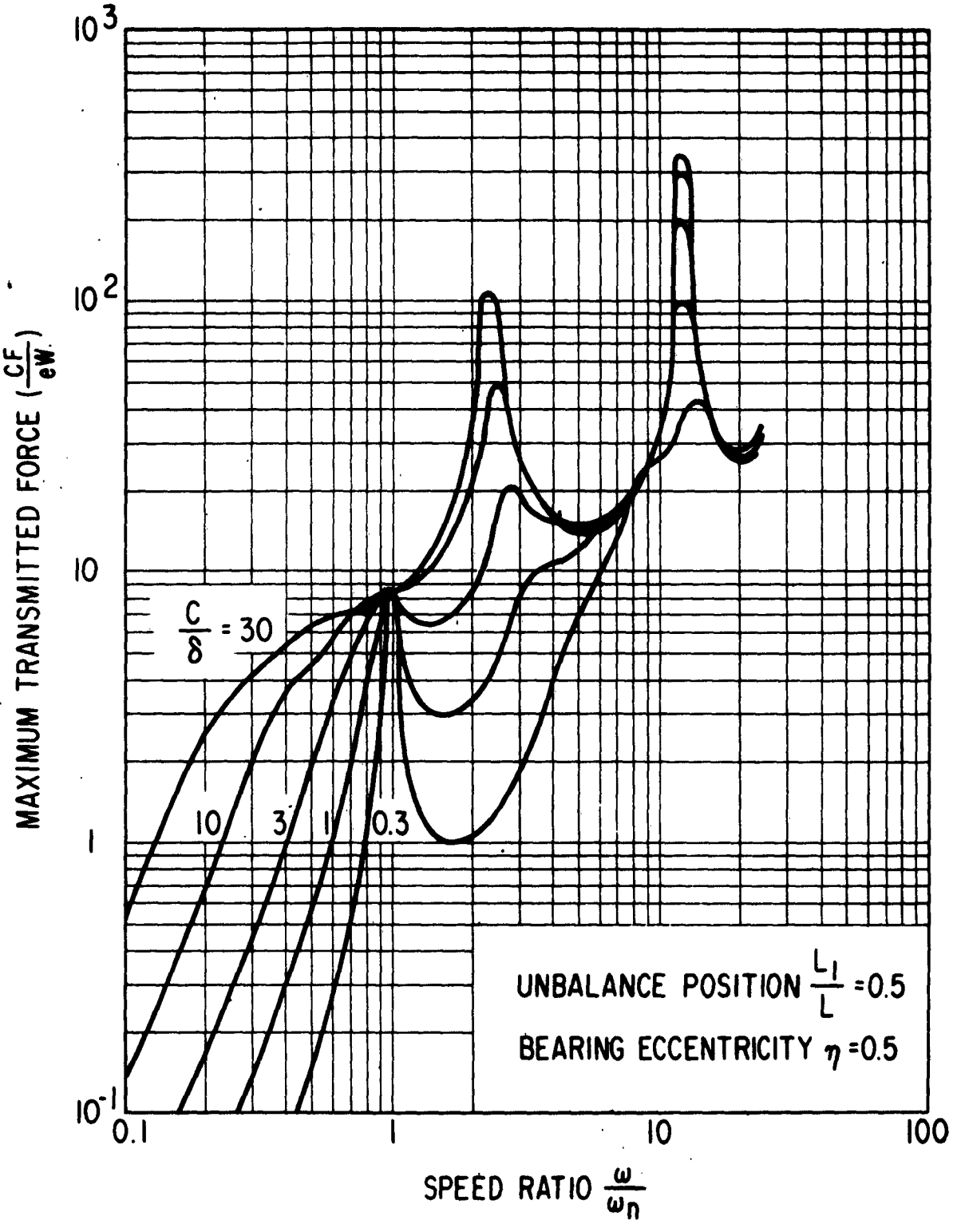

Fig. 20 Maximum Transmitted Force vs. Speed - Axially Symmetrical Unbalance

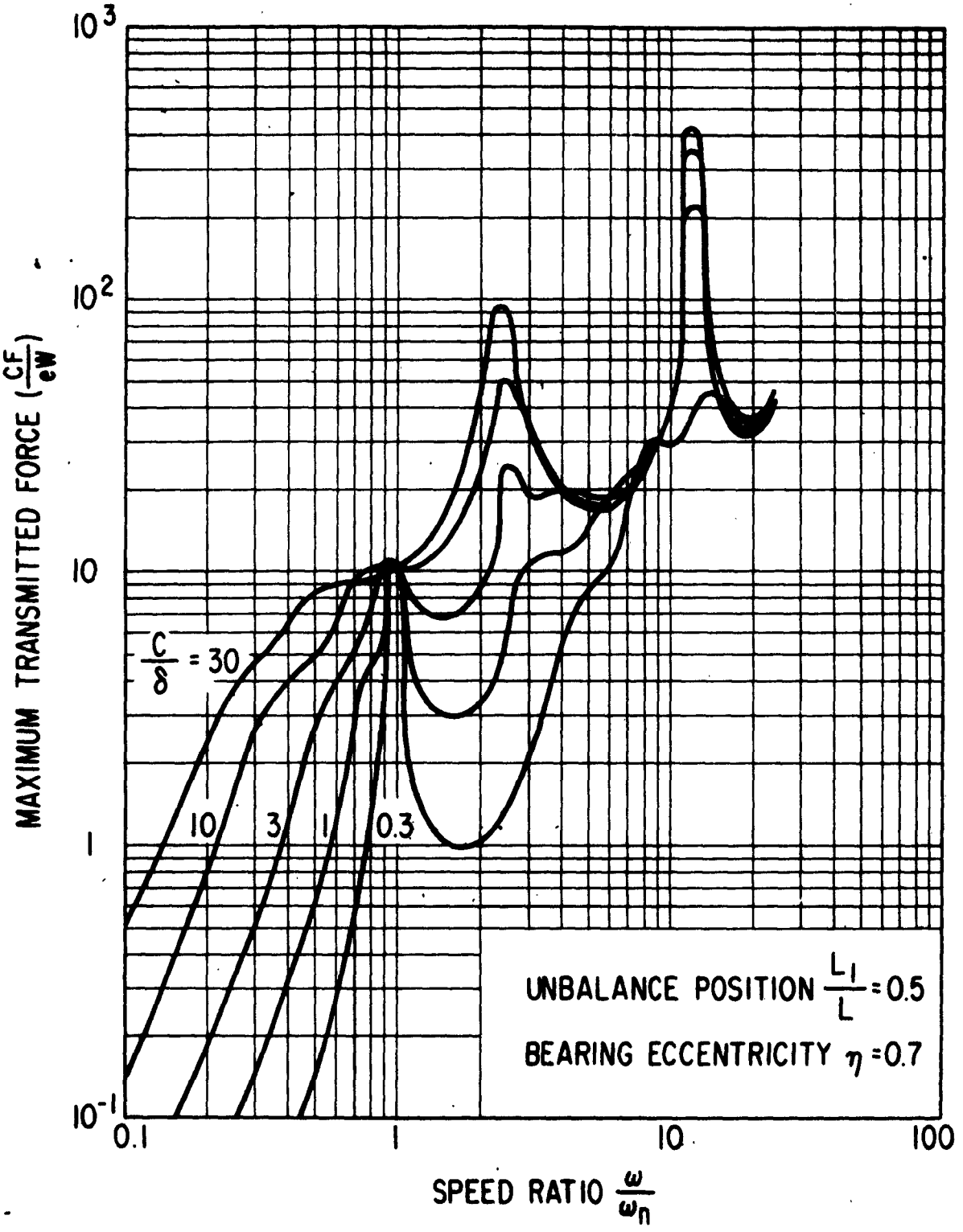

Fig. 21 Maximum Transmitted Force vs. Speed - Axially Symmetrical Unbalance

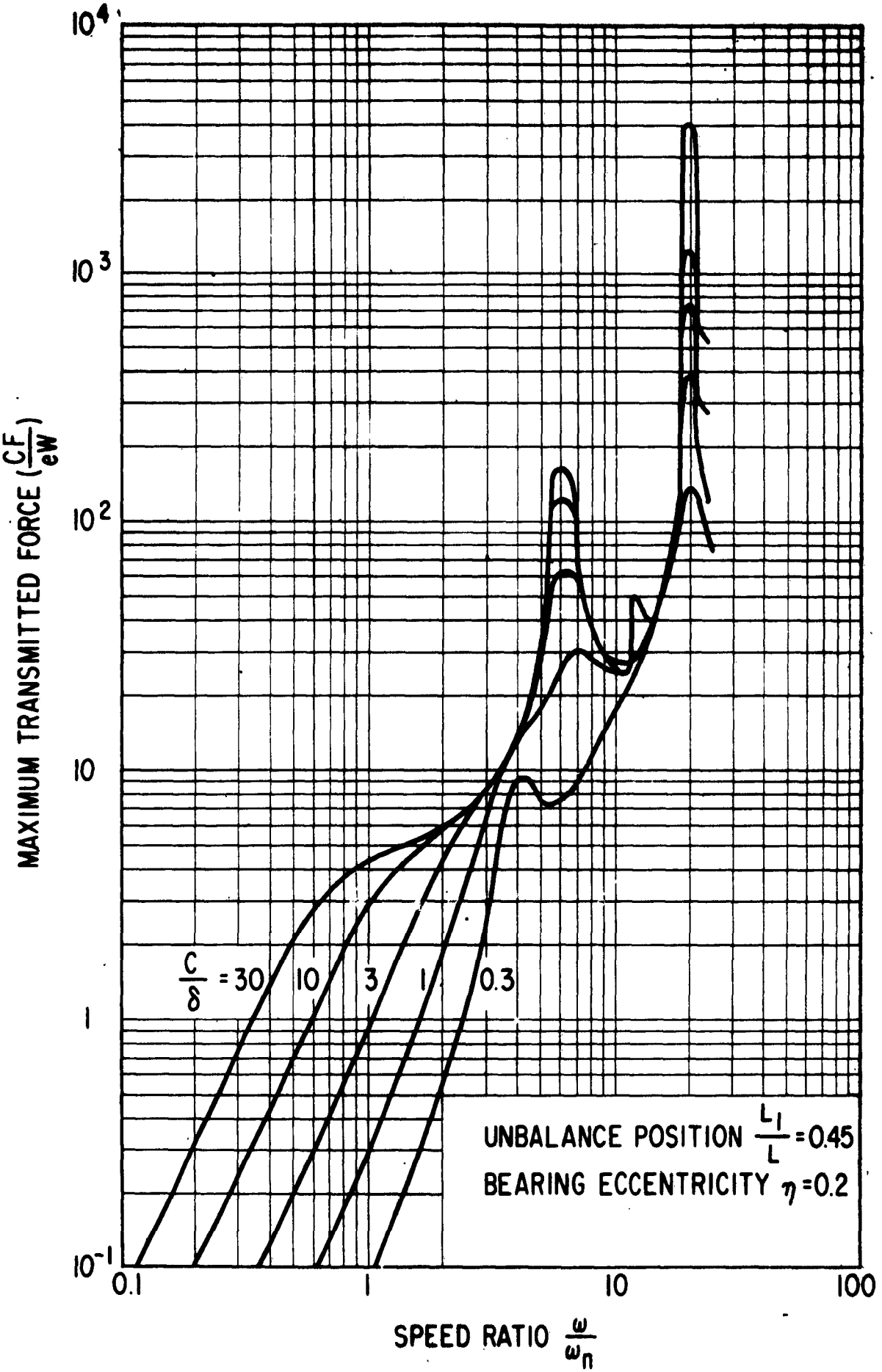

Fig. 22 Maximum Transmitted Force vs. Speed - Axially Asymmetrical Unbalance

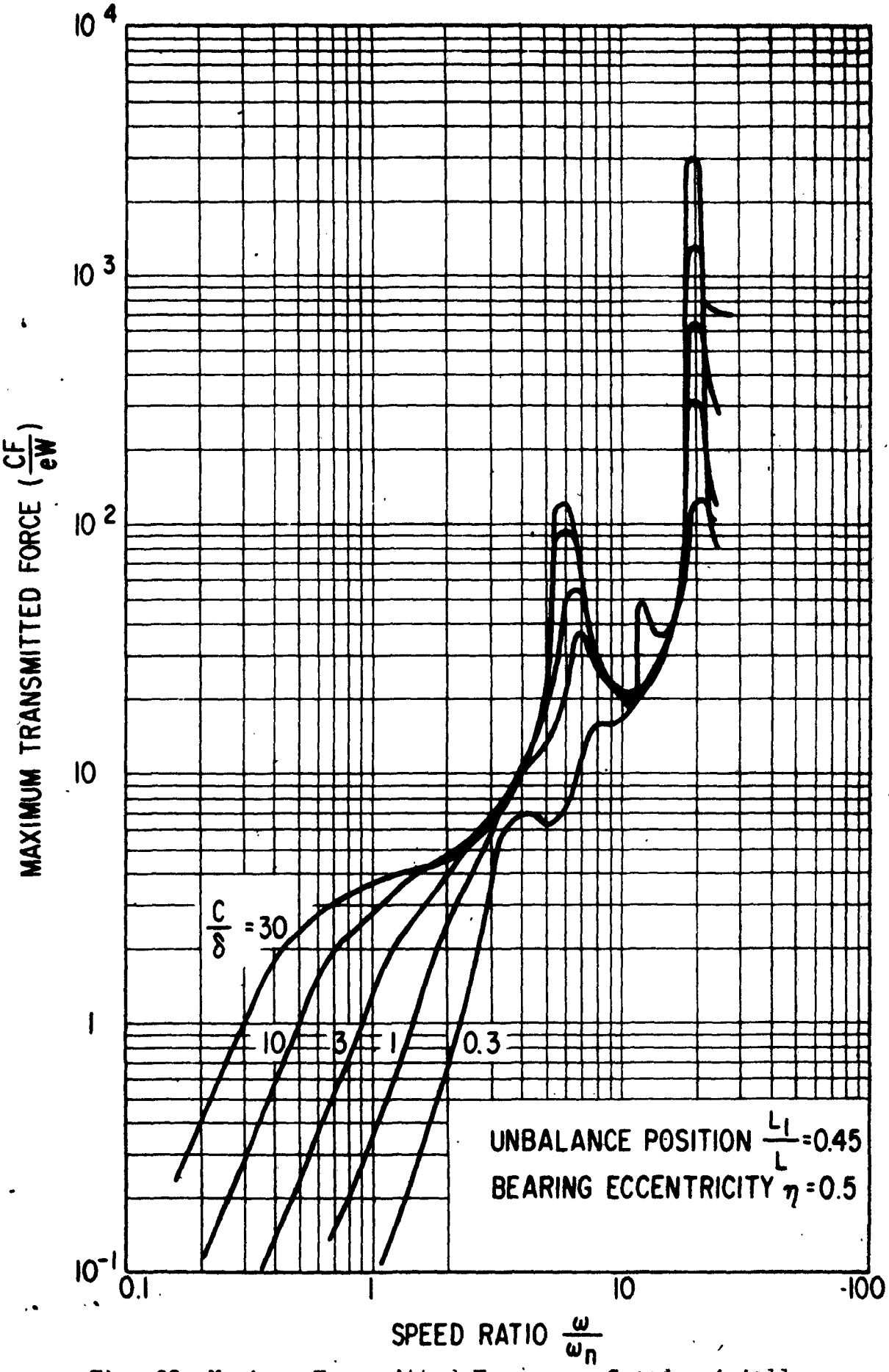

Fig. 23 Maximum Transmitted Force vs. Speed - Axially Asymmetrical Unbalance

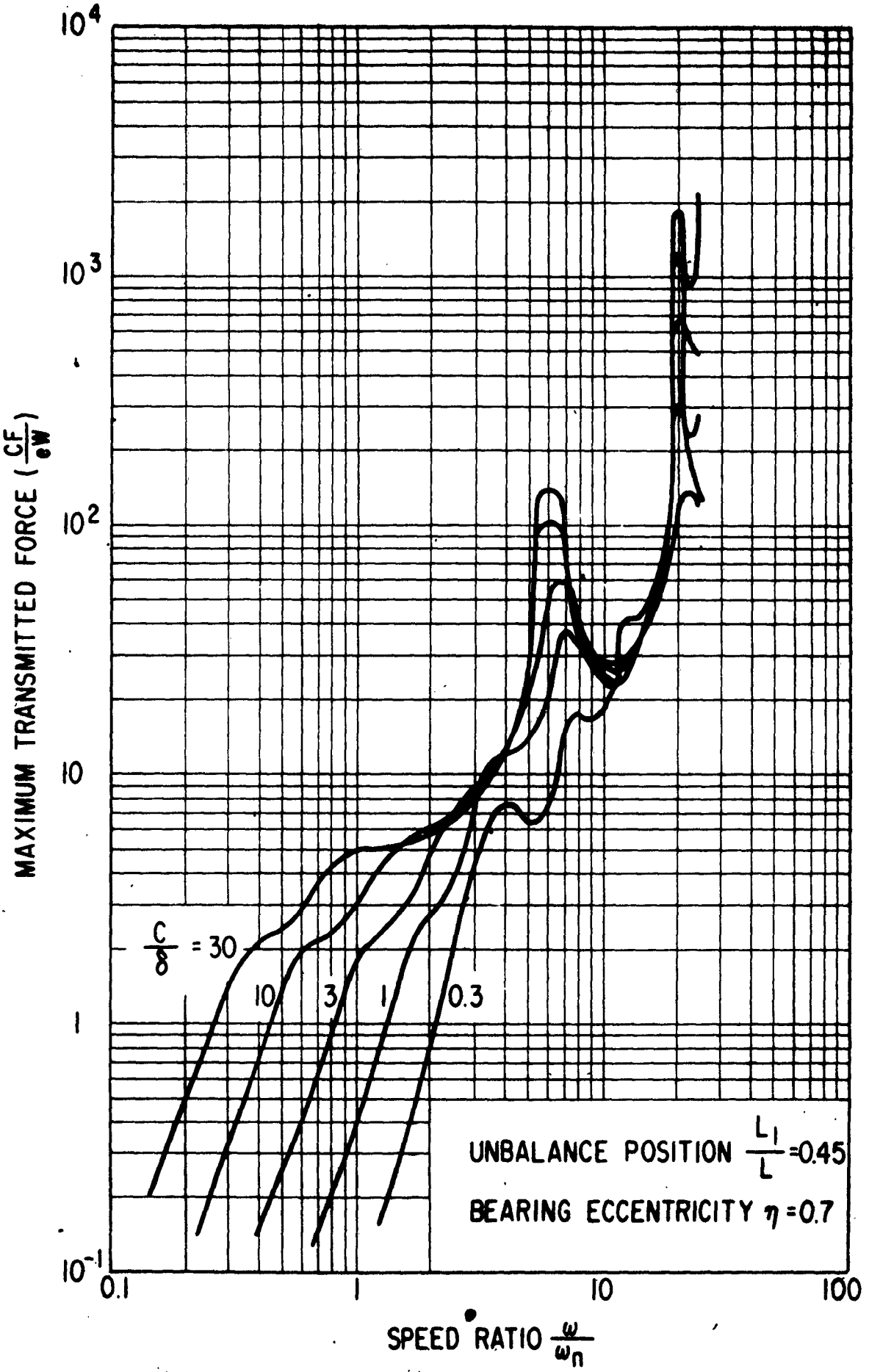

Fig. 24 Maximum Transmitted Force vs. Speed - Axially Asymmetrical Unbalance

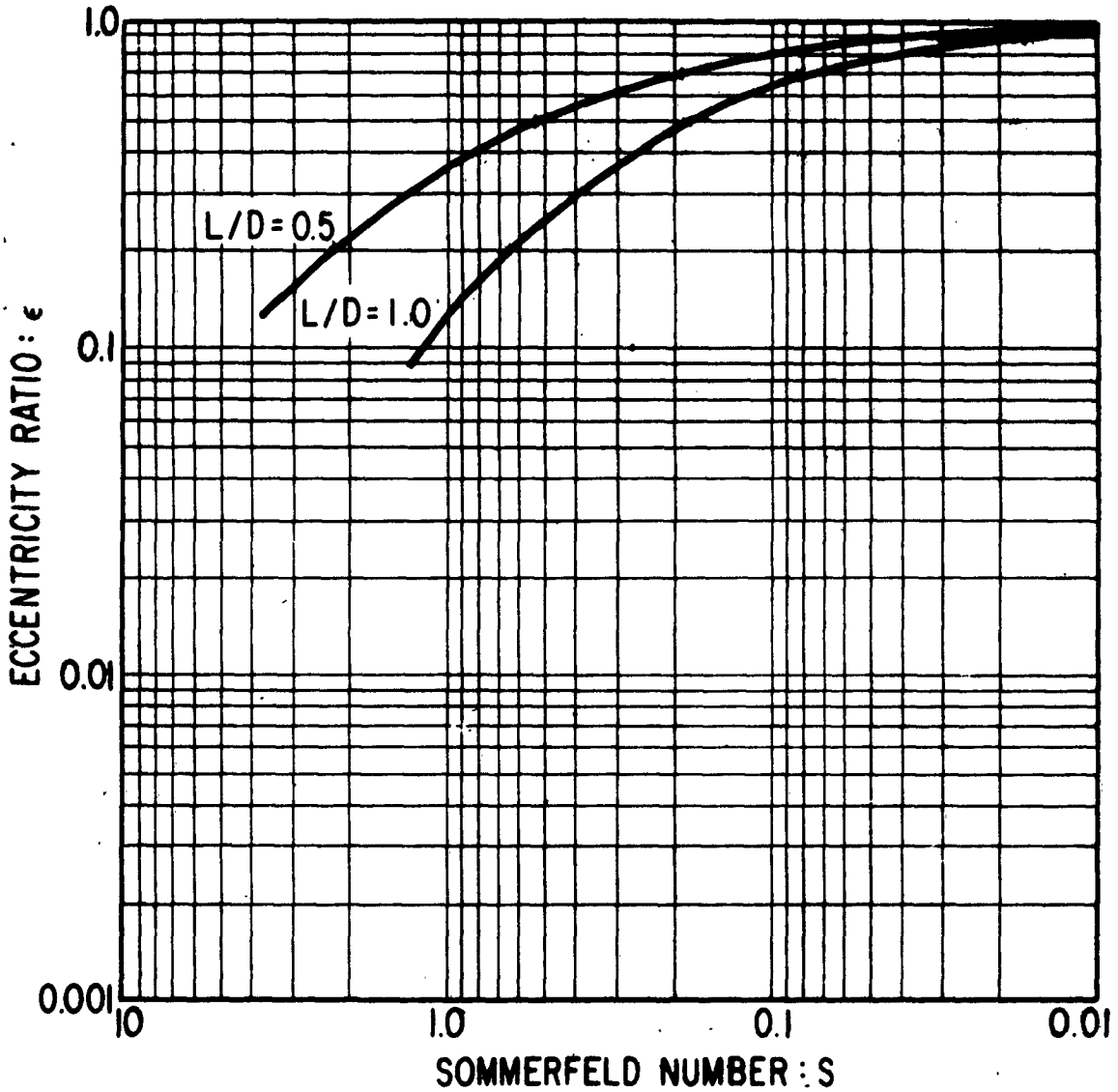

Fig. 25 Sommerfeld Number vs. Eccentricity for L/D = 0.5, 1.0

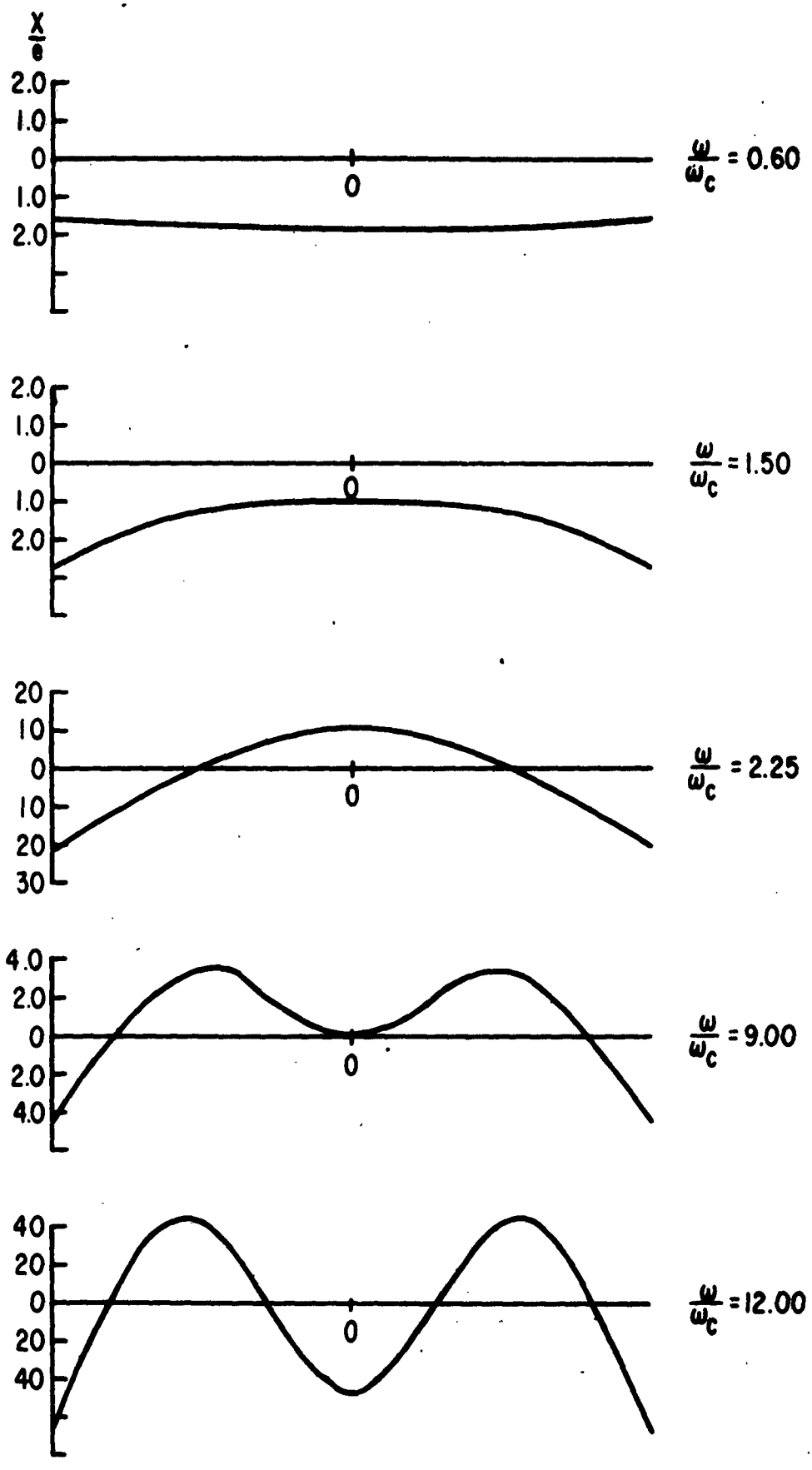

Fig. 26 Mode Shapes for Symmetrical Unbalance

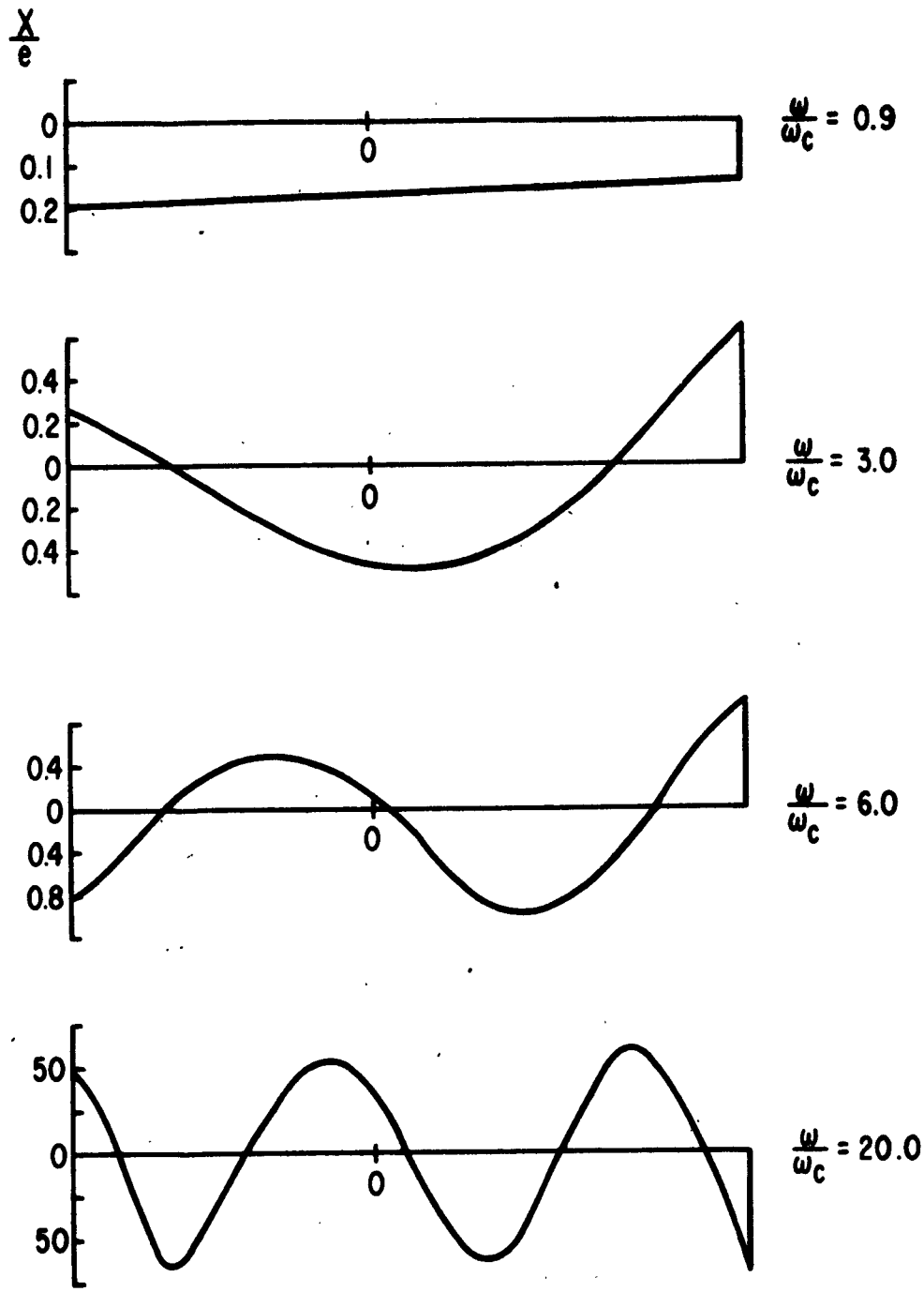

Fig. 27 Mode Shapes for Asymmetrical Unbalance

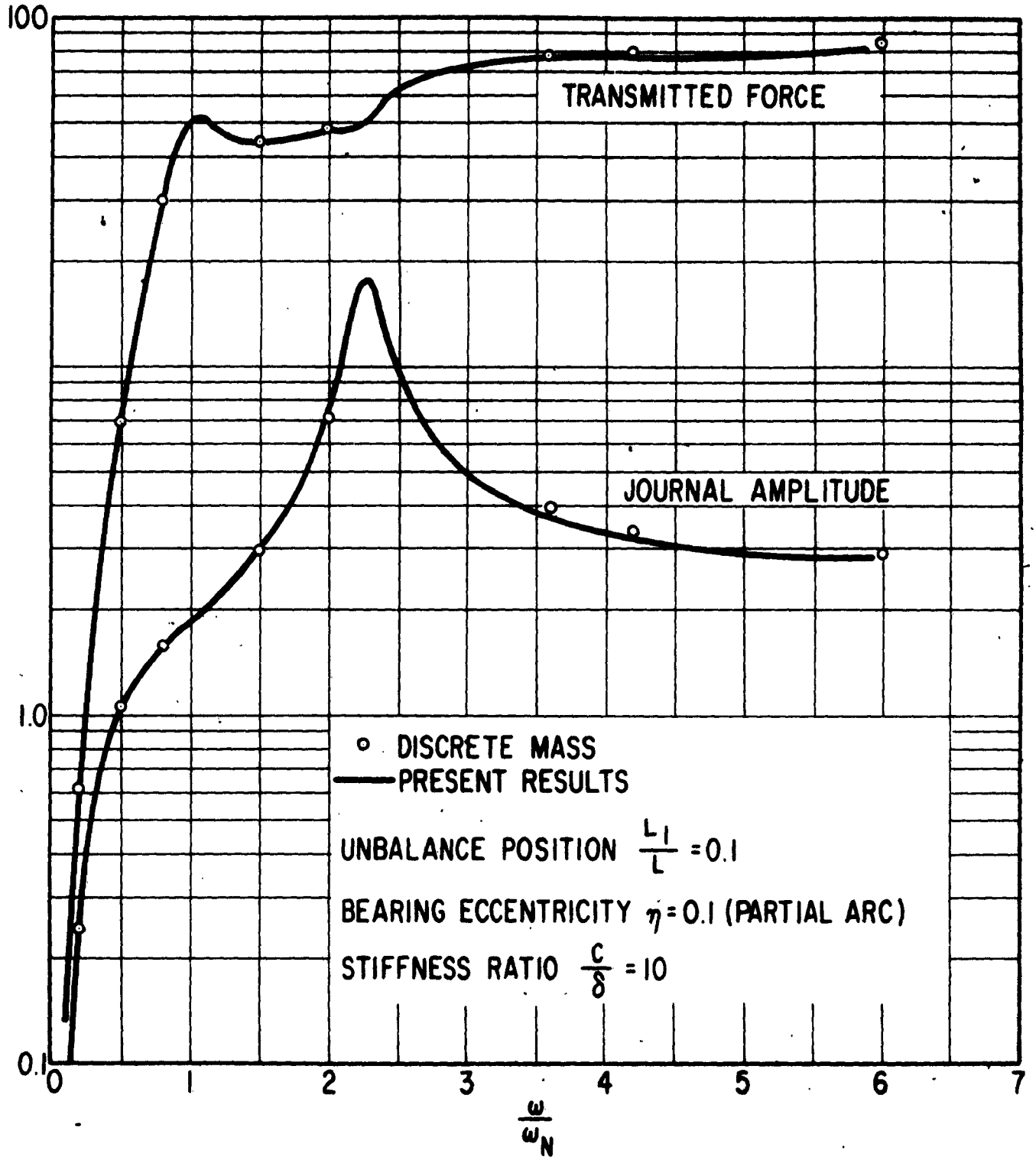

Fig. 28 Comparison Between Results of Present Analysis and Discrete-Mass Rotor Calculation

NOTATION

A	Area of cross-section of rotor
a, b	Whirl ellipse major and minor diameter
$A_1 B_1 C_1 D_1$	Constants of integration, region 1
$A_2 B_2 C_2 D_2$	
C	Bearing clearance
$C_{xx} C_{xy} C_{yx} C_{yy}$	Velocity coefficients for bearing damping
D	Bearing diameter
$E_1 F_1 G_1 H_1$	Constants of integration, region 2
$E_2 F_2 G_2 H_2$	
E	Modulus of elasticity
e	Eccentricity of unbalance
e	Base of natural logarithms, 2.71828....
F	Force
g	Gravitational acceleration
I	Second moment of area of rotor section
i	$\sqrt{-1}$
$K_{xx} K_{xy} K_{yx} K_{yy}$	Spring coefficients for bearing stiffness
L	Length of rotor
L	Length of bearing
L_1, L_2	Length of regions 1 and 2
$\mathscr{L}$	Length ratio L_1/L
M	Rotor mass
$M(X)$, $M(Y)$	Coordinate bending moments
N	Rev/Min
R	Bearing radius
S	Sommerfeld number $\left[\frac{\mu NLD}{W}\right]\left[\frac{R}{C}\right]^2$
t	Time
V	Shear Force
W	Rotor weight
W_1	Static Bearing load, $\frac{W}{2}$

w	Weight density
$X(z)$	Time-dependent displacement
$x(z)$	x-displacement
$Y(z)$	Time-dependent displacement
$y(z)$	y-displacement
z	Rotor length coordinate
$\alpha_1, \ldots$	Variables defined in text
α	Phase angle
β	Phase angle
δ	Deflexion of uniformly loaded shaft, $(\frac{5}{384})(\frac{wAL^4}{EI})$
η	Bearing eccentricity
θ	Bearing attitude angle
λ	Frequency parameter $\left[\frac{wA\omega^2}{gEI}\right]^{1/4}$
v	Stiffness parameter, $(EI\lambda^3)\cdot(\frac{C}{W})$
π	3.14159 ...
ρ	Mass density
μ	Viscosity
ω	Angular velocity rad/sec
ω_c	Critical speed of uniform rotor in rigid bearings.